

Analysis and Feasibility of Asphalt Pavement Performance-Based Specifications for WisDOT

Hussain Bahia
Pouya Teymourpour
Dan Swiertz
Cheng Ling
Remya Varma
Tirupan Mandal
Preeda Chaturabong
Erik Lyngdal
Andrew Hanz

University of Wisconsin- Madison

WisDOT ID no. 0092-15-04

December 2016



RESEARCH & LIBRARY UNIT



WISCONSIN HIGHWAY RESEARCH PROGRAM

WISCONSIN DOT
PUTTING RESEARCH TO WORK

Technical Report Documentation Page

1. Report No. 0092-15-04	2. Government Accession No	3. Recipient's Catalog No	
4. Title and Subtitle Analysis and Feasibility of Asphalt Pavement Performance-Based Specifications for WisDOT		5. Report Date : December 2016	
7. Authors H. Bahia, A. Hanz, P. Teymourpour, D. Swiertz, C. Ling, P. Chaturabong, T. Mandal, R. Varma, E. Lyngdal and Andrew Hanz		6. Performing Organization Code WHRP 0092-15-04	
9. Performing Organization Name and Address University of Wisconsin- Madison 3350 Engineering Hall, 1415 Engineering Dr., Madison, WI, 53717		8. Performing Organization Report No.	
12. Sponsoring Agency Name and Address Wisconsin Department of Transportation Research & Library Unit 4802 Sheboygan Ave. Rm 104, Madison, WI 53707		10. Work Unit No. (TRAIS)	
15. Supplementary Notes		11. Contract or Grant No. WisDOT SPR# 0092-15-04	
16. Abstract: <p>Literature review of most recent methods used for effective characterization of asphalt mixtures resulted in selecting a set of test methods for measuring mixture resistance for rutting and moisture damage at high temperature, fatigue cracking at intermediate temperatures, and thermal cracking at low temperatures. The methods were used to collect results for a large number of mixtures that vary in their composition including 3 sources of aggregates, 2 binders with and without polymer modification, different amounts of Recycled Asphalt Materials (RAM), and different volumetric properties. In addition, the sensitivity of specific mixture performance properties to variation of asphalt content and filler content was studied, and best methods to determine the effect of high RAM content on binder grades were evaluated.</p> <p>Based on the analysis of results collected, the Hamburg Wheel Tracking Test at 45 °C is recommended for use to evaluate resistance of mixtures to rutting and moisture damage, and the Semi-Circular Bend (SCB) test at intermediate temperature of the PG grade, with one notch depth, is recommended for fatigue resistance. For thermal cracking it is recommended at this time to continue testing with the Disk Compact Tension (DCT) test as well as the low temperature SCB test following AASHTO TP105 until more data is available. The recommendation also included a specification framework for each of the distress, and tentative limits for the key performance indicators from each of the selected tests. The indicators selected include Creep rate, Stripping Inflection Point (SIP) and Strip rate for rutting and moisture damage; Flexibility Index for Fatigue Cracking, and Fracture Energy for Thermal Cracking. Frameworks include different limits for traffic level and climate conditions, as well as aging condition in case of thermal cracking.</p> <p>The results also demonstrate the importance of controlling aggregate properties and asphalt binder content during production as both significantly influenced lab measured resistance to cracking. Limited data showed that use of high RAM content field trials had similar PG grades and mechanical properties as conventional mixes. Results to study methods for estimating change in blended binder grade due to use of RAM demonstrated that evaluation of the mortar can be applied to further evaluate the effects of RAM type and content.</p>			
17. Key Words Asphalt mixtures, Modified asphalts, Hamburg Wheel Tracking Test, Flow number, Confined conditions, Unconfined conditions, Semi-Circular Bend Test, Disc Compact Tension, Performance Specifications, Asphalt tests		18. Distribution Statement No restriction. This document is available to the public through the National Technical Information Service 5285 Port Royal Road Springfield VA 22161	
18. Security Classification (of this report) Unclassified	19. Security Classification (of this page) Unclassified	20. No. of Pages 132	21. Price

Disclaimer

This research was funded through the Wisconsin Highway Research Program by the Wisconsin Department of Transportation and the Federal Highway Administration under Project 0092-15-04.

The contents of this report reflect the views of the authors who are responsible for the facts and accuracy of the data presented herein. The contents do not necessarily reflect the official views of the Wisconsin Department of Transportation or the Federal Highway Administration at the time of publication.

This document is disseminated under the sponsorship of the Department of Transportation in the interest of information exchange. The United States Government assumes no liability for its contents or use thereof. This report does not constitute a standard, specification or regulation.

The United States Government does not endorse products or manufacturers. Trade and manufacturers' names appear in this report only because they are considered essential to the object of the document.

Executive Summary

This study was undertaken to evaluate the feasibility of using performance-related properties of mixtures to supplement the Superpave mixture volumetric specifications in Wisconsin. The study started with a wide scope literature review and discussions with the Project Oversight Committee that resulted in selecting a set of mixture performance tests with high potential for implementation. The experimental part of the study included four experiments in which a large number of mixtures, mainly produced in the lab, were evaluated for rutting resistance, moisture damage effects, fatigue cracking resistance, and thermal cracking. The study also included comparing effects of short term and long term oven aging of loose mixtures. The results are used to propose specification framework for each of the main distresses (Rutting and Moisture Damage, Fatigue Resistance, and Thermal Cracking Resistance). The framework includes specific testing procedures and specification parameters. It also provides very preliminary limits derived from the averages and distribution of the values measured for the mixtures tested. The following points provide a summary of the findings.

1. **Dynamic Modulus E*** (Section 3.1.1 in report): The values of E* measured at 4 temperatures (4.2, 21.1, 37.2, and 54.4 °C) vary based on the aggregates used, the mixture design (NT or HT) and the binder grade. The E* values, at a given temperature and frequency of loading, can vary by as much as 165%, or as small as 65% of the minimum value measured due to the mixture composition variation. This range is important and could have significant impact on stresses and strains in a typical pavement section.
2. **Rutting and Moisture Damage Resistance** (Section 3.1.2 in report): The Flow Number test in the confined and unconfined condition was used, as well as the Hamburg Wheel Tracking Test (HWTT), to measure effect of repeated loading and moisture at high temperatures on rutting rates. It is found that the HWTT results in a similar mechanism of rutting to the Flow Number. However there is not a one-to-one match of the rutting rate due to the fact that HWTT provides partial confinement that is lower than the confinement in the FN test. The HWTT mechanism of rutting changes significantly after the Stripping Inflection Point (SIP), which appears to be mainly due to moisture effects. It is recommended that the HWTT is used for measuring both rutting resistance as well as moisture damage potential. The parameters selected include the creep rate, the SIP, the strip rate, and the passes to 12.5 mm rut depth. Also it is recommended to conduct the test at 45 °C. The following table represents the specification framework recommended. The framework includes consideration of Climate (North and South), and traffic volume (LT, MT, and HT). It also include a provision for taking into account traffic speed.

<i>Mixture Rutting Resistance Framework: All tests done at 45 °C</i>				
Climatic Region/ Traffic		LT	MT	HT
North	Minimum Creep Rate (mm/1000 passes)	-1.50	-0.75	-0.375
	Minimum Passes to 12.5 mm	6,000	9,000	12,000
South	Minimum Creep Rate (mm/1000 passes)	-1.25	-0.625	-0.312
	Minimum Passes to 12.5 mm	7,500	11,250	15,000
*: These limits are for normal traffic speed, if slow speeds are expected the limits should be increased				
Moisture Damage Potential Framework				
<ul style="list-style-type: none"> - If Ratio of stripping slope to Creep slope: ≥ 2.75, passes to SIP should be checked - Passes to the Stripping Inflection Point (SIP): Same as Passes to 12.5 mm - Stripping Slope: $\geq - 2.25$ for all mixtures 				

3. **Fatigue Cracking Resistance (Sections 3.1.3.1 and 3.1.3.2 in this report):** Based on the literature review and the recently completed WHRP 0092-14-06 study, the Semi-Circular Bend (SCB) test was selected as the potential test for this distress type. Two procedures (SCB-LSU and SCB-IFIT) were included in this study. Both procedures are found to have deficiencies in terms of producing logical trends in measuring effect of mixture and aging variables included in the experiments. Therefore the modified SCB-LSU procedure recommended in WHRP 0092-14-06 is recommended for the specification framework. The main reason for this recommendation is the use of the Post-Peak Slope in the analysis, which appears to be a useful parameter to measure effects of oxidative aging and use of RAP. The following table presents the framework proposed. The mixture property used is the Flexibility Index (FI).

Fatigue Resistance at Intermediate Temperatures - SCB Test Framework									
Traffic	LT			MT			HT		
Construction	Overlay	Other Construction		Overlay	Other Construction		Overlay	Other Construction	
PG-LT	-28	-28	-34	-28	-28	-34	-28	-28	-34
Test Temp.	19	19	16	19	19	16	19	19	16
Minimum FI (Short-Term Aged 4hrs)	*	6.0		*	12.0		*	18.0	
Minimum FI (Long-Term Aged 12hrs)	*	2.5		*	5.0		*	7.5	

* The limits for Overlay should be increased by 50% to account for the excessive movements at the pavement joints or cracks. This increase should be left to the discretion of the material engineer of the project.

4. **Thermal Cracking Resistance (Section 3.1.3.4 of this report):** For thermal cracking the Disc-Compact- Tension (DCT) and the SCB test developed by the University of Minnesota (SCB-UMN) were included in the study. Due to the challenges faced in interpretation of the statistical analysis results and the lack of good fit of the regression models, it was difficult to decide if the DCT or the SCB-UMN should be used. Also there were mixed trends for the effect of long term aging on the values of the fracture energy, which is the parameter recommended for this distress. Therefore both tests and both aging conditions are included in the recommended framework until further studies allow expanding the database and validating which test and aging condition is preferred.

Low Temperature Cracking Resistance Framework									
Traffic	LT			MT			HT		
Construction	Overlay	Other Construction		Overlay	Other Construction		Overlay	Other Construction	
PG-LT	-28	-28	-34	-28	-28	-34	-28	-28	-34
Test Temp	-18	-18	-24	-18	-18	-24	-18	-18	-24
DCT Minimum Fracture Energy (Short-Term Aged 4hrs) J/m ²	*	300		*	400		*	500	
DCT Minimum Fracture Energy (Long-Term Aged 12hrs) J/m ²	*	250		*	300		*	350	

SCB-UMN Minimum Fracture Energy (Short-Term Aged 4hrs) J/m ²	*	200	*	350	*	500
SCB-UMN Minimum Fracture Energy (Long-Term Aged 12hrs) J/m ²	*	TBD	*	TBD	*	TBD

* The limits for Overlay should be increased by 50% to account for the excessive movements at the pavement joints or cracks. This increase should be left to the discretion of the material engineer of the project.

5. **Experiment 2: Sensitivity of Selected Performance Tests to Production Variation (Section 3.3 of this report):** The sensitivity of fatigue cracking parameters to variability of asphalt binder content and filler content within allowable construction tolerance were studied in Experiment 2. Based on results of this experiment it is concluded that minor changes to P200 (e.g. +/- 2.0%) during production would not be expected to significantly affect the FI and Post-Peak Slope measured by the SCB-IFIT procedure; however, changes in asphalt within the tolerance limits could significantly affect FI, and changing aggregate sources could change all responses. This confirms the concern expressed in earlier works that the results of this procedure could be over-sensitive to the asphalt content. Therefore, if the FI is used in the specifications, the limits should be set low enough to allow for the production variability (e.g. +/- 0.3%) in asphalt content. Also, aggregate source changes should be restricted to avoid failing of the specifications.

6. **Experiment 3: Development of Supplemental Guidelines for Required Performance Testing for High Recycled Content Mixes (Section 3.4 of this report):** To provide supplemental guidelines to control the properties of mixture with high RAM content, the results from binder extraction and blending charts procedure were compared with the mortar testing procedure for a limited number of combinations. The results indicate that the mortar procedure offers a solvent-free alternative to extraction and recovery and may offer the advantage of directly characterizing materials based on the amount of blending that actually occurs in high RAM mixtures. Since some solvents may degrade or otherwise mask the properties of some binder modifiers, the mortar procedure may be a viable alternative over extraction and use of blending charts.

7. **Experiment 4: In-Service Field Validation (Section 3.4 of this report):** An attempt was made to validate the limits proposed in the specifications frameworks proposed. Although, only one project could be sampled due to various challenges, imaging analysis of cored samples taken from 3 projects, as well as testing of recovered asphalt binders were completed. The data were also complemented by results from another recent study in WI. The limited results analyzed did not identify any significant performance concerns with the high RAM mix designs relative to the control as for most performance tests the high RAM designs performed as good as or better than the control designs when tested for the Fracture Energy. The exceptions are the ΔT_c values of the top 1/2" of the STH 77 mix and the STH 26 mix were slightly more negative than the control, but did not exceed the warning limit established by previous research. Given the relatively young age of the pavements, it is promising that no differences were observed, however monitoring of pavement performance over time is required to verify the results of the initial laboratory work conducted in the High RAM Pilot Project, and the initial forensic research presented in this study. It is recommended that the most promising tests be selected and applied on cores on an annual or bi-annual basis to continue to track material properties and to begin to develop relationships with pavement performance.

Table of Contents

Disclaimer	i
Technical Report Documentation Page.....	ii
Executive Summary	iii
Table of Contents	vi
List of Figures.....	viii
List of Tables	xi
1. Introduction & Research Approach.....	1
1.1 Background	1
1.2 National Efforts to Implement Mixture Performance Based Specifications	1
1.3 WisDOT Efforts to Implement Mixture Performance Based Specifications.....	2
1.4 Project Objectives	2
1.5 Research Approach.....	3
2. Experimental Design and Materials.....	4
2.1 Selection of Test Methods.....	4
2.2 Materials	5
2.3 Experimental Designs	6
3. Analysis of Results and Summary of Findings	12
3.1 Experiment 1: Evaluation of Mixtures that meet Specification.....	12
3.1.1 Experiment 1a- Dynamic Modulus (E^*) Testing	12
3.1.2 Experiment 1a- Flow Number (FN) and Hamburg Wheel Tracking Testing (HWTT).....	14
3.1.3 Experiment 1b: Evaluation of Long Term Aged Mixtures using SCB and DCT.....	37
3.2 Experiment 2: Sensitivity of Selected Performance Tests to Production Variation	76
3.3 Experiment 3: Development of Supplemental Guidelines for Required Performance Testing for High Recycled Content Mixes.....	77
3.3.1 Overview of the Results	77
3.3.2 Comparison of RAP and RAS Blends	80
3.3.3 Summary of Findings	82
3.4 Experiment 4: In-Service Field Validation.....	83
3.4.1 Background	83
3.4.2 Analysis Methods	84
3.4.3 Experimental Plan	87
3.4.4 Results and Analysis	88

3.4.5 <i>Summary and Conclusions</i>	96
4. Conclusions and Recommendations	97
5. References	100

List of Figures

Figure 1. Master Curves of E^* versus frequency at 21.1 C for the 24 mixtures tested.....	13
Figure 2. Results of Confined and Unconfined FN Testing.....	15
Figure 3. Correlation of strain of dry HWT and confined FN to tertiary point of HWTT test for four mixtures commonly used in WI. Mixtures were produced with different aggregates and binder grades.	16
Figure 4. Power Law Fit for HWTT results, (a) normal scale, and (b) log-log scale	17
Figure 5. Correlation of slope between dry HWTT and confined FN by the Power Law Method.....	17
Figure 6. Correlation of creep slopes of dry HWT and slopes of confined and unconfined FN test by the Power Law Method.....	18
Figure 7. Comparison of rut depth in dry and wet HWT.....	19
Figure 8. HWT temperature based on NCHRP Project 20-07/Task 361	21
Figure 9. Defining the creep slope and the strip slope from the first derivative of the 6-order polynomial fit of the HWT test results.....	21
Figure 10. Example of HWT results at 50 °C for Cisler MT mixtures.....	22
Figure 11. Ratio of strip slope to creep slope for the 24 mixtures tested in this study. (a) MT mixes, and (b) HT mixes.....	23
Figure 12. SIP Passes and Passes to 12.5 mm rut depth for the 24 mixtures tested in this study. (a) SIP - MT mixes, (b) SIP- HT mixes, (c) 12.5 mm passes MT mixes, and (d) 12.mm passes HT Mixes.	24
Figure 13. Best-subsets regression for passes to 12.5 mm at 50 °C.....	25
Figure 14. HWT results at 45 °C for the Wimme and for the Waukesha aggregates. (a) Passes to 12.5 mm for Wimme aggregates, (b) Passes to 12.5 mm for Waukesha aggregates, (c) SIP for Wimme aggregates, (d) SIP for Waukesha aggregates.....	28
Figure 15. Stepwise regression for Passes at 12.5 mm at 45 °C in terms of binder, aggregate and mixture properties	29
Figure 16. Stepwise regression for Passes to SIP at 45 °C in terms of binder, aggregate and mixture properties	30
Figure 17. Stepwise regression for Creep Slope at 45 C in terms of binder, aggregates and mixture properties	31
Figure 18. Results of the HWTT testing for three mixtures with and without anti-strip additive.	33
Figure 19. Variation of J_c Values estimated from the SCB Test Results for All Mixtures. (a) after 12 hours lab aging, and (b) after 2 hours of lab aging	40
Figure 20. Peak Load and Peak Displacement for 25.4 mm Notch Length (LT= Long Term Aged, ST=Short Term Aged).	41
Figure 21. Peak Load and Peak Displacement for 31.8 mm Notch Length.....	41
Figure 22. Peak Load and Peak Displacement for 38.1 mm Notch Length.....	42
Figure 23. Stepwise regression and Multi-linear Regression model for the J_c estimated from the SCB-LSU procedure.....	44
Figure 24. Regression Model from WHRP 14-06 Draft Report	45
Figure 25. SCB-LSU Flexibility Index of Short and Long Term aged Mixtures for (a) Mixtures with PGxx-28 binders and (b) Mixtures with PG xx-34 binders	46
Figure 26. Results of Stepwise Regression for the FI calculated from the SCB-LSU testing at 25-mm notch depth.....	47

Figure 27. Best set models for (a) Slope value (m), and (b) Peak Load for the SCB-LSU testing at 25-mm notch.....	48
Figure 28. Comparison of Measured Values of FI from the SCB-LSU with values predicted using the model proposed by WHRP 14-06 study	50
Figure 29. Summary of Flexibility Index for all mixtures: (a) Short Term aged (b) Long Term aged	52
Figure 30. Best Sub-set Model for FI from the IFIT procedure.....	53
Figure 31. Results of Statistical Models for the Fracture Energy, Post Peak Slope, and Peak Load for the UIUC-IFIT results.....	54
Figure 32. Summary of DCT Results @ -18°C (LT PG =-28°C).....	59
Figure 33. Summary of DCT Results @ -24°C (LT PG =-34°C).....	60
Figure 34. Cross Section of Failed DCT samples for Different Aggregate Types	65
Figure 35. DCT Fracture Energy Results for Mixes from Various Aggregate Sources	67
Figure 36. Effect of Aggregate Source and Aging on DCT Fracture Energy.....	68
Figure 37: DCT Fracture Energy Results for Mix Designs Produced Using Various Aggregate Sources in SE MN	69
Figure 38. Location of 2013 Construction MnDOT DCT Pilot Study (Johanneck, et al., 2015)	70
Figure 39. Summary of DCT Fracture Energy Results for Mix Design, Adjustment, and Production MNDOT DCT Pilot Study (Johanneck, et al., 2015).....	70
Figure 40. Results of the SCB-UMN cracking test for mixtures with HT designs and V grade binders. Mixtures with V-28 binders are tested at -18 C and mixtures with V-34 binders are tested at -24 C.	73
Figure 41. Gf for the mixtures produced with the S-28 binders as compared to mixtures with the V-28 binders for the 15% PBR	74
Figure 42. (a) RAP grade change rate comparative analysis, and (b) RAS grade change rate comparative analysis.....	79
Figure 43. Low Temperature Grade Change analysis for RAP/RAS Combinations (estimated from Grade Rate Changes of Figure 2).	80
Figure 44. Intermediate Temperature Grade Change analysis for RAP/RAS Combinations (estimated from Grade Rate Changes of Figure 2).....	81
Figure 45. High Temperature Grade Change analysis for RAP/RAS Combinations (estimated from Grade Rate Changes of Figure 2).	82
Figure 46. Location of WisDOT High RAM Pilot Projects.....	83
Figure 47. Total Distress vs. ΔT_c – Olmstead County Test Section, WRI Source Study (Reinke, et al., 2015)	85
Figure 48. Schematic of Sample Cutting for Image Analysis (Roohi, 2012).....	86
Figure 49. Microstructural parameters from imaging analysis in iPas (Roohi, 2012)	87
Figure 50. Schematic of Definition of Aggregate Proximity and Length of Proximity (Roohi, 2012)	87
Figure 51. High Temperature PG of Recovered AC from STH 77 High RAM and Control Mixes.....	89
Figure 52. Low Temperature PG of Recovered AC from STH 77 High RAM and Control Mixes	89
Figure 53. Low Temperature PG of Recovered AC from STH 77 High RAM and Control Mixes	90
Figure 54. High Temperature PG of Recovered AC from USH 141 and STH 26 High RAM and Control Mixes	91
Figure 55. Low Temperature PG of Recovered AC from USH 141 and STH 26 High RAM and Control Mixes	92

Figure 56. ΔT_c of Recovered AC from USH 141 and STH 26 High RAM and Control Mixes.....	92
Figure 57: DCT Fracture Energy at -24°C – Comparison of STH 77 High RAM and Control Mixes.....	93
Figure 58: SCB-IFIT Flexibility Index at 25°C – Comparison of STH 77 High RAM and Control Mixes	95
Figure 59: IPas Results for High RAM and Control Mixes – Comparison of Total Proximity Length (mm/100cm ²)	96

List of Tables

Table 1. Selected Performance Test Methods.....	4
Table 2. Aggregate Source Information.....	5
Table 3. Binder Testing Results.....	6
Table 4. Aging Conditions Used in this Study.....	7
Table 5. Experiment 1a. Short Term Aged Mixtures (Full Factorial = 24 combinations).....	7
Table 6. HWTT Extended Experiment.....	8
Table 7. Experiment 1b. Long Term Aged Mixtures (Full Factorial = 48 combinations).....	9
Table 8. Production Variation Experimental Design using SCB-I.....	10
Table 9. Experiment 3 Design.....	11
Table 10. Minimum and Maximum Values of E* Measured for the 24 Mixtures Tested.....	12
Table 11. Unconfined Flow Number Limits for Wisconsin Mixtures from WHRP 0092-08-06.....	14
Table 12. Creep Slope of Eight Mixtures using Wet and Dry HWT.....	20
Table 13. WisDOT High-RAM Specification for HWT.....	22
Table 14. Reduced Test Temperature Subset.....	26
Table 15. HWT results for testing at 40 C.....	27
Table 16. Sensitivity of HWT Parameters to Selected Responses.....	32
Table 17. Limits for Passes to 12.5 mm used by various State Agencies for the HWT test.....	34
Table 18. HWT testing temperature selected by various State Agencies (NCHRP 219).	35
Table 19. Proposed HWT Limits at 45 °C to Limit Permanent Deformation.....	37
Table 20. Experimental Design for the SCB-LSU Testing.....	38
Table 21. Volumetric Properties for the Mix Designs Used in this Study.....	38
Table 22. ANOVA Analysis of the SCB- Jc Test Results.	42
Table 23. ANOVA Analysis of the SCB Test Results for Peak Load, Peak Displacement, and Fracture Energy.....	43
Table 24. Sensitivity Analysis of the SCB-LSU response to Mixture Design and Conditioning Factors.....	51
Table 25. Sensitivity Analysis of the SCB-IFIT Responses to the Mixture and Aging Variables.....	55
Table 26. Proposed Intermediate Temperature Cracking Framework.....	57
Table 27. Summary of Existing Specifications for the DCT test.....	58
Table 28. Estimated Effect of Binder Replacement on LT PG.....	60
Table 29. Analysis of Trends of Mixtures' Main Variables with DCT Average Values of Response Parameters for the PG xxx-28 Binder.....	61
Table 30. Analysis of Trends of Mixtures' Main Variables with DCT Average Values of Response Parameters for the PG xxx-34 Binder.....	61
Table 31. Trends Observed in Main Effects – DCT.....	62
Table 32. ANOVA Results for DCT Fracture Energy ($\alpha = 0.05$).....	63
Table 33. Results of Multi-Linear Regression Analysis Including Main Effects and Mixture Properties.....	64
Table 34. Effect of Aggregate Source and PG Selection on DCT Fracture Energy at -12°C (Buttlar, et al., 2016).....	66
Table 35. Summary of Mixes Used to Evaluate Effects of Aggregate Source on DCT Fracture Energy.....	66
Table 36. Sensitivity Analysis for the DCT Test.....	71
Table 37. Initial Framework for Control of Low Temperature Cracking.....	75
Table 38. ANOVA Analysis for Production Variation Experiment at Confidence Level of 95%.....	77

Table 39. Continuous Grading Properties for the Recovered Binders.....	78
Table 40. Overview of High RAM Projects for WisDOT Pilot Program.....	84
Table 41: Summary of DCT Parameters for Field Cores and Laboratory Aged Mixtures	94
Table 42: Summary of SCB-IFIT Parameters for Field Cores	95
Table 43. Rutting Resistance Framework: All tests done at 45 °C	97
Table 44. Intermediate SCB Test Framework.....	98
Table 45. Low Temperature Cracking Tests Framework	98

1. Introduction & Research Approach

1.1 Background

The fundamental objective of an asphalt mix design is to select an aggregate skeleton and a single asphalt binder content that will balance the constructability and the performance properties of the compacted pavement layer. It is well established that while increasing the asphalt content in the mixture may be desirable for some mixture properties (such as durability and flexibility), it often comes at the detriment of other properties, such as stability and rutting resistance (Asphalt Institute, 2014). High performing mixtures must therefore exhibit a balance of properties controlling primary pavement distresses such as rutting resistance, moisture resistance, and cracking resistance.

The Wisconsin Department of Transportation (WisDOT) currently follows a modified version of the Superpave mix design procedure, which results in the selection of a single asphalt binder content that achieves a design air void content and meets other designated volumetric parameters such as Voids in Mineral Aggregate (VMA). Aggregate physical and volumetric properties are likewise controlled by agency specified source and consensus properties. Currently, the WisDOT mix design method (WisDOT Method 1559) does not utilize any performance testing of the mixture for validation of the design asphalt content, or acceptance of mixtures in the field other than assessing the moisture susceptibility of the mixture using the Modified Lottman Test (ASTM D 4867). Since the adoption of the Superpave mix design method, however, several new asphalt binder and mixture technologies have become common practice and have had a significant effect on improving field performance, calling into question the efficacy of the volumetric design approach in capturing mixture performance.

This research study is conducted to identify which performance related properties of mixtures should be evaluated, which tests should be used, and how this information will be incorporated into WisDOT's asphalt pavement mixture design and quality management program (QMP).

1.2 National Efforts to Implement Mixture Performance Based Specifications

The original Strategic Highway Research Program (SHRP) that introduced a performance based specification for asphalt binders (Performance Grading) system also included mixture performance based testing. SHRP researchers advocated for the use of performance related mechanical testing of mixtures in order to produce empirical relationships with field performance. Despite this effort, the original SHRP performance models proved unreliable, the performance test equipment was found to be complex and expensive, and the planned Superpave performance evaluation was not fully or widely implemented.

The National Cooperative Highway Research Program (NCHRP) revisited the topic of asphalt mixture performance testing with NCHRP Project 09-19, with the final report published in 2002. The study promoted the use of a cylindrical specimen test called the Simple Performance Tester (SPT) to predict rutting and fatigue distress, while the use of Indirect Tensile (IDT) testing was used to predict low temperature cracking, as it was intended in the SHRP program. The SPT later evolved into the Asphalt Mixture Performance Tester (AMPT), which is mainly a tri-axial testing apparatus capable of measuring key structural design parameters. Concurrent with the development of the SPT, the FHWA continued work on the development of a Mechanistic-Empirical pavement design procedure, which at that time was called the Mechanistic-Empirical Pavement Design Guide (MEPDG).

The MEPDG design software relies heavily on the asphalt mixture complex modulus (E^*), which is a fundamental property that can be measured using the AMPT. Several AASHTO testing standards have been developed supporting the AMPT, yet its usage in practice remains low. The initial cost of the machine,

sample preparation, testing time, and required technical proficiency of the operator have all been cited as drawbacks to the more widespread implementation of the AMPT.

In response to concerns over the shortcomings of a purely volumetric design approach, and the lack of widely approved performance tests, several agencies and research institutions have developed new testing procedures for asphalt mixtures or adapted testing procedures from other industries. Case studies by several of these agencies were presented at the Transportation Research Board annual meeting in 2014, and are summarized in the Transportation Research Board E-Circular E-C189 (Transportation Research Board, 2014). California, New Jersey, Texas, Wisconsin and Louisiana were among the states shared their experience with implementing performance-based specifications. Although the results with different specifications have been generally promising, no clear consensus exists as to which performance tests best capture field performance while being practical enough to be used on routine basis.

1.3 WisDOT Efforts to Implement Mixture Performance Based Specifications

In 2014 WisDOT developed a pilot program for HMA with higher recycled asphalt materials content (high RAM) that required use of performance based test methods during mix design and production. Following the balanced mix design concept mixture tests were selected to address rutting resistance after short term aging and durability after long term aging. Durability tests included the semi-circular bend (SCB) at intermediate temperatures and disc-shaped compact tension (DCT) at low pavement temperatures. Asphalt binder extraction and grading from aged mix was also required. Results of asphalt mixture fracture tests and recovered binder grading after 12 and 24 hour loose mix aging were used to demonstrate the change in properties with aging and to recommend loose mix aging as a viable alternative to the current long term aging protocol in AASHTO R30. High RAM results were also compared to a conventional mix to assess the impacts of increased recycled binder content on the evolution of binder and mix properties with aging. Four projects were let throughout the State utilizing the High RAM specification and in general economic benefits were seen for all projects. The program highlighted several important considerations for future work, such as the relatively poor performance of 12.5 mm NMA mixtures using the Hamburg Wheel Tracking Test. Summaries of the projects and lessons learned are available on the Wisconsin Asphalt Pavement Association (WAPA) website as presentations given at WAPA annual meetings (<http://www.wispave.org/wapas-56th-annual-conference-and-business-meeting/>).

An ongoing project within the Wisconsin Highway Research Program (WHRP) is also using mixture performance testing to evaluate durability of asphalt mixtures. Project 0092-14-06: Critical Factors Affecting Asphalt Concrete Durability is expected to be completed in late Summer 2016 and is investigating the use of the SCB among other tests to evaluate how mixture design parameters affect durability of asphalt mixtures.

1.4 Project Objectives

The purpose of this research is to aid WisDOT in implementing an asphalt mixture performance based specification that addresses the primary modes of failure commonly observed in the State. In support of this goal, the following objectives are identified:

- Identify and evaluate asphalt mixture testing procedures that can effectively discriminate the performance of commonly used mixtures in the State of Wisconsin and produce logical trends in the data.
- Establish the relationship between performance test results with surrogate measures for production testing applications.

- Ensure quality of mixtures with high RAP contents through the use of performance based testing.
- Develop a criteria-type framework with suggested performance limits for future evaluation.

1.5 Research Approach

This project includes four major experiments: (1) evaluating mixtures that meet current specification, (2) evaluating the effects of production variability on mixture performance, (3) provide additional guidance for high-RAM mixtures, and (4) in-service field validation of the findings.

The first experiment included an extensive literature review of existing performance test methods and the selection of methods of highest interest to WisDOT for further evaluation. Materials and mix designs from several contractors were used to replicate commonly used WisDOT mixtures in the laboratory and these mixtures were evaluated using the proposed test methods. Mix design variables were changed in a factorial design to evaluate the effects of mix design variables on performance.

The second experiment involved fixing several mix design variables and adjusting the design asphalt content and dust (P200) content in the mixture within current WisDOT tolerances and evaluating the effects on mixture performance.

The third experiment provides guidance for determining the effective binder properties for high-RAM mixtures using linear blending charts and a developmental grading procedure developed at UW-Madison.

In the final experiment, field cores were used to compare to laboratory mixtures in order to develop relationships between laboratory test methods and field performance.

2. Experimental Design and Materials

2.1 Selection of Test Methods

The research team performed an extensive literature review of available performance test methods to select methods best suited for this study. Seven criteria were identified to evaluate the test methods as abbreviated below:

1. Specification by other state agencies
2. The presence of existing AASHTO or ASTM standards
3. The existence of well-established precision and bias statements
4. The distress targeted by the test method and its relevance to Wisconsin conditions
5. The possibility of overlap with other WisDOT and WHRP research projects including efforts to implement AASHTOWare ME, or high Recycled Asphalt Material (RAM) pilot projects
6. Past WHRP, internal WisDOT and other national research projects use of the test
7. The cost and labor intensiveness of each proposed test

Based on these criteria, the research team asked WisDOT Flexible Pavement Technical Oversight Committee (TOC) to evaluate the criteria based on importance in implementation. The criteria were ranked and the literature review was conducted according to the criteria that were deemed most important.

Based on the findings, the test methods listed in Table 1 were selected. The conditions used for each test method are outlined in the respective results section.

Table 1. Selected Performance Test Methods

Performance Property	Test Method	Reference/Standard
Rutting	1. Flow Number 2. Hamburg Wheel Tracking	1. AASHTO TP79 2. AASHTO T324
Moisture Damage	Hamburg Wheel Tracking	AASHTO T324
Stiffness	Dynamic Modulus	AASHTO TP79 with temperatures and frequencies from AASHTO T342
Intermediate Temperature Cracking	1. SCB-LSU 2. SCB-IFIT	1. Draft ASTM 2. AASHTO TP124
Low Temperature Cracking	1. SCB-UMN 2. DCT	1. AASHTO TP105 2. ASTM D7313

Experiment three compared results of linear blending charts (AASHTO M323, X1) with results from an experimental, mortar-based method that does not require extraction of the binder from the RAP and RAS. RAP and RAS binders used in the blending charts were prepared by solvent extraction following AASHTO T164 using toluene and recovered following ASTM D5404. All binder test procedures follow industry standard aging and testing protocol unless otherwise noted. In all cases, aging and testing conditions will be specified. The mortar grading approach follows the procedure outlined in Swiertz and Bahia (2011).

In addition to the performance testing methods listed above, imaging analysis was used to quantify aggregate structure and potentially provide a surrogate measure of performance. Imaging analysis is

completed using the Image Processing and Analysis (iPAS) software partially developed at UW Madison. Details of the software and its use can be found in Roohi et al. (2012).

2.2 Materials

Aggregate

Mix design information for mixtures currently in use in Wisconsin was collected from several contractors throughout the State DOT in order to capture a representative distribution of materials. Three primary coarse aggregate sources were identified from the mix designs, including one dolomite/limestone source and two granite-based sources. Note that the mix designs also include fine aggregates that may not necessarily be from the same source as the coarse aggregate, such as natural sand material. Information for the coarse aggregate sources is included in Table 2 as taken from the 2016 WisDOT Approved Products List. Based on contractors' experience with the aggregate listed in Table 2, it is expected that the selected sources will show a wide range in moisture damage susceptibility and mechanical properties; with Waukesha aggregate rarely requiring the use of anti-stripping additives, Cisler sometimes requiring the use of anti-strip, and Wimmie often requiring anti-strip use based on WisDOT specified Tensile Strength Ratio testing. All coarse aggregates are 100% crushed material (i.e. 100% two-face fracture per ASTM D5821).

Table 2. Aggregate Source Information

Source Name	WisDOT Test No.	Primary Aggregate Type	LA Wear (% Loss at 500 Rev.)	Bulk Specific Gravity	Absorption (%)
Cisler	225 29 2016	Crushed Granite	17.2	2.680	0.41
Waukesha Lime & Stone	225 4 2016	Crushed Limestone	20.5	2.712	1.43
Wimmie	225 43 2016	Crushed Granite	24.3	2.705	0.88

Recycled Materials

The RAP used for all experiments was supplied from a single project to ensure consistency. Sufficient RAP material was gathered at the onset of the project from a source in Northern Wisconsin. RAP materials were screened over a 3/8" sieve to remove large pieces prior to use. RAS materials used in Experiment 3 were supplied from a source in South-Central Wisconsin and are post-consumer waste materials.

Asphalt Binder

Two base asphalt binders were selected for this study based on the PG requirements specified by WisDOT for surface mixtures in the State. A PG 58-28S was selected to represent binders used in the Southern climate zone and a PG 58-34S was selected to represent the binders used in the Northern climate zone. One level of modification was also included for each of the base grades using current Combined State Binder Group specifications to achieve a 'V' grade. Base binder grading information is shown in Table 3. It should be noted that the PG 58-28 V has a much higher $G^*/\sin\delta$ value for the RTFO-aged material at 58 °C, as compared to the other binders. Also, according to the Jnr (non-recoverable creep compliance) value, the 58-28V could qualify as an E grade.

Table 3. Binder Testing Results

Binder Grade	Original Binder		RTFO Binder				Softening Point (°C)
	G*/sin(δ) (kPa) @ 58°C	G*/sin(δ) (kPa) @ 64°C	G*/sin(δ) (kPa) @ 58 °C	G*/sin(δ) (kPa) @ 64 °C	Jnr, 3.2 kPa (kPa ⁻¹) @ 58 °C	%R, 3.2 kPa (%) @ 58 °C	
PG 58-28 S	1.266	0.583	3.401	1.485	3.0	1.2	41.9
PG 58-28 V	1.627	0.873	8.096	4.223	0.42	47.9	51.1
PG 58-34 S	1.418	0.685	3.895	1.822	2.4	3.1	41.0
PG 58-34 V	2.009	1.103	5.027	2.750	0.54	55.2	48.0

Mix Design Information

WisDOT currently specifies three mixture design levels based on the 20 year design ESALs for a given roadway. Low Traffic (LT) designs cover less than two million design ESALs, Medium Traffic (MT) covers from 2-8 Million ESALs, and High Traffic (HT) covers more than eight million ESALs. For this project, the MT and HT design levels were chosen for the initial experimental plan. Select LT mixtures were included in a Hamburg Wheel Tracking test extension plan, as described in later sections. The primary design specification differences between the traffic levels as they pertain to this research are minimum VMA limits, level of compactive effort, coarse aggregate fracture requirements, and fine aggregate angularity, as specified in the WisDOT Standard Specification for Construction, Section 460. Since all of the coarse aggregates used in this study are 100% fractured, this requirement is not a factor studied in this research. A summary of remaining relevant mix design information has been gathered into a database available to WisDOT in electronic format. The summary of mix designs is included in Appendix A of this report.

All designs were first verified using WisDOT production tolerances at their respective design asphalt content, as indicated on the mix design provided by the contractor. If the design was found to pass the required specification, the mixture was considered acceptable and samples were compacted to the air void level required for a given test procedure. If the design failed to meet the specification, adjustments were first made to the asphalt content, then to the job mix formula aggregate ratios to correct the problem. In some cases new designs had to be created, such as the 50% RAP mixtures, an existing design was modified and several asphalt contents were checked to determine the asphalt content that produced a mixture within specification limits. For this reason, although three general levels of RAP binder replacement (15%, 30%, and 50%) were included in the experimental matrix for Experiment 1b, the actual binder replacement was allowed to fluctuate to accommodate the specification. In the statistical analysis for this experiment, the actual RAP binder replacement for a given mixture is always used.

2.3 Experimental Designs

Four primary experiments were designed to achieve the project objectives. Details of each experiment are presented in the following sections.

Experiment 1: Evaluation of Mixtures that meet Specification

Mixtures meeting current WisDOT specification were evaluated at two aging conditions for this experiment. Short term oven aging (STOA) followed AASHTO R30 recommendations for performance samples of four hours loose mix aging at 135 °C. Long term oven aging (LTOA) followed the WisDOT high RAM pilot project recommended procedure of 12 hours loose mix aging at 135 °C. It is important to note that the LTOA procedure used in this study is for comparison against the STOA and does not include

the initial four hour conditioning period (i.e., the LTOA procedure is not the STOA + 12 hours at 135 °C). This information is summarized in Table 4.

Table 4. Aging Conditions Used in this Study

Aging Condition	Procedure	Reference
Short Term Oven Aging (STOA)	4 hours Loose Mix at 135 °C	AASHTO R30, Section 7.2 Short Term Conditioning for Mixture Mechanical Property Testing
Long Term Oven Aging (LTOA)	12 hours Loose Mix at 135 °C	WisDOT High RAM Pilot SPV

Experiment 1 was split into two parts (1a and 1b) to cover testing after short term aging (Experiment 1a) and testing after long-term aging (Experiment 1b) as discussed in the following sections.

Experiment 1a: Evaluation of Short Term Aged Mixtures using E, FN, and HWTT*

The primary pavement distress associated with short-term aged asphalt mixtures is permanent deformation (rutting). Therefore, the test methods selected for this experiment focus on mixture stiffness and resistance to permanent deformation using the Dynamic Modulus (E*), Flow Number (FN), and Hamburg Wheel Tracking Test (HWTT). The RAP content of the mixtures in this experiment was held nominally at 15% binder replacement, which is roughly the average for surface mixtures in Wisconsin. Aggregate type was varied to verify whether expected differences in moisture susceptibility could be detected using the HWTT. The complete factorial used for Experiment 1a is shown in Table 5; all testing includes two replicates.

Table 5. Experiment 1a. Short Term Aged Mixtures (Full Factorial = 24 combinations)

Factor	Level	Level Description	Comment
Aggregate Type	3	Cisler Waukesha Wimmie	Based on common mineralogy in Wisconsin and selected to show spread in moisture resistance
Design Level	2	MT (2-8M ESAL) HT (>8M ESAL)	Evaluate higher level traffic mixtures (most critical)
MSCR Grade	2	S V	MSCR designations in place to improve rutting resistance
Low Temperature PG (Block)	2	-28 -34	WisDOT regional surface LT grades

Estimated Number of Tests for Experiment 1b: 2 replicates x 24 combinations = 48 tests for each test method

Although it was initially planned to conduct FN testing in the un-confined conditions, as recommended for the MEPDG software, review of completed WHP studies (WHP 0092-08-06 and 0092-09-01) clearly indicated that it is better to use the “Confined” testing condition since the confined condition is a better simulation of the asphalt mixture in the pavement layers. The confinement is due to the presence of the mixture surrounding the wheel path where the tire load is applied. With the approval of the Project Oversight Committee (POC), the FN testing started following the Confined condition. However during the initial testing, it was discovered that in the confined condition, it is unlikely to see the

change in creep rate that is required to estimate the FN value. In addition, during execution of the confined FN testing, the AMPT used by the research team was removed from service for repair. After a meeting with the POC, it was decided that the remaining FN samples would be replaced with an extension of the HWTT testing plan. The original experimental plan for the HWTT was designed for testing at 50°C and included only MT and HT mixtures as shown in Table 5. The experimental design for the HWTT extension plan did not include the same factors but focused more on expanding the mixture designs used to LT and also included testing of mixtures with anti-strip additives. The complete design is shown below in Table 8. The eight mixture types most commonly specified in Wisconsin are included in the design with two aggregate sources at two additional test temperatures: 45 °C (for all mixtures) and 40 °C (for a subset of the Wimmie mixtures using PG -34 binder). The RAP content was held constant at 15% nominal binder replacement. In addition, three mixture combinations were tested with liquid anti-strip additive (Wimmie MT-S-28, Wimmie MT-S-34, and Waukesha MT-S-34) to evaluate the effect of anti-strip on the HWTT results. Two replicates were tested for each type of mixture.

Table 6. HWTT Extended Experiment

Traffic Level	LT	MT	HT
Binder Type	58-28S	58-28S	58-28H
	58-34S	58-34S	58-34H
		58-28H	
		58-34H	

Factor	Levels	Description	Comment
Aggregate Source	2	Waukesha Wimmie	Aggregates with the best and worst expected moisture sensitivity
Mix-Binder combinations	8	Shown Above	Mixes most commonly used in Wisconsin

All combinations tested at 45 °C, Wimmie PG XX-34 combinations also tested at 40 °C.

Experiment 1b: Evaluation of Long Term Aged Mixtures using SCB and DCT

Cracking is the primary pavement distress associated with long-term aged asphalt mixtures. Therefore, the test methods selected for this experiment focus on mixture resistance to cracking using the SCB (LSU, IFIT, and UMN procedures) and DCT, and use samples treated for long-term aging. Aggregate source was held constant based on the concept that provided the aggregate quality standards are met, the source most near the project would be used and other mix design factors would be varied to improve cracking resistance. Aging was included as a factor to capture the change in durability with aging and evaluate the ability of the selected tests to measure this change. Conceptually, the presence of increased recycle content has the potential to change the rate at which the mix ages due to the presence of highly aged asphalt and increased blending with time. In this experiment RAP binder replacement was therefore tested at three levels. The complete factorial used for Experiment 1b is shown in Table 7; all testing includes two replicates.

Table 7. Experiment 1b. Long Term Aged Mixtures (Full Factorial = 48 combinations)

Factor	Level	Level Description	Comment
% Binder Replacement	3	15% 30% 50%	Evaluate effects of increased RAP binder on cracking resistance
Design Level	2	MT (2-8M ESAL) HT (>8M ESAL)	Evaluate higher level traffic mixtures (most critical)
MSCR Grade	2	S V	Effect of modification on intermediate and low temperature durability
Low Temperature PG (Block)	2	-28 -34	WisDOT regional surface LT grades
Aging	2	4 hour loose mix @ 275 °F 12 hour loose mix @ 275 °F	Aging expected to negatively impact durability

Estimated Number of Tests for Experiment 1b:

SCB-LSU, SCB-IFIT: 4 samples (3 for SCB-LSU, 1 for SCB-IFIT) x 48 combinations = 192 samples

SCB-UMN: 2 replicates x 48 combinations = 96 tests

DCT: 2 replicates x 48 combinations = 96 tests

Experiment 2: Sensitivity of Selected Performance Tests to Production Variation

The sensitivity of selected performance tests to production variables is important to both practitioners and state agencies. From a state agency perspective, it establishes what a reasonable level of variation in the test output is, given the current production variation tolerances. From a contractor perspective, it provides insight as to what blend or JMF changes are needed to improve a certain performance aspect and avoid failing results. Relative to the cracking tests cited above, the intermediate and low temperature cracking tests are relatively new and therefore precision statements and sensitivity to mix composition has yet to be established. Since work on establishing a precision statement is ongoing through draft AASHTO and ASTM standards for the selected test methods, this research focused on sensitivity to mix composition. Similar to work by Bonaquist on the Flow Number test in WHRP 0092-09-01, the primary factors considered for this experiment include:

- Asphalt binder grade
- Asphalt binder content
- Mix traffic level
- Aggregate angularity

Filler Content and mix traffic level are already varied in Experiments 1a and 1b, and asphalt binder grade is similarly addressed in these experiments. Therefore, asphalt binder content, aggregate angularity (through source), and filler content were varied for this experiment based on the specification tolerance limits when preparing the performance samples. High and medium traffic levels (MT and HT) were included as a blocking factor with PG 58-28S used for MT mixes and PG 58-28V for HT mixes. RAP binder replacement is held constant at 15% nominal for all mixtures. The STOA protocol was also used for all mixtures. The test method selected for this experiment is the SCB-IFIT procedure; the SCB-IFIT test method was found during this research to be comparatively easy to run, less material intensive, and

preliminary analysis of Experiment 1b data showed promising trends in the results for this test. The complete factorial for Experiment 2 is shown in Table 8.

Table 8. Production Variation Experimental Design using SCB-I

Factor	Level	Level Description
Asphalt Binder Content	3	Design AC – 0.3% Design AC Design AC + 0.3%
P200 Content	3	Design – 2% Design Design AC + 2%
Aggregate Source	3	Cisler Waukesha Wimmie
Mix Traffic Level	2	MT HT

Experiment 3: Development of Supplemental Guidelines for Required Performance Testing for High Recycled Content Mixes

It is expected that the binder in RAP and RAS materials will blend to some degree with the virgin binder used during production of the mix. As the proportion of RAP and RAS binder replacement increases, the effect that these materials have on mixture performance is expected to increase. It is therefore desirable to develop a method to predict the effects of RAP and RAS binder on the mixture blended binder properties. Traditionally this is accomplished through the use of blending charts as specified in Appendix X1 of the AASHTO M323. Although the accuracy of linear blending charts has been proven for unmodified binders, RAS binders have been shown to produce strongly non-linear blending characteristics at low temperature in a previous WHRP study (Bonaquist, 2011).

This study compared two methods to estimate blended binder properties in terms of performance grading parameters. The first is following the method presented in WHRP project 0092-10-06, which assumes linear blending for RAP, and linear blending for RAS, at sufficiently small percentages. The second method is a mortar grading procedure developed as part of the Asphalt Research Consortium. The mortar grading procedure is a draft AASHTO standard and was selected because it eliminates the need for use of solvents and is representative of the actual blending that occurs between materials. The draft standard is included in Appendix C of this report. All extractions were performed using toluene as the solvent and binders were recovered from solution with the Rotovapor method. The experimental design for this testing is shown in Table 9.

Table 9. Experiment 3 Design

Factor	Level	Description
Total Percent Binder Replacement	2	15% 50%
Binder Type	2	PG 58-28 PG 58-34
RAP/RAS Ratio*	3	95% RAP, 5% RAS 85% RAP, 15% RAS 70% RAP, 30% RAS

**With total percent binder replacement held constant, the ratio of RAP to RAS binder is changed*

Experiment 4: In-Service Field Validation

This experiment is designed to provide an opportunity for initial validation of the selected performance tests in their ability to correlate with actual field performance. Field cores from three WisDOT high RAM pilot projects as well as cores from control sections associated with these projects are used as the basis for this validation. Four tests were initially selected for this validation experiment, including the SCB (TP-124), DCT, extracted binder testing, and aggregate structure analysis using iPAS. During the execution of the work plan, however, it was discovered that two of the three projects provided 4” cores, which cannot be tested using the SCB or DCT tests, so testing for these sections included only extracted binder analysis and iPAS image analysis. In addition to the cores, the WisDOT performance database was cross-referenced to rank field performance of these sections.

3. Analysis of Results and Summary of Findings

This section includes presentation of the results collected and the main findings drawn from the analysis of the results. The section is organized by experiment and by the mixture testing method used.

3.1 Experiment 1: Evaluation of Mixtures that meet Specification

Experiment 1a included testing of Short Term Oven Aged (STOA) samples and focused on high temperature conditions for rutting resistance and moisture damage. It also included testing complex modulus E^* at four temperatures varying between 4.2 and 54.4 °C. Experiment 1b included testing STOA samples as well as Long-Term Oven Aged (LTOA) samples but focused on testing resistance to cracking at intermediate and low temperatures. The following sections summarize the results and findings.

3.1.1 Experiment 1a- Dynamic Modulus (E^*) Testing

The Dynamic Modulus (E^*) testing is conducted at four temperatures and at five frequencies for each temperature following the experimental design outlined in Table 5. The average results for the two replicates are averaged and plotted as a function of frequency. The trends of E^* versus frequency measured at the five temperatures are shifted along the frequency scale to generate the Master Curve (MC) for each mixture. These MCs are used for pavement response analysis in design software such as the MEPDG (Pavement ME). It is expected that mixture components and volumetric properties affect the E^* MC position and curvature.

Figure 1 includes the MCs fitted for all 24 combinations tested in the study. The plots show that there are some changes in the E^* trends for the various mixtures, but they are relatively small. Since the plots use logarithmic scales it could be difficult to distinguish the differences in values. Therefore, a table of the lowest and highest values measured at each combination of temperature and frequency is prepared to show the range in values measured (not estimated from the MCs) as a percent of the minimum value measured. The data in Table 10 shows the range between the minimum and maximum E^* representing the effect of traffic design level (HT and MT) and the effect of changing the PG grades (S and V for -28 and -34).

Table 10. Minimum and Maximum Values of E^* Measured for the 24 Mixtures Tested

Temperature (°C)	Frequency (Hz)	Minimum E^* , Ksi			Maximum E^* , Ksi			Range as % of Minimum
		Cisler	Waukesha	Wimmie	Cisler	Waukesha	Wimmie	
4.2	0.1	319	417	429	739	827	669	159
4.2	1	465	591	637	1090	1231	943	165
4.2	10	885	1007	1076	1830	1944	1493	120
21.1	0.1	94	128	94	157	201	143	114
21.1	1	169	217	175	293	357	280	112
21.1	10	307	365	341	591	656	542	114
37.2	0.1	37	50	34	56	83	51	126
37.2	1	63	76	58	88	133	86	130
37.2	10	95	128	101	154	213	147	124
54.4	0.1	22	29	27	37	42	41	89
54.4	1	36	35	39	45	61	46	73
54.4	10	54	53	54	77	90	72	68

Values in blue are the minimum values, and in red are the maximum for each row. Also Min and Max Range is shown.

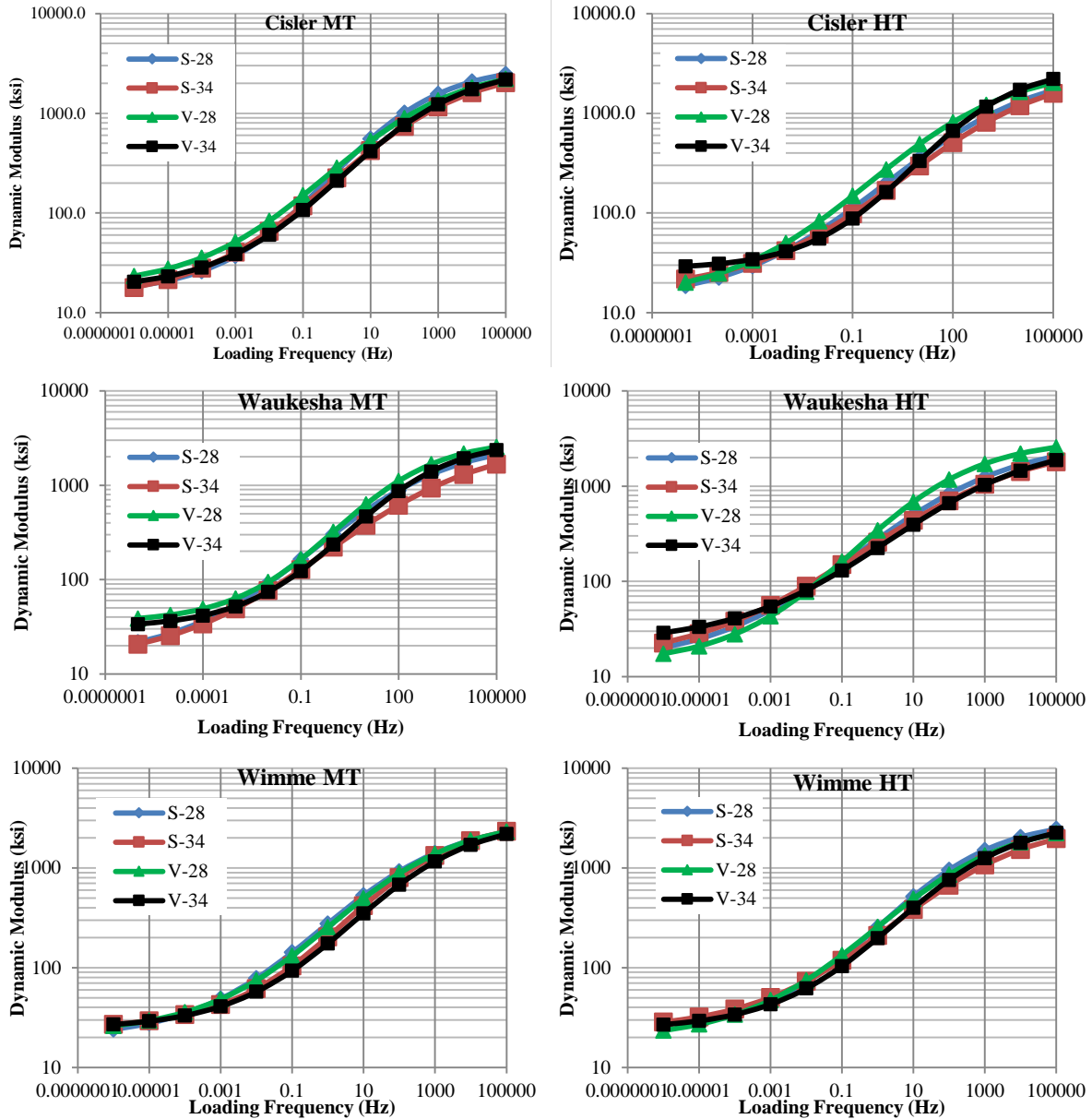


Figure 1. Master Curves of E^* versus frequency at 21.1 C for the 24 mixtures tested

The results show that the source of the aggregates is somewhat important as the Cisler mixtures are showing the minimum values, or close to the minimum in almost all cases. On the other hand, the Waukesha mixtures are showing the maximum values in all cases. The range in values as a percentage of the minimum varies between a low of 68% at the highest test temperature of 54.4 °C, and a high of 165% of the minimum at the lowest temperature of 4.2 °C. These ranges are significant as they are much higher than the experimental error for the measurements. It is clear that the range in E^* increases with lowering the temperature of the test. The values of E^* can be used in the MEPDG software to estimate pavement responses. In most cases, higher moduli values are favorable as they reduce the strains in pavements for a given truck loading, and could provide longer fatigue life due to lower strains. However modulus values by themselves cannot be used to predict distress since fatigue and rutting is affected by crack resistance and

by elastic recovery, respectively. What this data set is showing is that aggregates can play an important role, and the trends in Figure 1 shows that binders can also have an impact for a given mixture. The data can also be used to refine the prediction of the modulus in the MEPDG software using the Hirsch model. A database for all E* testing has been developed and is available to WisDOT in electronic format as part of this final report. Summary of E* values estimated from fitting master curves at the temperature of 21.1°C is Appendix B of this report.

3.1.2 Experiment 1a- Flow Number (FN) and Hamburg Wheel Tracking Testing (HWTT)

At the beginning of this project the Flow Number (FN) test (AASHTO TP79-15) was proposed as the method to measure rutting resistance of mixtures. The test can be conducted with or without confining pressure; however, a previous study by WHRP (WHRP 0092-08-06) determined that the range in unconfined FN values for Wisconsin mixtures at four design traffic levels may be within the experimental error of the test (shown in Table 11). The research team and project oversight committee (POC) agreed that confined FN testing should therefore be conducted for this study.

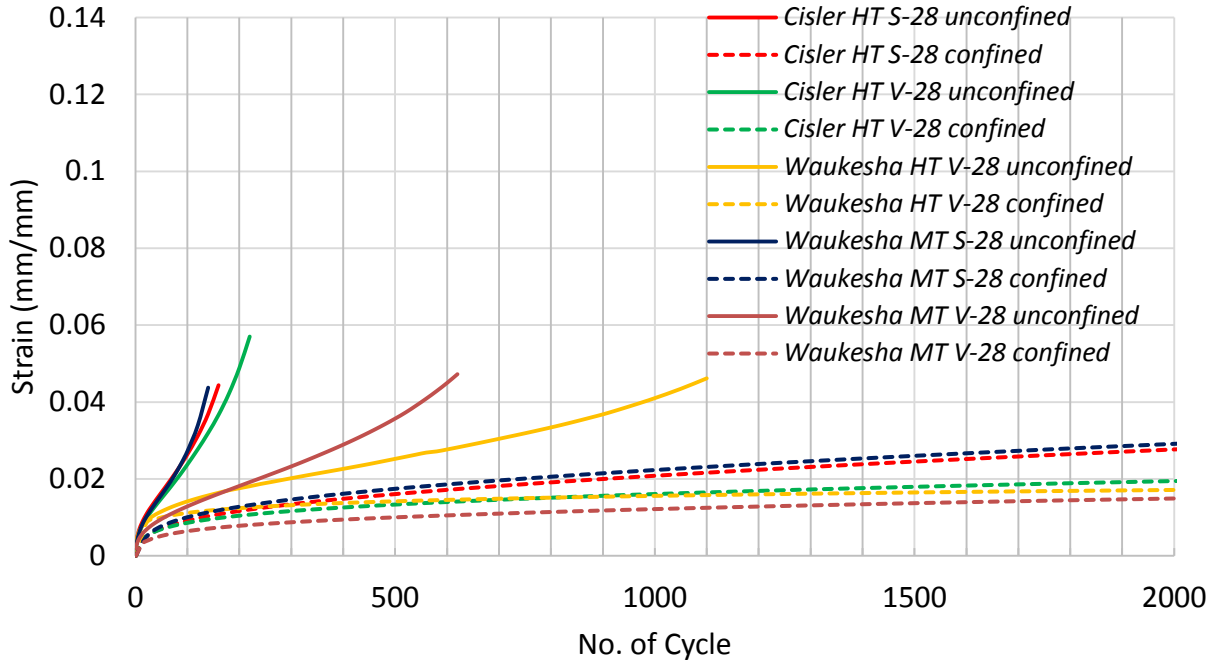
Table 11. Unconfined Flow Number Limits for Wisconsin Mixtures from WHRP 0092-08-06

Traffic Level (Million ESALs)	Minimum Flow Number (Cycles)
3	15
10	50
30	135
100	415

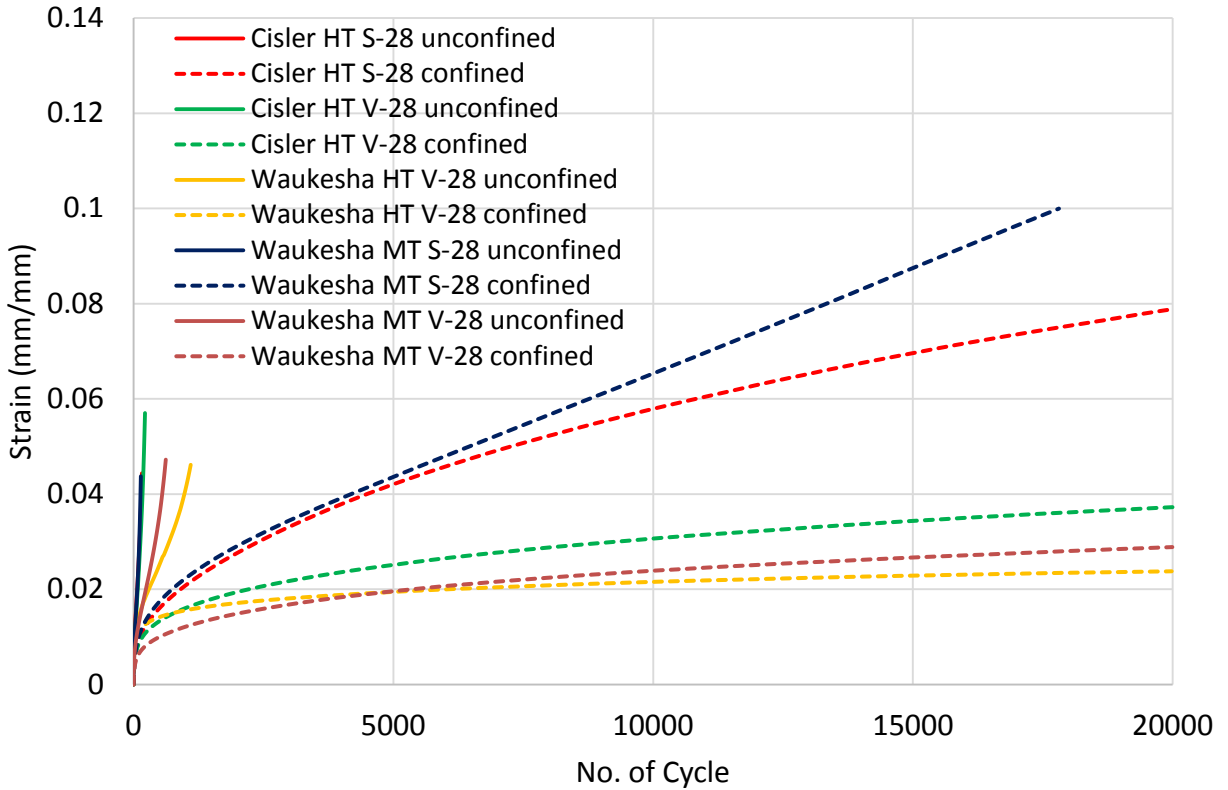
Testing was initiated using the AMPT equipment in the WisDOT Central Laboratory. Figure 2 includes the results of the confined and the unconfined axial flow number testing for five of the mixtures produced in this project. As expected, the unconfined testing results in very low number of cycles to tertiary failure ranging between less than 100 cycles to approximately 800 cycles. The results of confined testing, on the other hand, show that no tertiary behavior could be identified, and thus they cannot be used to measure a FN value.

However, the ranking of these five mixtures in terms of accumulated strain does not change due to the confinement. As shown in Figure 2, the mixtures with the least resistance to rutting in the unconfined condition are the Waukesha MT-S-28 and the Cisler HT-S-28; the same mixtures also show the highest rate of secondary creep in the confined condition. The best mixtures in rutting resistance are the Waukesha HT-V-28 followed by the Waukesha MT-V-28 for the unconfined, and for the confined conditions these two mixtures gave almost identical resistance to rutting.

FN testing was stopped part way through the project due to mechanical problems with the AMPT equipment which could not be fixed in a reasonable time frame. The research team met with the POC and proposed focusing on the Hamburg test as the potential method for measuring rutting resistance. To support the use of the HWT in place of the FN test, a limited sub-study comparing results of the HWT and confined FN test was conducted to verify that both tests are capturing the permanent deformation resistance of the mixtures. A summary of this sub-study is presented in the following sections.



(a) Close up plot of the Unconfined FN results (maximum scale 2000 cycles)



(b) Larger scale of 20,000 cycles showing no Tertiary creep for the confined samples

Figure 2. Results of Confined and Unconfined FN Testing

3.1.2.1 Comparison of confined FN testing and HWTT

A limited study was done to verify if the mechanism of rutting measured in the HWTT is the same as the confined FN test and if the HWTT can be used as a surrogate for the FN test. Since the HWTT is conducted in the wet condition (samples are submerged in water), it was necessary to isolate the possible moisture damage effect by conducting the HWTT in dry conditions. Strain accumulation in the flow number test and estimated strain in HWTT can be compared to verify that the mechanisms of rutting are similar and equivalent in both tests.

Figure 3 shows the correlations of strains at equivalent cycles between in the dry HWTT and the confined FN to the tertiary point of the dry HWT test for four mixes. These correlations show an excellent linear relationship with R^2 in range of 0.97-0.99. However, as shown by the correlation lines, the slopes and intercepts of relationships vary among mixes; therefore, the specifications limits for dry HWTT need to be verified and selected independent of the limits used currently for FN.

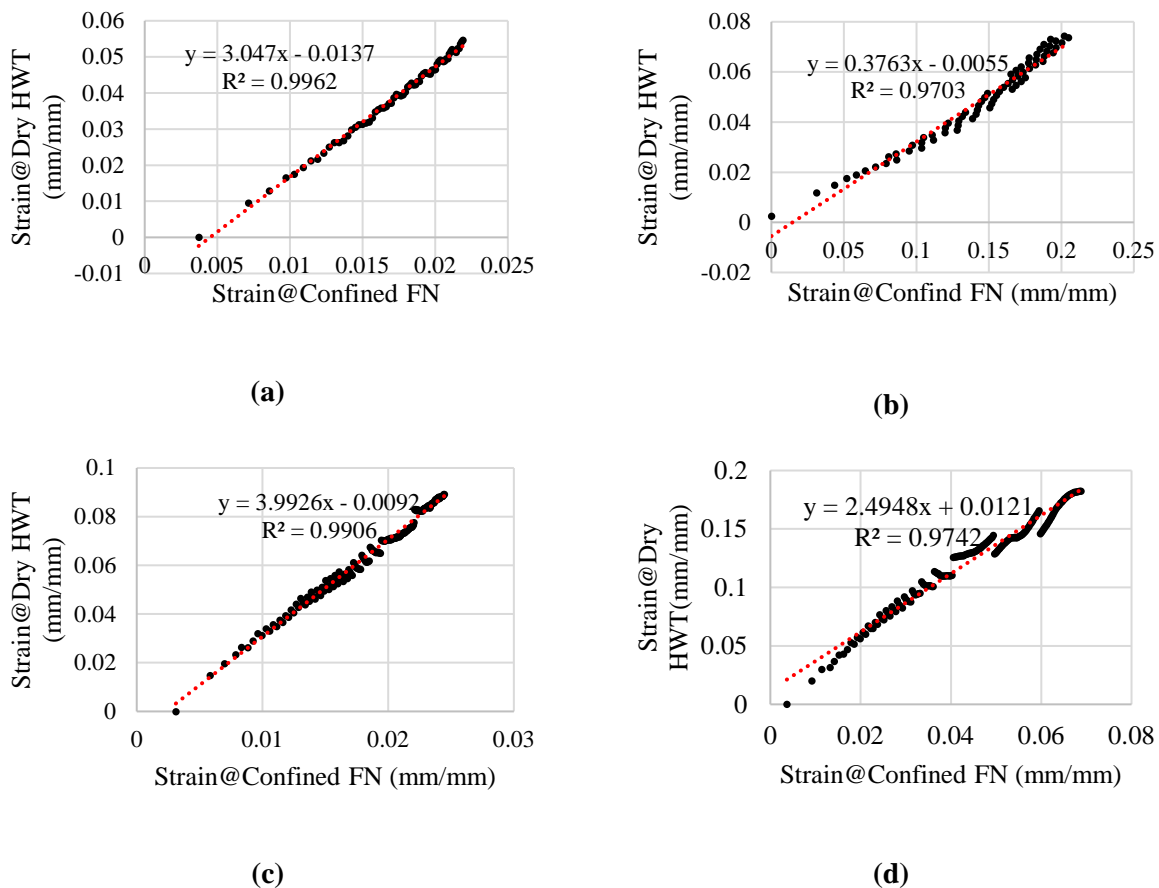


Figure 3. Correlation of strain of dry HWT and confined FN to tertiary point of HWTT test for four mixtures commonly used in WI. Mixtures were produced with different aggregates and binder grades.

The Power Law model is widely used in many pavement design methods including the AASHTO Pavement ME software. The model does not recognize the tertiary zone in the rutting mechanism and assumes that the main stages of rutting are the initial consolidation of the mixture and the secondary creep.

The concept behind this model is that the tertiary stage represents the ultimate failure and thus need not to be modeled.

As shown in Figure 4, the Power Law model can be fitted such that a slope is determined from the power factor (b) in the equation of $\epsilon_p = a(N)^b$, where ϵ_p stands for the permanent strain and N stands for the number of cycles. The logarithmic creep slopes (values of “b” power factor) of confined FN test and dry HWTT can be determined and compared to evaluate if using the two tests can give the same information.

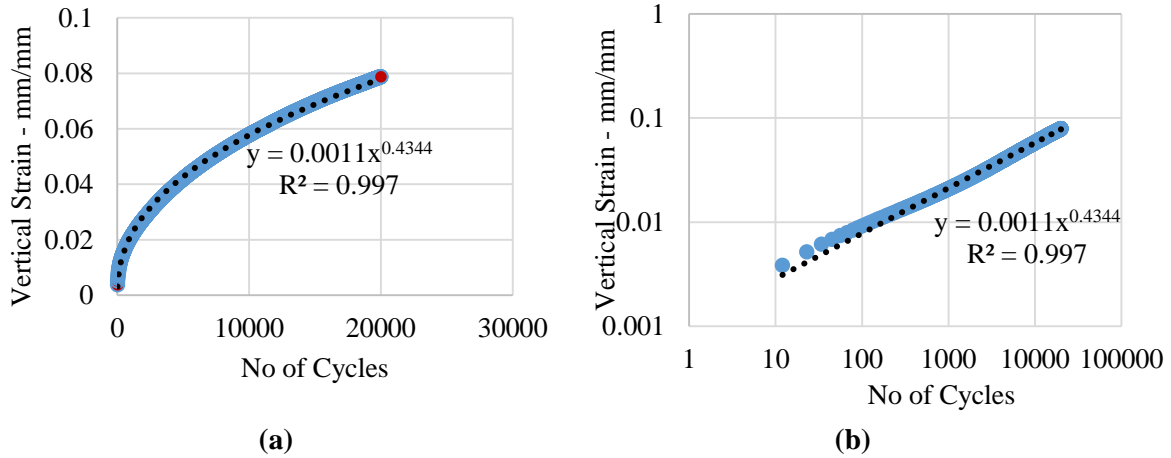


Figure 4. Power Law Fit for HWTT results, (a) normal scale, and (b) log-log scale

The relationship of the slope values of confined FN and dry HWTT by Power Law are shown in Figure 5, which illustrates that there is no equality between the two tests but there is a very strong linear relationship.

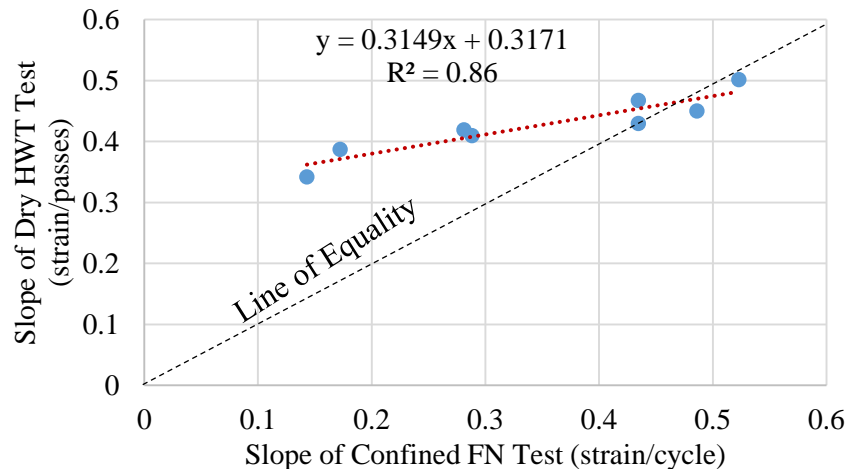


Figure 5. Correlation of slope between dry HWTT and confined FN by the Power Law Method.

The results show that the creep slope estimated from the dry HWTT show a positive and rational relationship with those of confined FN. Most of the HT mixes, which requires more angular aggregates, are

significantly above the line of equality. These results are logical since the contact stress of confined FN (87 psi) is lower than that of dry HWTT (estimated at approximately 105 psi). This is also in agreement with previous research from Quintus et. al (2012) in which it is shown that higher stress results in higher permanent strain slope. For the confined FN at 10 psi confining pressure, it can be shown that the prediction model takes the form shown in Equation 1.

$$Y = 0.3149X + 0.3171, R^2 = 0.8559$$

Where: Y= Slope at Dry HWT (strain/passes)

X= Slope at Confined FN (strain/cycles)

Equation 1

The results are also considered logical since the HWTT samples are considered to have lower confinement than the FN test since they are only confined by the mixture sample itself rather than by applying an actual confining pressure. In other words the confinement in the FN test can be considered much more than the HWT and thus it is logical to expect higher creep rate in the HWTT as compared the FN test.

To verify the effect of confinement on the relationship between dry HWTT and FN, unconfined FN testing was conducted for the same mixes. Five mixes with significantly different creep slope values were selected to evaluate the unconfined FN test relationship to HWTT. The remaining test conditions in the unconfined FN were kept the same as the confined FN test (same test temperature and deviator stress), but without the confining pressure. The results are plotted with the confined FN results as shown in Figure 6.

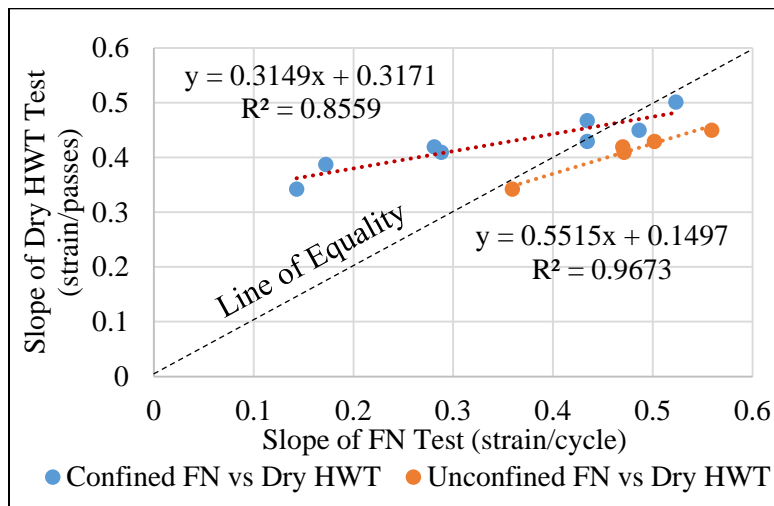


Figure 6. Correlation of creep slopes of dry HWT and slopes of confined and unconfined FN test by the Power Law Method.

Results indicate that the creep slopes of unconfined FN testing for all mixtures are significantly higher than the confined FN slopes, and are under the line of equality with the dry HWTT slopes. These results are also logical since the confining pressure of 10 psi is expected to reduce the rutting rate (lower value of the slope) as compared to the unconfined test. Also, since the HWTT provides some confinement

by the sample on sides of the wheel, the unconfined FN slopes should be higher and thus under the equality line with HWTT results. These results are also in agreement with the previous study from Quintus et.al (2012) in which lower confining pressure resulted in higher creep slope for the FN testing. Figure 6 also shows that there is a significant linear relationship between dry HWTT and unconfined FN, and a simple linear relationship as shown in Equation 2 can be used.

$$Y = 0.5515X + 0.1497, R^2 = 0.9673$$

Where: Y= Slope at Dry HWT (strain/passes)
X= Slope at Unconfined FN (strain/cycles)

Equation 2

The results of the dry HWT show that the rutting mechanism in the HWTT can be considered similar to the FN test. However, due to the difference in the confinement level in the HWTT as compared to the FN, the creep slope values are not equivalent. The other main difference between the two tests is the conditioning of the sample. In the HWT samples are conditioned by submersion in water while all FN testing is conducted in a dry chamber. To investigate the possible effects of water conditioning, the HWT was also conducted using water conditioning and the dry and wet results are compared. Figure 7 shows an example of rut depth in dry and wet HWT for a single mix design.

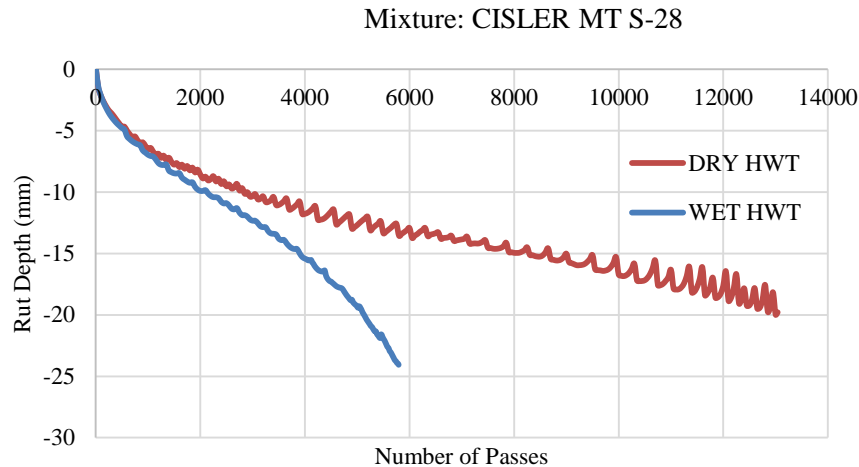


Figure 7. Comparison of rut depth in dry and wet HWT.

To verify the effect of the moisture conditioning in the wet HWT on the creep rate as modeled by the power law, the tertiary stage data was truncated and the model was fit to determine the power function (slope of the log-log plot). This was done to avoid any confounding effects of moisture damage. The results for the wet and dry HWT before the SIP and tertiary points are listed in Table 12. The creep slopes in wet and dry conditions are used to calculate the moisture slope sensitivity, shown in Equation 3. The sensitivity to wet conditioning ranges from 2% to 15% of the wet slope. All mixtures show relatively low values of sensitivity that can be considered to be within the experimental error of the HWT results.

$$Sensitivity = \frac{(Wet\ Creep\ Slope - Dry\ Creep\ Slope)}{Wet\ Creep\ Slope} * 100$$

Equation 3

Table 12. Creep Slope of Eight Mixtures using Wet and Dry HWT.

Mixture Type	Wet	COV.	Dry	COV.	Sensitivity
Cisler MT S-28	0.51	1%	0.50	2%	2%
Cisler HT V-28	0.37	10%	0.35	4%	4%
Cisler HT S-28	0.47	3%	0.42	0%	9%
Cisler MT V-28	0.42	8%	0.38	2%	10%
Waukesha HT S-28	0.45	2%	0.39	8%	15%
Waukesha HT V-28	0.37	5%	0.36	6%	2%
Waukesha MT S-28	0.47	8%	0.45	4%	4%
Waukesha MT V-28	0.37	10%	0.33	1%	10%

The results indicate that the sensitivity to moisture is relatively small (less than 15%), and that the wet creep slope is always higher than the dry creep slope. These observations indicate that the creep rates in wet HWT are only marginally affected by moisture damage, and that the wet creep slopes are more conservative than the dry in terms of measuring rutting resistance. These findings are logical since moisture damage is unlikely to happen in the first few hours in HWT testing. Creep slope relates to rutting primarily due to plastic flow (Aschenbrener, 1995). Also, the ranking of creep slope for wet and dry HWT are the same. The rankings show that the V-28 mixtures are more resistant to permanent deformation than S-28 mixtures, and the HT mixtures show lower slopes than the MT mixtures in almost all cases.

3.1.2.2 HWTT Results and Analysis

All mixtures for this experiment were tested in accordance with AASHTO T324-16, which does not specify a testing temperature directly, but states that selection of test temperature should be based on local specification. For the present study, testing temperature was initially selected as 50 °C based on testing completed for the WisDOT high RAM pilot project.

The final project report for NCHRP Project 20-07/Task 361: “Hamburg Wheel-Track Test Equipment Requirements and Improvements to AASHTO T 324” released during this study details the findings of a nationwide survey on testing requirements for AASHTO T324. Based on the findings of the survey, State agencies are specifying test temperatures in several ways. Some agencies are using a single temperature exclusively for all of their testing (Texas, for example, uses 50 °C for testing all mixtures). Some agencies are specifying temperature based on the base PG of the mixture (Colorado, for example, specifies that a PG 58 is tested at 45 °C, while a PG 64 is tested at 50 °C). Figure 8 shows the testing temperature used by states that currently use the HWT to characterize mixtures based on information reported by the NCHRP Project 20-07/Task 361 report.

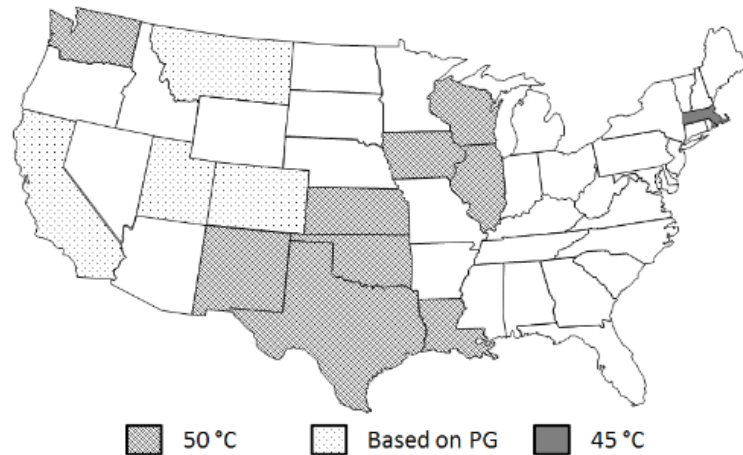


Figure 8. HWT temperature based on NCHRP Project 20-07/Task 361

All HWTT data was analyzed using an Excel based spreadsheet following the analysis method proposed by the Iowa DOT. The analysis method involves fitting a sixth degree polynomial to the wheel passes vs. deflection curve, and inserting a tangent line at the location where the first derivative of the polynomial is at a minimum near the end of the test; the slope of this tangent is referred to as the stripping slope. A tangent line is also inserted at a point where the second derivative of the polynomial is zero prior to the stripping initiation point; the slope of this tangent is the creep slope. This method is shown graphically in Figure 9.

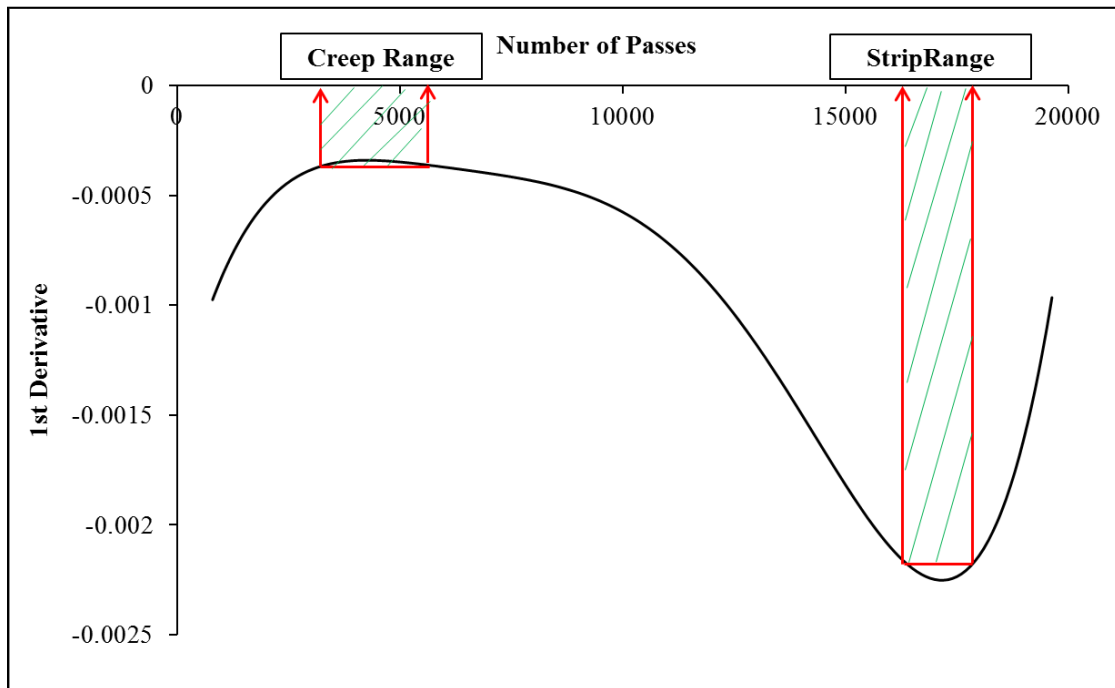


Figure 9. Defining the creep slope and the strip slope from the first derivative of the 6-order polynomial fit of the HWT test results.

The ratio of the stripping slope to the creep slope can be used to quantitatively determine whether stripping is occurring and if a Stripping Inflection point (SIP) can be calculated. WisDOT specifies that a stripping slope to creep slope ration must be greater than 2.0 in order to calculate a SIP; this ratio was found to be greater than 2.0 in all mixture combinations used in this study. The number of passes that corresponds to the intersection of the two tangent lines is referred to as the SIP.

The WisDOT high-RAM special provision provides tentative limits on number of passes to 12.5 mm (0.5 inches) rut depth, as well as SIP based on the original grade of the binder used in the mixture. This specification is shown in Table 13; note that the minimum SIP limits are the same as number of passes to 12.5 mm. Approximate M332 equivalent grades are shown in red since at the time of this report WisDOT is transitioning away from the M320 system in favor of M332.

Table 13. WisDOT High-RAM Specification for HWT

Asphalt Binder Grade	Number of Passes	Maximum Rut Depth (inches)
PG 76-XX (PG 58E)	20,000	0.50
PG 70-XX (PG 58V)	15,000	0.50
PG 64-XX (PG 58H)	10,000	0.50
PG 58-XX (PG 58S)	5,000	0.50

3.1.2.2.1 HWTT Results at 50 °C

Figure 10 shows an example of the results for the Cisler MT mix produced with three binders (S-28, V-28 and V-34). Results show that the HWTT is generally repeatable and that there a significant effect of binder grade for the high temperature (S versus V). There is also an effect of the low temperature grade (-28 vs -34) that can be observed. The mixture with the V-28 grade shows much better resistance to rutting than the mixture with the V-34 grade. It should be noted however that The V-28 binder had a slightly lower Jnr value and a much higher G*/sinδ value than the V-34 binder (see Table 3).

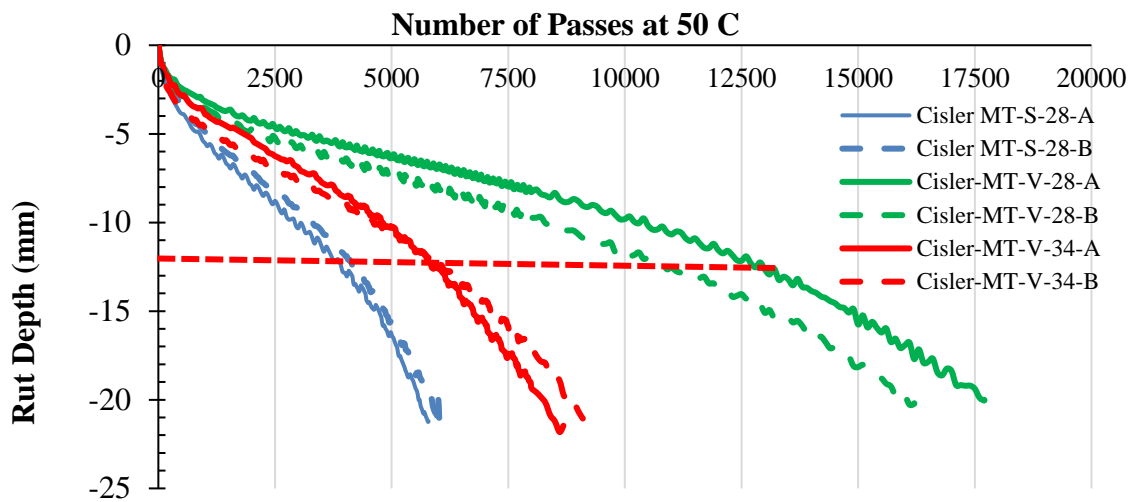


Figure 10. Example of HWT results at 50 °C for Cisler MT mixtures. (dashed red lines represent specification limits)

Figure 11 shows the strip to creep slope ratios for all mixtures tested at 50 °C. It is clear that all mixtures show a ratio of slopes greater than 2.0 and thus the SIP should be checked based on the requirements listed in the proposed WisDOT criteria. Based on this criteria, it is generally assumed that if the ratio is higher than 2.0, the mixture has the potential for moisture damage. Aggregate sources in this study were selected based on their history of moisture susceptibility (i.e. the range in strip to creep slope ratios is expected to be high, with some mixtures below 2.0 and some above 2.0). Clearly this was not observed during this study. It was also expected that the Wimmie aggregates show more moisture damage potential than the other aggregates, however the data shows the Wimmie in many cases has a lower ratio, which is also a contradiction with the experience with these aggregates' sources.

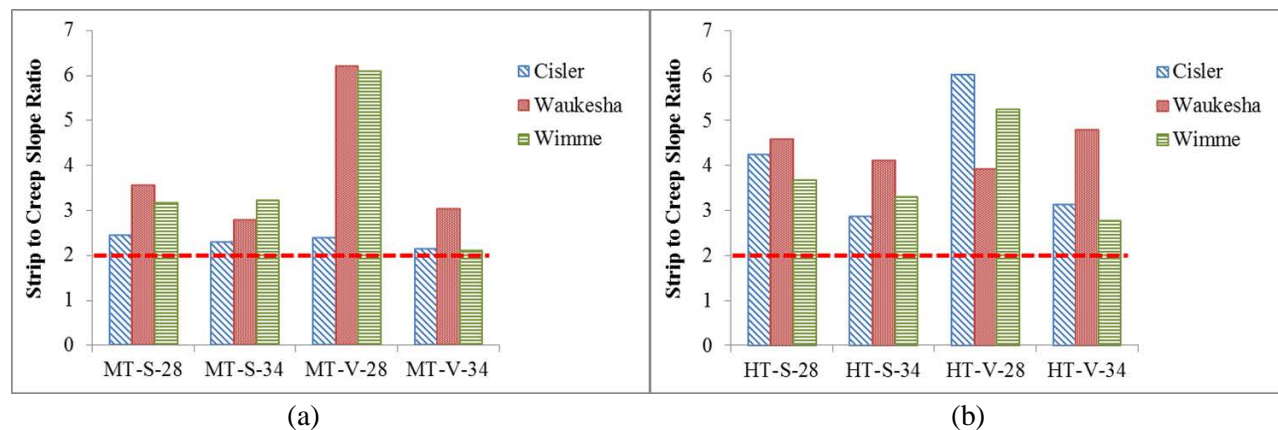


Figure 11. Ratio of strip slope to creep slope for the 24 mixtures tested in this study. (a) MT mixes, and (b) HT mixes (dashed red lines represent specification limits)

The results for the SIP passes and the passes to 12.5 mm rut depth are shown in Figure 12. Several noteworthy observations can be made directly from Figure 12. All mixture combinations, V-28 notwithstanding, appear to perform similarly in terms of number of passes to 12.5 mm and SIP, possibly indicating the HWT at 50 °C cannot differentiate between the mixtures used in this study. The results also show that the SIP and 12.5 mm passes are similar in most cases and thus could be considered redundant.

Interestingly, the majority of mixtures fail the existing HWT specification despite of observational evidence in the field suggesting these mixtures are performing adequately in rutting and moisture damage resistance. Based on Figure 12, all MT mixtures fail the existing specification, and 16 of 32 HT mixtures fail either passes to 12.5 mm, SIP, or both. The effect of modification on the -34 base grades also does not appear to have a significant effect on the response parameters of interest, whereas similar modification of -28 base grades produces a pronounced effect on both parameters. Since both V binders are modified to meet the same specification, this is not an expected result.

To determine the sensitivity of the HWT at 50 °C to the mix design variables controlled during this experiment, an analysis of variance (ANOVA) was used at the 95% level of significance and blocking for low temperature binder grade. Findings suggest that aggregate source ($p=0.02$), mix design level ($p=9.7 \times 10^{-6}$), and binder modification ($p=<2.2 \times 10^{-16}$) all significantly affect the number of passes to 12.5mm. The SIP ANOVA resulted in similar results with p -values of 0.0005, 0.02, and 5.92×10^{-16} for aggregate source, mix design level, and binder modification, respectively. Both analyses show that binder modification is the most significant factor affecting the response variables selected. Since all three aggregate sources represent

quarried, 100% fractured materials, one might expect the aggregate source to be less significant, particularly for number of passes to 12.5mm.

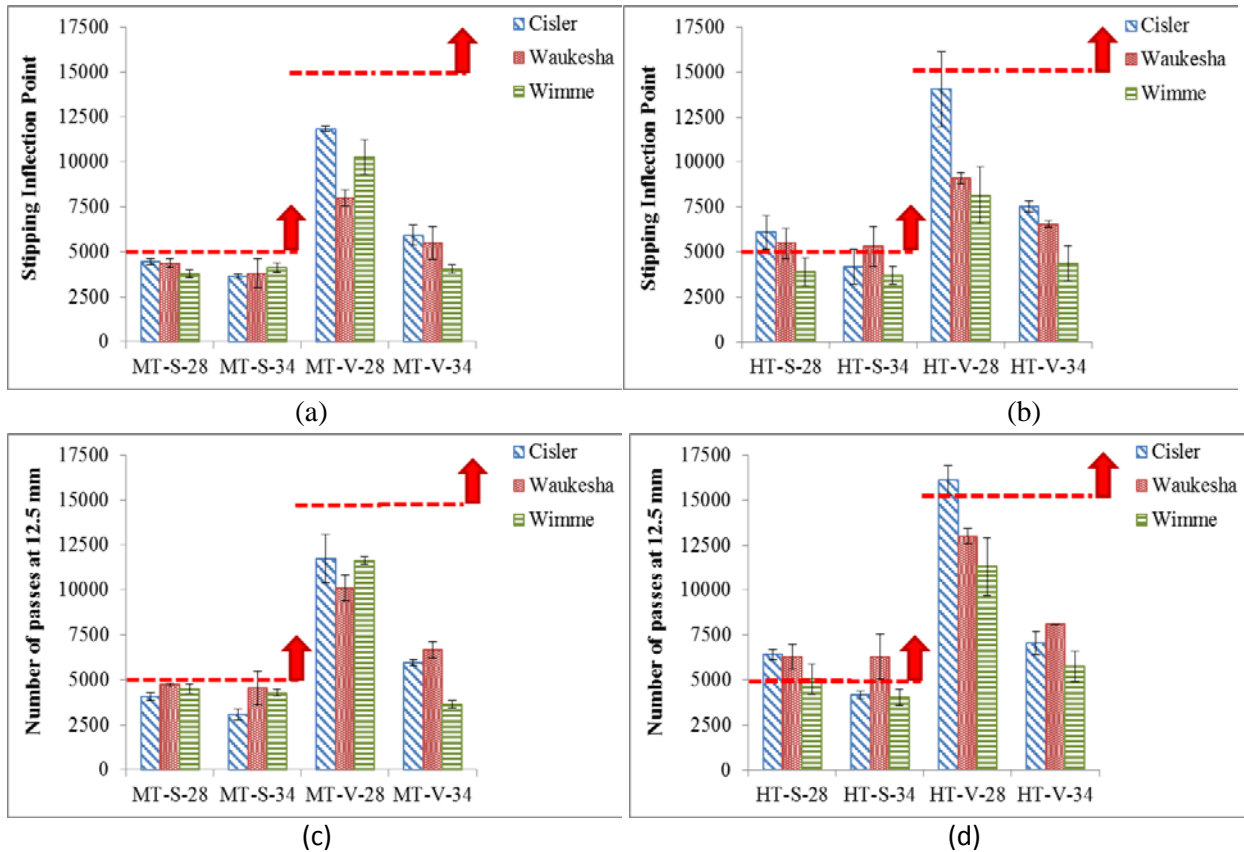


Figure 12. SIP Passes and Passes to 12.5 mm rut depth for the 24 mixtures tested in this study. (a) SIP - MT mixes, (b) SIP- HT mixes, (c) 12.5 mm passes MT mixes, and (d) 12.5 mm passes HT Mixes. (dashed red lines represent specification limits)

Best-subsets regression was used to determine the relative sensitivity of the aggregate, mix design and binder property factors that control the number of passes to 12.5 mm and SIP. A summary table for passes to 12.5 mm is shown below in Figure 13. In initial analysis iterations, binder Jnr at 3.2 kPa was used as the primary binder property; however, the binder testing data shown in Table 3 shows that although Jnr values for the S and V binders are similar among the low temperature grades, the $G^*/\sin(\delta)$ parameters are significantly different, particularly for the V-28 and V-34. Observing Figure 12, it appears the V-34 performs similarly to the S-28 and S-34, prompting the use of $G^*/\sin(\delta)$ in the final analysis iteration. The analysis clearly indicates that binder stiffness, as quantified with the $G^*/\sin(\delta)$ rutting parameter at 58 °C, dominates the mixture behavior in the HWT at 50 °C with an explained variance in the data of 81.6% (R^2_{ADJ}) using $G^*/\sin(\delta)$ as the predictor alone. Using model that selects binder and mix design properties together as an example (highlighted in Figure 13), the explained variance increases only marginally. Nevertheless, a regression equation was generated for the selected model to determine whether the predicted trends matched expected outcomes.

The regression equation for number of passes to 12.5 mm includes two binder properties and two mix design properties. The model shows that for an increase in $G^*/\sin(\delta)$ and Phase Angle (denoted as PA), the number of passes to 12.5 mm increases and decreases, respectively. This is expected, since stiffer binder

should strain less for a given stress, and more elastic (lower phase angle) binders should recover strain. The two mix design factors selected by the model, total AC and added AC do not appear to show consistent trends, although one might expect that as total AC is increased, the mixture becomes less stiff since binder controls a greater proportion of mixture behavior.

A significant finding highlighted in Figure 13 is that aggregate properties do not appreciably affect the performance (as measured by passes to 12.5 mm) of the mixtures in the HWT at 50 °C. Given the differences in aggregate physical properties noted among the mix designs, this finding is unexpected and may suggest that the testing temperature is causing the binder properties to dominate. Note that the softening points for all binders tested in this study aside from S-28 were below 50 °C. Regression analysis findings for SIP, creep slope, and stripping slope at 50 C all generally agree with the observation that binder properties alone appear to dominate performance in the HWT at 50 °C for these mixtures.

Statistical Indicators of model						Variables included in the model								
Vars	R-Sq	R-Sq (adj)	R-Sq (pred)	Mallows Cp	S	LAS Abrasion	% Natural sand	Binder LT	G*/sin d	PA	Total AC	Added AC	P8	P200
1	82	81.6	79.9	41.5	1516.5				X					
1	30.5	29	24.6	286.2	2980.7					X				
2	86.5	85.9	84.4	22	1327.3				X				X	
2	84.3	83.6	81.8	32.6	1432.1				X		X			
3	88.6	87.9	85.9	14	1232.5				X		X	X		
3	87.8	87	85.2	18	1277.1				X				X	X
4	89.8	88.9	86.9	10.3	1179.1				X	X	X	X		
4	89.4	88.4	86.3	12.6	1207	X			X		X	X		
5	90.5	89.4	87.4	9	1151.4	X			X	X	X	X		
5	90.4	89.2	86.9	9.8	1162.1				X	X	X	X		X
6	91.2	89.9	87.5	8	1126.6	X			X	X	X	X	X	
6	91	89.7	87.7	8.6	1134.2	X		X	X	X	X	X		
7	91.7	90.2	88	7.5	1106.1	X		X	X	X	X	X		X
7	91.6	90.2	87.9	7.7	1108.2			X	X	X	X	X	X	X
8	92	90.4	87.9	8	1098.6	X	X	X	X	X	X	X	X	
8	91.9	90.2	87.7	8.7	1108.6	X	X	X	X	X	X	X		X
9	92	90.1	87.6	10	1112.5	X	X	X	X	X	X	X	X	X

Best Model

Number of passes at 12.5 mm = 11314 + 1420.8 G*/sind - 52.9 PA - 4223 Total AC+ 3426 Added AC

Term	Coef	Coef	T-Value	P-Value	VIF
Constant	11314	5879	1.92	0.061	
G*/sind	1420.8	95	14.95	0	1.34
PA	-52.9	23.5	-2.25	0.029	1.34
Total AC	-4223	995	-4.24	0	1.11
Added AC	3426	793	4.32	0	1.11

Figure 13. Best-subsets regression for passes to 12.5 mm at 50 °C.

The outcome of the regression analysis indicates that the binder properties dominate most of the behavior measured at 50 °C, while the mixture properties and aggregates show only minor influence on the main responses of the Hamburg. These results prompted the need to review what temperatures are used by other states and whether using lower temperatures could make the results of the HWT more reasonable in relating to mixture factors other than binder grade and to give reasonable passing level for many mixtures that have been used successfully in Wisconsin. Considering all of the results collected at 50 °C, the following list includes the disadvantages of using this temperature identified by the research team:

- Influence of binder properties on mixture response is too high at 50 °C.
- Most mixtures fail typical criteria proposed in Wisconsin (5,000, 10,000, 15,000, and 20,000 passes); establishing new lower limits for mixtures with a proven history of performance could be difficult due to the inherent variability of the test.
- Illogical correlations between passes to 12.5 mm and the design level of mixtures (HT versus MT) were noted.
- Several mixtures are within one standard deviation of each other, which makes the use of the results to differentiate between mixtures very difficult.

Based on initial findings at 50 °C for this study and the results of the NCHRP 20-07 survey above, an extended HWTT experiment was designed to test a subset of mixtures at 45 °C and 40 °C. Mixtures with varying expected degrees of moisture damage potential and permanent deformation resistance were selected for testing at 45 °C. The aggregate source with the highest expected degree of moisture susceptibility (Wimmie) was also selected for testing at 40 °C. The subset of mixtures tested at reduced temperatures is listed in Table 8 and is shown again in Table 14.

Table 14. Reduced Test Temperature Subset

Traffic Level	LT	MT	HT
Binder Type	58-28S	58-28S	58-28V
	58-34S	58-34S	58-34V
		58-28V	
		58-34V	
Aggregate type	Waukesha and Wimmie		
Tested at 45 C	Yes	Yes	Yes
Tested at 40 C	Only Wimmie with PG 58-34S or V		

3.1.2.2.2 HWT Results at 40 °C

Data for the selected mixture combinations tested at the 40 °C test temperature is shown in Table 15. Two of the mixtures did not exhibit a stripping inflection point and only one mixture exhibited 12.5 mm deformation after the maximum limit of cycles for the machine (20,000 cycles). Only a creep slope could be calculated for this test temperature for the mixtures that did not exhibit an inflection point. This finding suggests practically that if the HWT is to be used to evaluate number of passes to 12.5 mm and more importantly SIP, testing at 40 °C is too low for the mixtures used in this study.

Table 15. HWT results for testing at 40 C

Aggregate	Traffic Level	Binder	Temp.	Passes to 12.5 mm	Creep Slope (*1000) mm/pass	SIP passes
Wimmie	LT	S-34	40 °C	10650	-0.812	11845
	MT	S-34		>20000	-0.281	15399
	MT	V-34		>20000	-0.144	>20000
	HT	V-34		>20000	-0.204	>20000

The results also show that the HT mixture gives a higher creep rate than the MT mixture of the same source, which is contradictory to the experience and the logic of HT design versus MT designs. However the results give logical trends with the change from LT to MT and also for changing the binders from S grade to V grade since MT shows lower creep rate and more cycles than LT, and mixtures with V grades show lower creep rate than S grades. The data set is very limited and thus cannot be used to decide if this temperature should be recommended for testing. Although the data set is limited, it is clear that the limit of 5,000 cycles for S grade binders can be easily met by the LT mix, which is of a concern since these mixtures are expected to be weakest of all. This could imply that all mixtures could pass the current proposed criteria if 40 °C is used as the test temperature. This is completely the opposite of the findings at 50 °C testing, in which almost all mixtures failed the same criteria.

3.1.2.2.3 HWT Results at 45 °C

Testing at 45 °C included more combinations of aggregates and binders. As shown in Figure 14, Wimmie and Waukesha aggregates were used and LT, MT, and HT designs were tested for S-28 and S-34 grades. Using the limits of 5,000 passes for S-xx binder grades and 15,000 passes for V-xx grades, it is found that only one mixture with S-xx grade will fail, while only three mixtures of the V-xx grade will fail the cycles to 12.5 mm specification but will pass the SIP limits. Also, there is a logical trend in passes to limits for the MT versus the HT designs, but the trend for changing from LT to MT is not consistent for both aggregate sources; for the Waukesha aggregates, the MT mixes are failing at lower passes than the LT.

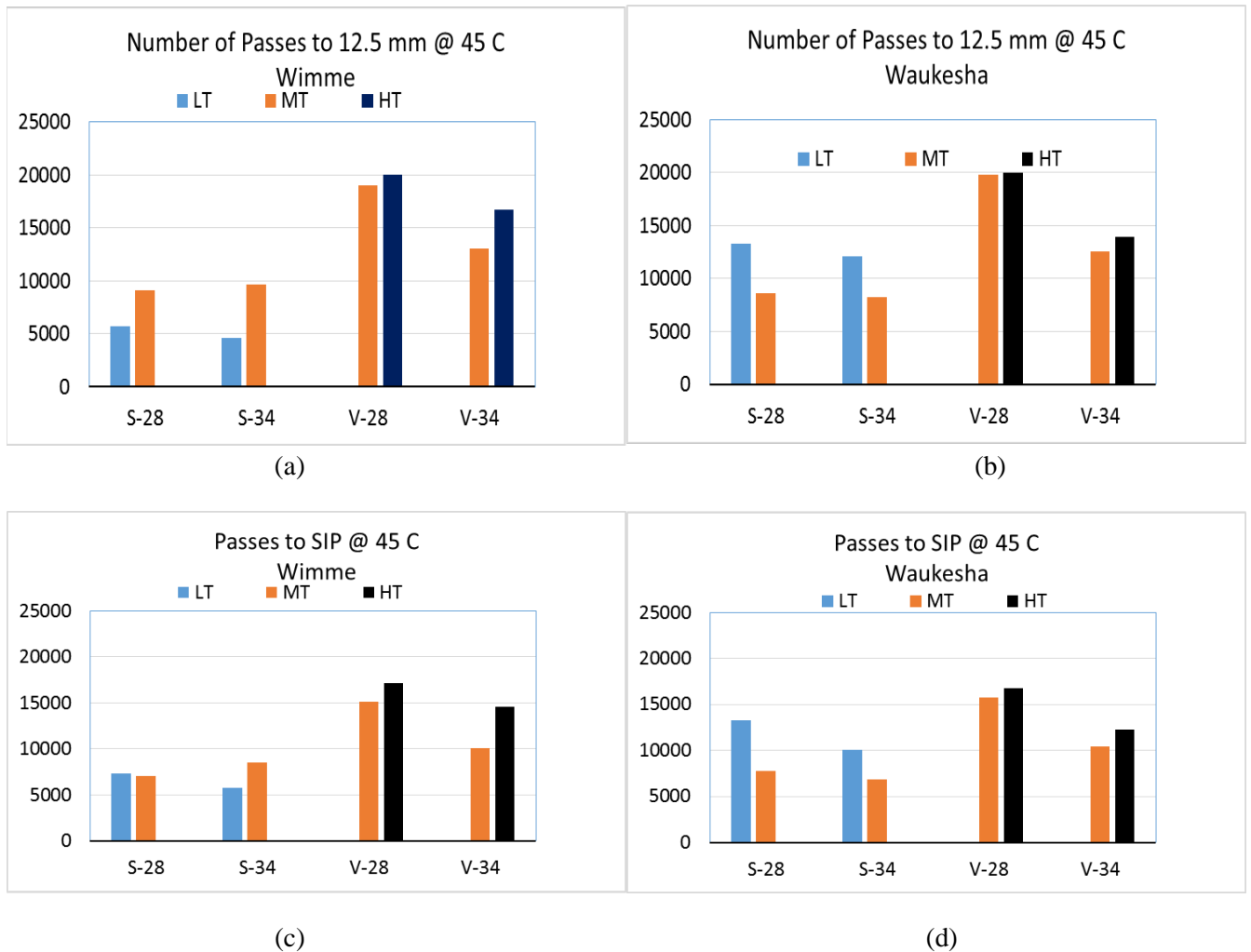


Figure 14. HWT results at 45 °C for the Wimme and for the Waukesha aggregates. (a) Passes to 12.5 mm for Wimme aggregates, (b) Passes to 12.5 mm for Waukesha aggregates, (c) SIP for Wimme aggregates, (d) SIP for Waukesha aggregates

It should be mentioned that all mixtures when analyzed with the IOWA DOT procedure to estimate the creep and strip slopes, showed a ratio more than 2.0 for the strip to creep slope, with the exception of one mix (Wimme S-28). The ratio of this mix was 1.89, which is very close to 2.0.

A statistical analysis was conducted at 45 °C in a similar fashion to the analysis conducted at 50 °C to find which binder or mixture parameters can best explain the changes in HWT results. Using the same responses (Passes to 12.5 mm, SIP and creep rate) as at 50 °C, the results of the stepwise regression are shown in Figure 15 through 17. In Figure 15 it is shown that passes to 12.5 mm rut depth can be predicted very well using the aggregate sources as represented by the LA Abrasion, the Fine Aggregate Angularity (FAA) value, the binder Jnr and $G^*/\sin\delta$, and the Percent of Effective binder (Pbe). The R^2 value adjusted for number of variables is close to 93%.

Statistical Indicators of model						Variables included in the model							
Vars	R-Sq	R-Sq (adj)	R-Sq (pred)	Mallows Cp	S	LAS Abrasion	FAA	Binder Jnr	Binder LT	G*/sin d	Pbe	VMA	D/B Ratio
1	71.5	70.6	67.8	93.8	3333					X			
1	62.7	61.5	57.6	131.3	3812.1			X					
2	82.5	81.3	79.1	49	2659.3		X			X			
2	80.9	79.6	76.9	55.7	2776.1			X		X			
3	88.3	87.1	85.6	25.8	2206.3	X	X			X			
3	86.3	84.8	82.7	34.5	2391.8		X			X	X		
4	92.1	90.9	89.3	11.8	1850.6	X	X			X	X		
4	91.9	90.7	89	12.7	1876.2	X	X			X		X	
5	94	92.9	90.9	5.6	1641.6	X	X	X		X	X		
5	92.7	91.3	89.4	11.1	1810.3	X	X			X	X	X	
6	94.5	93.2	91.1	5.4	1599.5	X	X	X		X	X		X
6	94.1	92.7	90.1	7.3	1664.1	X	X	X		X	X	X	

Best Model

Number of Passes at 12.5 mm = 6813 - 699 LA Abrasion + 1261 FAA - 1358 Binder Jnr + 1427 G*/sind - 7353 Pbe

Term	Coef	SE Coef	T-Value	P-Value	VIF
Constant	6813	10224	0.67	0.511	
LA Abrasion	-699	169	-4.15	0	1.22
FAA	1261	194	6.5	0	2.11
Binder Jnr	-1358	471	-2.88	0.008	2.78
G*/sind	1427	199	7.16	0	2.03
Pbe	-7353	1626	-4.52	0	1.27

Figure 15. Stepwise regression for Passes at 12.5 mm at 45 °C in terms of binder, aggregate and mixture properties

The coefficients in the model for passes to 12.5 mm all have logical signs, meaning that the trend in change of passes to 12.5 mm with change in the model factors are logical. The model shows reduced passes with an increase in LA Abrasion loss, increase in binder Jnr and increase in Pbe. Also it shows that passes increase with increases in FAA and in G*/sin(δ). All of these trends indicate the model is very good in predicting changes in passes to 12.5 mm in HWT.

Figure 16 shows the stepwise regression and the model for the passes to SIP. The model is not as strong as the passes to 12.5 mm as it shows the maximum R² adjusted to be 78%. The factors selected by the model includes the LA Abrasion, the FAA, the G*/sin(δ) and the VMA. Although the model contains slightly different factors than the previous model for passes to 12.5 mm, the trends of change in passes to SIP with change in factors remain logical.

Statistical Indicators of model						Variables included in the model							
Vars	R-Sq	R-Sq (adj)	R-Sq (pred)	Mallows Cp	S	LAS Abrasion	FAA	Binder Jnr	Binder LT	G*/sind	Pbe	VMA	D/B Ratio
1	60.7	59.4	56.8	32.1	2470.7					X			
1	59	57.6	53.3	34.8	2526.2			X					
2	71.8	69.9	66.3	17.1	2128.3			X		X			
2	70.3	68.3	63.8	19.5	2185.4			X	X				
3	74.7	71.9	67.2	14.8	2054.6			X		X	X		
3	73.9	71.1	66.4	16	2087			X	X		X		
4	80.8	78	73.2	7.4	1821.4	X	X			X		X	
4	77.2	73.8	68	13	1986.4		X	X		X	X		
5	82.6	79.2	73.8	6.7	1768	X	X	X		X		X	
5	81.5	78	72.2	8.3	1819.7	X	X			X		X	X

Best Model

Stripping Inflection Point = 12938 - 717 LA Abrasion + 889 FAA + 1080 G*/sind - 1894 VMA

Term	Coef	SE Coef	T-Value	P-Value	VIF
Constant	12938	10407	1.24	0.224	
LA Abrasion	-717	193	-3.72	0.001	1.29
FAA	889	184	4.84	0	1.54
G*/sind	1080	172	6.29	0	1.23
VMA	-1894	586	-3.23	0.003	1.2

Figure 16. Stepwise regression for Passes to SIP at 45 °C in terms of binder, aggregate and mixture properties

Figure 17 includes the stepwise regression and the multi-linear model for the creep slope, which can be used as a rutting only indicator with no confounding effects of moisture in the HWT. The model is very strong with R² adjusted of almost 92%. The parameters of the model include LA Abrasion loss, FAA, Binder Jnr and LT grade, and the Dust to Effective Binder ratio (D/B). The trends for the change in creep slope with changes in the parameter are logical as they follow what is known about the effects of these parameters on stability of mixtures.

Statistical Indicators of model						Variables included in the model							
Var s	R-Sq	R-Sq (adj)	R-Sq (pred)	Mallow s Cp	S	LAS Abrasi on	FA A	Binde r Jnr	Binde r LT	G*/ sind	Pbe	VM A	D/B Rati o
1	47.8	46	38.1	160.7	0.00033		X						
1	43.6	41.8	36	175.6	0.00035			X					
2	70.1	68.1	62.9	81.9	0.00026	X	X						
2	63.1	60.5	53.3	107.4	0.00029			X					X
3	82.6	80.8	77.1	38.8	0.0002	X	X						X
3	78.3	76	70.6	54.4	0.00022	X		X					X
4	90.7	89.4	85.9	11.5	0.00015	X	X	X					X
4	88.7	87	83.5	19	0.00016	X	X			X			X
5	93.1	91.8	88.9	4.8	0.00013	X	X	X	X				X
5	91.9	90.3	86.9	9.4	0.00014	X	X	X		X			X
6	93.3	91.7	88.6	6.1	0.00013	X	X	X	X		X		X

Best Model

Creep Slope = -0.000110 - 0.000130 LA Abrasion + 0.000107 FAA - 0.000172 Binder Jnr + 0.000023 Binder LT - 0.001371 D/B Ratio

Term	Coef	SE Coef	T-Value	P-Value	VIF
Constant	-0.00011	0.000784	-0.14	0.8900	
LA Abrasion	-0.00013	0.000014	-9.52	0.0000	1.27
FAA	0.000107	0.000016	6.87	0.0000	2.17
Binder Jnr	-0.00017	0.000031	-5.51	0.0000	1.95
Binder LT	0.000023	0.000008	3.01	0.0060	1.01
D/B Ratio	-0.00137	0.000163	-8.4	0.0000	1.25

Figure 17. Stepwise regression for Creep Slope at 45 °C in terms of binder, aggregates and mixture properties

In summary, the statistical analysis of the HWT results at 45 °C supports the selection of this temperature for testing and shows that not only binder properties are important, but also the aggregate source, FAA, and the mixture properties such as VMA and Pbe. The data set used is relatively small but the results are encouraging, showing that properties controlled today in the volumetric mix design and the selection of binder grades can reduce the risk of rutting.

3.1.2.2.4 Sensitivity Analysis of HWT at 45 °C

To estimate which of the mix design factors have the most influence on critical response variables in the HWT, a sensitivity analysis can be used. In Table 16 the mix design factors are listed in the first column and the percent change in the responses are estimated using the best fit models explained earlier. The percent of average values are calculated from using the models and changing the value of the factor between the minimum and maximum values shown. The change in the response calculated is then divided by the average and taken as percentage. For example, for the Number of Passes to 12.5 mm, changing the FAA between 39.8 and 47.1 in the best fit model resulted in a change (increase) in passes to 12.5 mm of 9,205 passes, which is 68% of the average of 13,527 passes. These percentages are therefore the indicators of sensitivity of response to the specific factor.

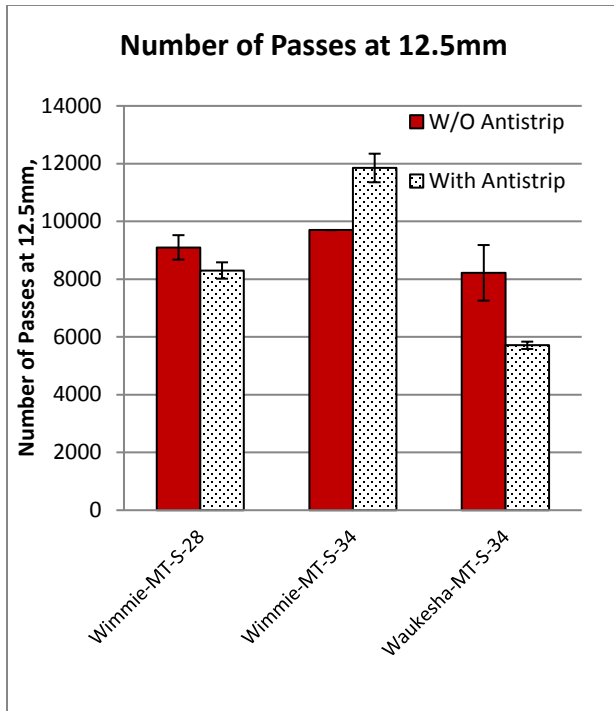
Table 16. Sensitivity of HWT Parameters to Selected Responses

Response Measured			Number of Passes at 12.5mm		Stripping Inflection Point		Creep Slope (mm/1000 passes)		Stripping Slope (mm/1000 passes)	
Factors	Ranges in Values		Change	% of Average	Change	% of Average	Change	% of Average	Change	% of Average
LA Abrasion (%)	Min	20.5	-2656	-20%	-2725	-24%	-0.494	-82%	-0.604	-26%
	Max	24.3								
FAA (%)	Min	39.8	9205	68%	6490	58%	0.781	130%		
	Max	47.1								
Binder Jnr (1/kPa)	Min	0.5	-2988	-22%			-0.378	-63%	-0.656	-28%
	Max	2.7								
Binder LT (°C)	Min	-34					0.138	23%		
	Max	-28								
G*/sind (kPa)	Min	3.48	7078	52%	5357	48%			1.230	53%
	Max	8.44								
Pbe (%)	Min	4.5	-5147	-38%					-0.983	-42%
	Max	5.2								
VMA (%)	Min	14.6			-3788	-34%				
	Max	16.6								
D/B Ratio	Min	0.67					-0.631	-105%	-0.791	-34%
	Max	1.13								
AVERAGE			13527		11161		-0.599		-2.322	
STD			6143		3879		0.455		0.944	
MIN			4200		5124		-1.972		-4.381	
MAX			25000		17455		-0.175		-0.317	

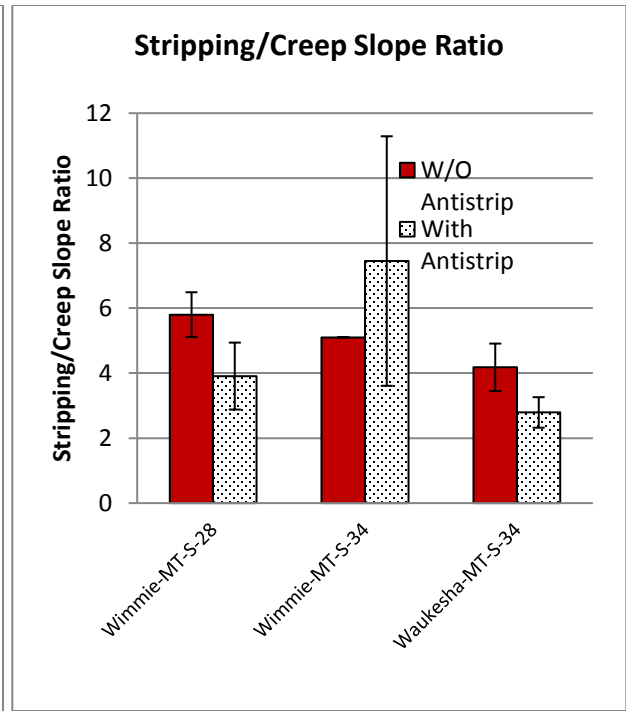
3.1.2.2.5 Effect of Anti-strip additive on HWTT results

As mentioned earlier, a limited experiment was conducted to study the effect of anti-strip additive on the HWTT results. Since the Wimmie aggregates are known to have more potential for moisture damage, two mixtures were included, one with S-28 binder and the other with S-34 binder. The third mixture was produced with Waukesha aggregates and the S-34 binder. The anti-strip additive used was in liquid form with the brand name of “Gripper X”. Based on contractor experience the dosage used was 0.5% by weight of asphalt binder. The results for the three mixes, with and without anti-strip additive, are shown in Figure 18 in terms of the four important parameters (Passes to 12.5 mm rut depth, ratio of strip slope to creep slope, creep slope, and strip slope).

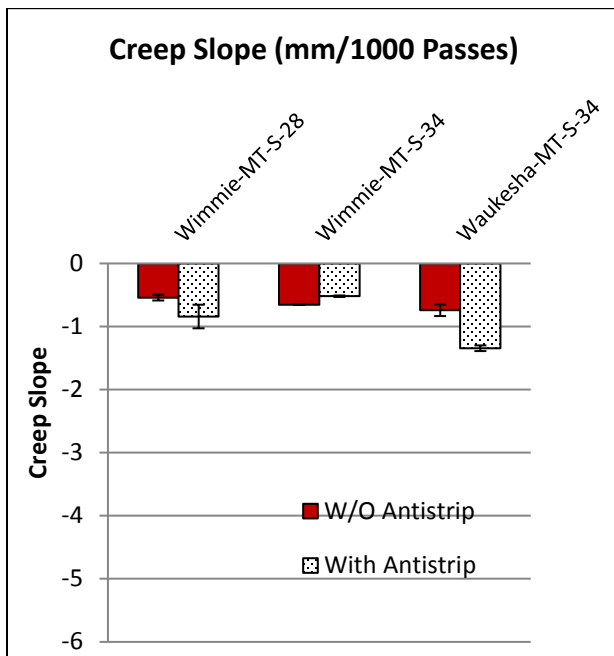
The trends of change with adding the antistrip are mixed with one mixture showing improvement in passes to 12.5 mm and in creep slope while the other two show reduction in passes to 12.5 mm and worse creep rate (more negative). The results show that HWTT is sensitive to use of anti-strip and the ratio of the strip to creep slope is changed with the use of such additive. The experiment shows potential for using the HWTT to measure effect of anti-strip additives but the number of samples tested are too small to draw any conclusions.



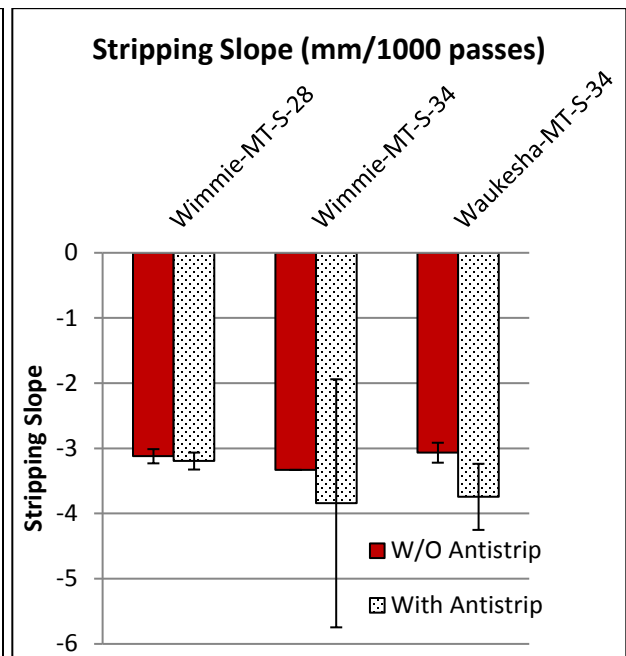
(a) Number of Passes to 12.5 mm Rut



(b) Stripping/Creep Slope Ratio



(c) Creep Slope



(d) Stripping Slope

Figure 18. Results of the HWTT testing for three mixtures with and without anti-strip additive.

3.1.2.3 Proposed HWTT Specification Framework

A number of State Agencies have been using the HWT test to specify mixture rutting and moisture damage performance. Table 17 is taken from the NCHRP 216 web document and lists the specifications framework used by a few select Agencies. (Note that the number of passes were incorrect and inverted in the table presented in the cited report.) It appears that most states focus on varying the limits for passes to 12.5 mm based on the binder grade. This is logical since binder grades are selected based on climate and traffic conditions. However, the effect of moisture is not taken into consideration and also the effect of aggregates or mix design variables are not considered.

Table 17. Limits for Passes to 12.5 mm used by various State Agencies for the HWT test.

Asphalt Binder Grade	Minimum Number of Passes at 0.5 inch Rut Depth*	
California DOT		
PG 58	10000	
PG 64	15000	
PG 70	20000	
PG 76 or higher	25000	
Illinois DOT		
PG 58 or lower	5000	
PG 64	7500	
PG 70	15000	
PG 76 or higher	20000	
Louisiana DOT		
PG 58	12000	
PG 64	20000	
PG 70 (OGFC)	7500	
Montana DOT		
	Produced Plant Mix	Mix Design
PG 58	10000	15000
PG 64	10000	15000
PG 70	10000	15000
Texas DOT		
PG 64 or lower	10000	
PG 70	15000	
PG 76 or higher	20000	

State Agencies have also varied the temperature of the test based on the binder grade used as listed in Table 18. It is not clear what the basis for selecting these temperatures are, and in the case of California and Montana, what the purpose of changing the limits and the testing temperature at the same time is. Also, there appears to be no direct link between the grade and the temperature selected or the concept of increasing the limits by 5,000 for each 6 °C change in the grade of the binder. In the regression model of this study at 45 °C, the effect of changing the $G^*/\sin(\delta)$ by 100% (which is approximately equivalent to a 6 °C reduction in grade) the maximum change in passes is approximately 1,500 cycles and not the 5,000 cycles used in the

current limits by various States. Perhaps this explains why some State Agencies decided to change the test temperature so that the limits are not biased against the heavily modified binders.

Table 18. HWT testing temperature selected by various State Agencies (NCHRP 219).

Asphalt Binder Grade	Test temperature (°C)
California DOT	
PG 58	45
PG 64	50
PG 70	55
Colorado DOT	
PG 58	45
PG 64	50
PG 70	55
PG 76	55
Montana DOT	
PG 58	44
PG 64	50
PG 70	56
Utah DOT	
PG 58	46
PG 64	50
PG 70	54

*: States Iowa, Illinois, Louisiana, Oklahoma, Texas, Washington and Wisconsin DOTs are using 50°C for all the tests.

The framework that is proposed based on the results on this study, and review of the survey summarized in the NCHRP 219 web document, includes the selection of parameters estimated from the HWT test, and the limits for acceptance based on binder and mixture design properties. For the parameters, the following list assumes that the HWT will be used to control the moisture damage potential and accumulation of rutting.

For moisture damage it is hypothesized that the change in creep rate is caused by the moisture damage, although it is also possible that tertiary creep (mixture instability) could cause the change in creep slope. In order to isolate the effects of moisture from rutting, the concept of using the stripping slope to the creep slope can be maintained as used currently. However the ratio of 2.0 appears to be too low and for all mixtures tested in this study at 50 °C and 45 °C the ratio was either close to, or above, the value of 2.0. At 45 °C the values range between 1.85 and 12.7, however one of the mixtures showed a value of 12.7, which appears to be an outlier because it is more than double the average of the ratio calculated as 4.85. Removing this one outlier, the average is at 4.09 and the standard deviation is 1.30. Therefore using these statistics and assuming the values are normally distributed, the limit of average minus one standard deviation can be used to propose that the ratio value of 2.75 is used to indicate potential for moisture damage or tertiary creep.

Although the ratio can be used to indicate instability it is still advisable that the strip slope is controlled since effect of moisture damage could be more pronounced in this stage. The range in strip slope is -1.01 (mm/1000 passes) and -4.17 (mm/1000 passes) for the mixtures in this study. The average without removing any outliers is -2.32 and standard deviation of -0.90. Considering that more than 50% of the mixtures show values of less than -2.3, the limiting slope can be set at - 2.25 (mm/1000 passes). In summary the following limits will be set for moisture damage:

1. Resistance to Moisture Damage:
 - 1.1 If Ratio of Stripping slope to Creep slope: $\leq - 2.75$, must check SIP
 - 1.2 Passes to the Stripping Inflection Point (SIP): Same as Passes to 12.5 mm
 - 1.3 Stripping Slope: $\geq - 2.25$ for all mixtures

For rutting resistance, a recent study by the University of Wisconsin evaluated the effect of the testing in a wet environment on the HWT results by testing in dry conditions. The findings indicated that the creep slope, which is the creep rate for the data before the SIP, is not affected significantly by the wet conditioning. Thus, using the creep slope could be a good indicator of rutting resistance and could be used in pavement design. The range of creep slope values in this study was between -0.20 and -2.0 (mm/1000 passes). The average was -0.60 and the standard deviation was 0.50. However, review of the data shows that there is a significant change due to the use of LT mixes. And since rutting limits should be proportional to traffic, the data should be grouped by the mix design level before setting up limits.

For a mixture acceptance framework based on permanent deformation, the following options are therefore possible:

1. Change temperature of test with binder grade but use same limits.
2. Use same test temperature (45 °C) but change limits based only on binder M332 traffic design level (S, H, V, or E).
3. Use same test temperature (45 °C) but change limits with traffic mix design level (LT, MT, HT) and climate (North and South).

Option 1 is possible but changing test temperature is not very practical and cannot take traffic into account directly. Changing temperature and limits could even make it more confusing. Option 2 is similar to the framework currently proposed by the WisDOT tech team in which the limits change with only the high temperature traffic grade of binder (S, H, V, or E). However this option cannot account for traffic design levels separately. In other words, all mixtures with S or V traffic grade binders have to meet the same passes at the test temperature. This cannot be considered optimum since rutting is affected by climate and thus different temperatures should be used in the test, or different limits should be required. Therefore, Option 3 is proposed for implementation in which a 2-dimensional matrix of (a) traffic and (b) climate are used, as shown in the following table with recommended limits based on the data in this study.

Preliminary limits shown in the table were adjusted by approximately 25% from the averages determined in the experiments and rounded to more logical numbers. This was done to allow accounting for the speed of the traffic. For example, the HT mix for South climate showed an average of 20,000 cycles to 12.5mm; to adjust for traffic speed the value is discounted by 25% (5000), thus the value of 15,000 is shown in the table. Similarly all other limits were treated the same in the sense that the averages are changed by 25%. It should be mentioned that the experiment for Hamburg testing at 45 °C included a limited number of mix types for each traffic category. Given the relatively small data set, these limits are considered

tentative and further studies are needed to validate the specified limits, and to propose increased limits for slower traffic.

Table 19. Proposed HWT Limits at 45 °C to Limit Permanent Deformation

Climatic Region/ Traffic		LT	MT	HT
North	Minimum Creep Rate (mm/1000 passes)	-1.50	-0.75	-0.375
	Minimum Passes to 12.5 mm	6,000	9,000	12,000
South	Minimum Creep Rate (mm/1000 passes)	-1.25	-0.625	-0.312
	Minimum Passes to 12.5 mm	7,500	11,250	15,000

*: These limits are for normal traffic speed, if slow speeds are expected the limits should be increased.

3.1.3 Experiment 1b: Evaluation of Long Term Aged Mixtures using SCB and DCT

Fatigue cracking is an important pavement distress at intermediate temperatures that is known to be caused by traffic and to be very sensitive to aging. In this study two tests were selected for evaluation of intermediate temperature cracking, both using the Semi-Circular Bend (SCB) geometry. The tests are referred to in this report as the SCB-LSU (Louisiana State University, ASTM Draft Standard) procedure and the SCB-IFIT (Illinois Flexibility Index Test, AASHTO TP124) procedure. Several key distinctions exist between the methods, such as variances in the rate of loading, testing temperature, number of notch depths tested, notch depth, and response parameters. Two additional test methods were selected to evaluate low temperature thermal cracking, the Disc-Shaped Compact Tension (DCT, ASTM D7313) and a low temperature SCB test developed during the low temperature pooled fund project (SCB-UMN, AASHTO TP105). These tests are both run at the low temperature PG+10 C of the virgin binder in crack mouth opening displacement control, but otherwise differ in geometry and loading rate.

For the cracking test experiment two aging conditions were selected to represent short and long term aging. Short term aging was conducted according to AASHTO R30 which involves aging the loose mix for 4 hours at 135°C. For long term aging the loose mix was aged for 12 hours at 135°C, based on a procedure developed by Asphalt Institute. The long term aging method in AASHTO R30 involves compacted mix aging for 5 days at 85°C. This method was not selected for this study due to practical concerns. Compacted mix aging was implemented in year 1 (2014) of the WisDOT high RAM pilot projects and was found to be impractical for production level acceptance testing. Loose mix aging and was used in the year 2 (2015) of the WisDOT high RAM pilot project. Hanz et al. concluded that the 12 hours at 135°C loose mix aging protocol used during the WisDOT High RAM project produced results similar to the AASHTO R30 long term aging protocol (Hanz, et al., 2016).

3.1.3.1 SCB-LSU Procedure

The SCB-LSU test was first introduced by Mull et al. (2002) to characterize the fracture resistance of crumb rubber modified asphalt mixtures. This test method is based on concepts used in fracture mechanics; the output of the test is the critical strain energy release rate, which is also known as the critical value of J-integral, or Jc. Mohammad et al. (2004) used the test to derive limits for the Jc to control fatigue cracking of mixtures in Louisiana. In this study an experimental plan was executed to study the sensitivity of the Jc

parameter to changes in mixture variables commonly controlled in WI. Table 20 includes a list of these variables and provides the justification for the levels selected.

Table 20. Experimental Design for the SCB-LSU Testing.

Factor	Level	Description	Justification
Percent Binder Replacement	3	15%, 30%, 50%	Increasing recycle content causes mix to be more prone to cracking if binder is not adjusted
Low-temperature Binder PG	2	-28 °C and -34 °C	Covers the binder grades range used in most mixes
Traffic Level	2	MT (E3) and HT (E30)	Evaluate the effects of gradation using different mixture designs (Medium Traffic and High Traffic)
Binder Modification	2	Low (S-Grade) and High (V-Grade)	Modification has been shown to improve durability properties
Aging	2	Short Term (ST) and Long Term (LT)	4 hours and 12 hours aging of loose mixtures

Table 21 includes the details of the mixtures' volumetric properties that were produced in the laboratory.

Table 21. Volumetric Properties for the Mix Designs Used in this Study.

Material Detail		%Binder Replacement	Total AC Rep	Added AC Rep	RAP AC Rep	Gmb Ave	Gmm Ave	VM A Ave	VB E Ave	D/B Ratio Rep
Cisler -15% PBR	MT-S-28	20	5.64	4.50	1.14	2.368	2.458	15.9	12.2	0.72
	MT-S-34			4.50	1.14	2.404	2.474	15.4	11.6	0.75
	MT-V-28			4.50	1.14	2.399	2.462	15.5	12.1	0.72
	MT-V-34			4.40	1.14	2.393	2.466	15.6	11.8	0.75
	HT-S-28	8	5.66	5.20	0.46	2.365	2.455	17.5	12.7	0.71
	HT-S-34			5.20	0.46	2.381	2.457	16.9	12.7	0.73
	HT-V-28			5.20	0.46	2.391	2.469	16.5	12.3	0.75
	HT-V-34			5.20	0.46	2.382	2.457	16.9	12.7	0.73
Cisler -30% PBR	MT-S-28	35	5.75	3.75	2.00	2.404	2.480	15.8	11.5	0.96
	MT-S-34			3.75	2.00	2.414	2.478	15.4	11.7	0.94
	MT-V-28			3.75	2.00	2.416	2.473	15.3	11.9	0.94
	MT-V-34			3.75	2.00	2.421	2.459	15.0	12.5	0.89
	HT-S-28	34	5.32	3.50	1.82	2.423	2.492	14.6	10.8	1.00
	HT-S-34			3.50	1.82	2.402	2.479	15.3	11.2	0.96
	HT-V-28			3.50	1.82	2.418	2.496	14.8	10.7	1.02
	HT-V-34			3.50	1.82	2.423	2.487	14.6	11.0	1.00
Cisler -50% PBR	MT-S-28	50	5.75	2.90	2.85	2.429	2.493	15.0	11.1	0.79
	MT-S-34			2.90	2.85	2.425	2.492	15.1	11.2	0.79
	MT-V-28			2.90	2.85	2.427	2.494	14.9	11.1	0.79
	MT-V-34			2.90	2.85	2.402	2.487	15.9	11.2	0.78

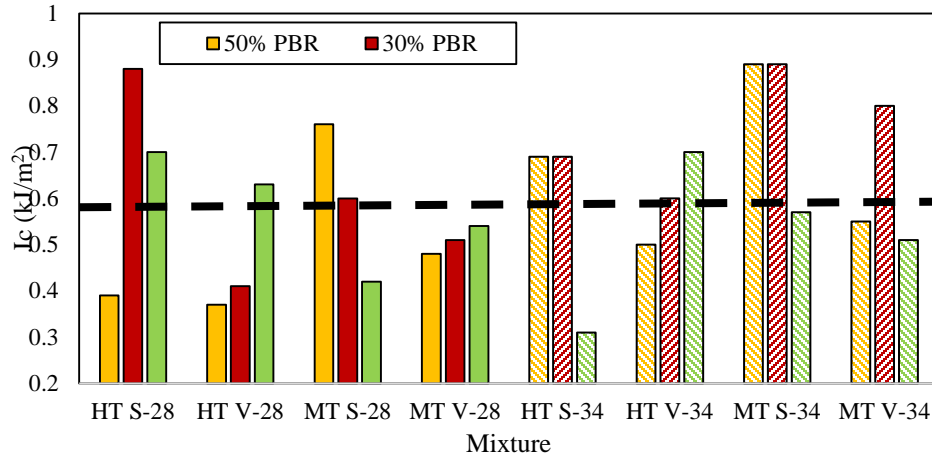
HT-S-28	60	5.25	2.10	3.15	2.441	2.521	14.1	9.7	0.93
HT-S-34			2.10	3.15	2.434	2.520	14.4	9.7	0.93
HT-V-28			2.10	3.15	2.442	2.513	14.0	10.0	0.88
HT-V-34			2.10	3.15	2.428	2.504	14.5	10.3	0.86

AC = Asphalt Content, Added AC = Adjustment in AC due to RAP binder replacement, RAP AC = AC in Recycled Asphalt Pavement, Gmm = Theoretical maximum specific gravity, Gmb = Bulk specific gravity, VMA = Voids in mineral aggregate, VBE = Volume of Effective Asphalt, D/B Ratio = Dust to Binder Ratio

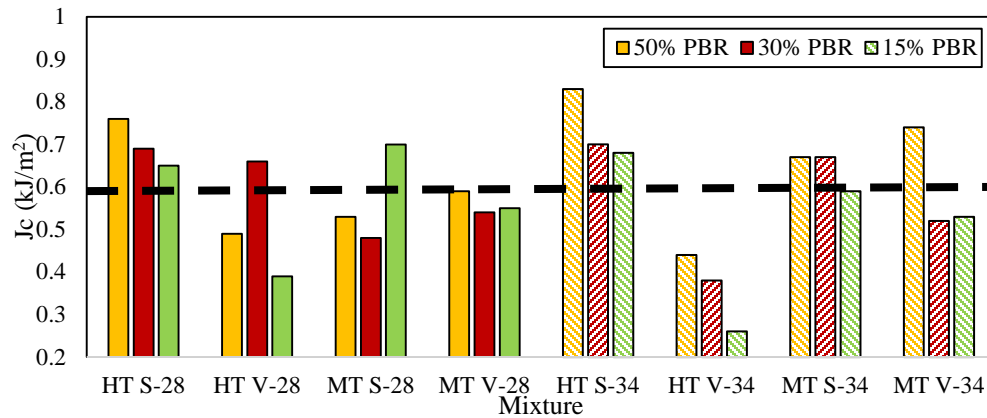
The SCB-LSU test provides the load displacement of samples tested at the Intermediate Temperature PG grade used in the mixtures. For PG 58-28 the testing temperature is 19 °C and for PG 58-34 the testing temperature is 16 °C. The response from the test allows determining the Peak Load, Fracture Energy, displacement at Peak Load, and Jc as the output parameters. However, as per the literature, Jc is considered the most important parameter to distinguish between cracking resistance of different asphalt mixtures. Three replicates are tested for each notch depth per mixture (with three notch depths). The outlier from each notch depth per mixture was removed from the data as per ASTM E 178.

Figure 19 show the Jc values determined for the mixtures in this study for long-term aged and short-term aged mixtures, respectively. The Jc values range from 0.26 to 0.89 kJ/m² for all mixtures. The dashed line shows the minimum Jc value (0.6 kJ/m²) for asphalt mixtures as proposed by Mohammad et al. (2004). From Figure 19, it can be seen that no consistent trends between change in Jc values and mixture factors could be found. For example, an increase of Percent Binder Replacement (PBR) does not show consistent increase or decrease in Jc values. Also, mixtures with low temperature grade of xx-28 do not always exhibit higher or lower Jc as compared to same mixture with PG xx-34 grades. Comparing the values of Jc to the limits proposed in Louisiana, it appears that more than 50% of the mixtures fail to meet this criterion.

The effect of PBR is important since it is expected that increasing the PBR should result in less durable mixes and therefore a lower Jc is expected. In the results shown in Figure 19, the Jc increases with a decrease in PBR content for only three out of 16 mixtures, whereas, Jc decreases with a decrease in PBR for nine out of 16 mixtures; for the rest of the mixtures, inconsistent trends are observed. For comparison with literature, Behnia et al. (2011) showed that fracture energy decreases when there is a significant increase in the PBR. Furthermore, the effect of binder modification is shown to result in a decrease in the Jc value for almost all of the mixtures; this trend contradicts the literature Mull et al. (2002) and Illinois Test procedure in which modified binders are found to increase the Jc value at intermediate temperature.



(a) Long-Term Aged Mixtures

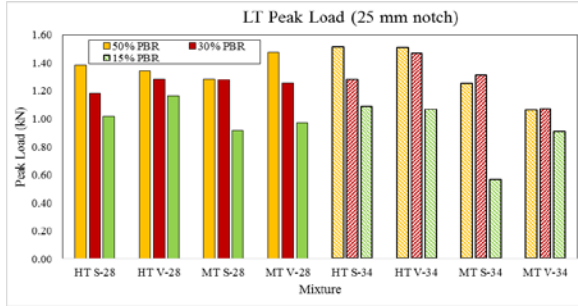


(b) Short-Term Aged Mixtures

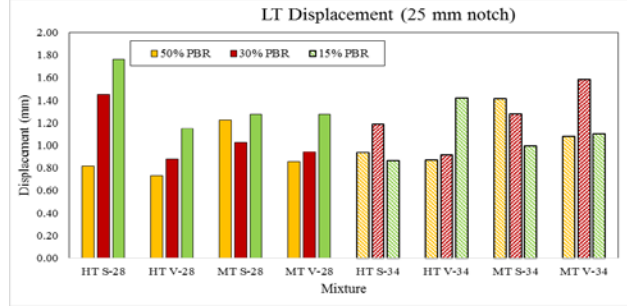
Figure 19. Variation of Jc Values estimated from the SCB Test Results for All Mixtures. (a) after 12 hours lab aging, and (b) after 2 hours of lab aging

As no clear trends could be seen from the Jc values, the results were further analyzed by looking into the peak load and peak displacement for each notch length per mixture. Figure 20, Figure 21 and Figure 22 show the average peak load and displacement for all mixtures for the notch depths of 25.4 mm, 31.8 mm, and 38.1 mm, respectively.

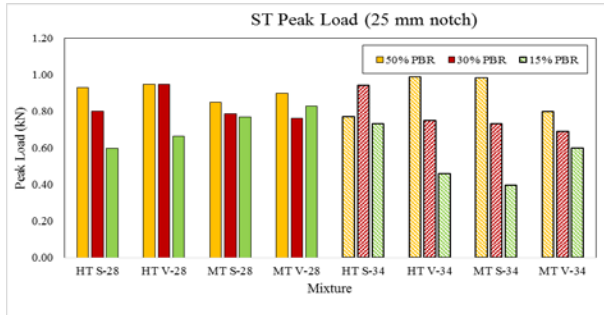
The results show that in general the Peak Load values increase with an increase in PBR while the Displacement at Peak Load decrease with an increase in PBR. The results also show that Peak Load values for the Long Term (LT) are almost always higher than the Short Term aged (ST) samples, while the Displacement values at Peak Loads are lower with increased aging. These trends are logical and encouraging as they show the test to be sensitive to aging and use of recycled asphalt. However, the effects of mixture volumetric and aggregate properties on the responses measured continue to be inconsistent. To further understand the sensitivity of the responses to the factors controlled in the experiment, statistical analysis is carried out as discussed in the next section.



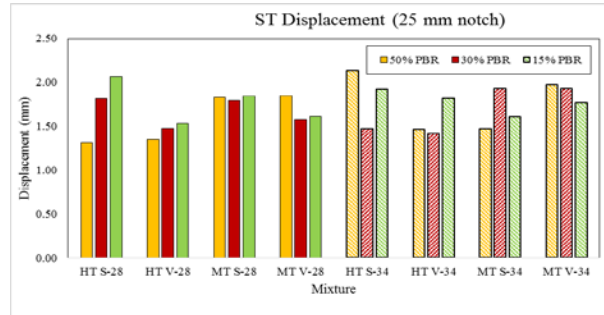
(a) LT Peak Load



(b) LT Peak Displacement

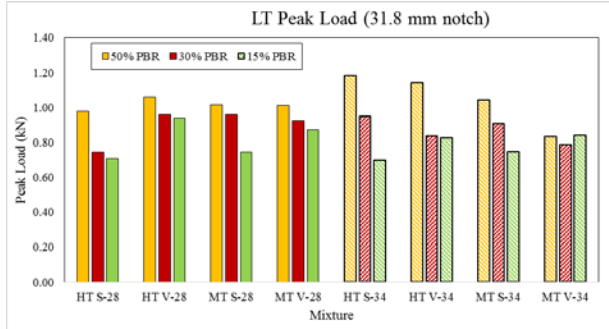


(c) ST Peak Load

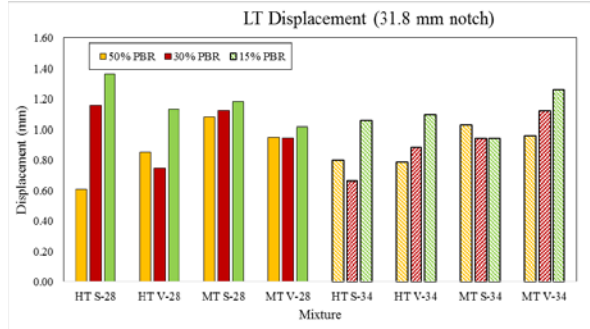


(d) ST Peak Displacement

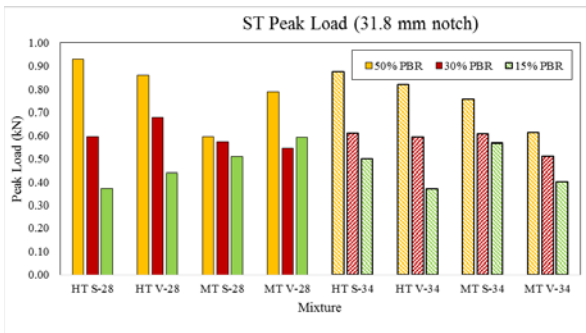
Figure 20. Peak Load and Peak Displacement for 25.4 mm Notch Length (LT= Long Term Aged, ST=Short Term Aged).



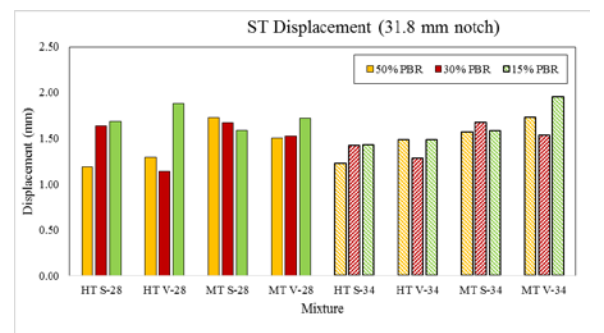
(a) LT Peak Load



(b) LT Peak Displacement



(c) ST Peak Load



(d) ST Peak Displacement

Figure 21. Peak Load and Peak Displacement for 31.8 mm Notch Length

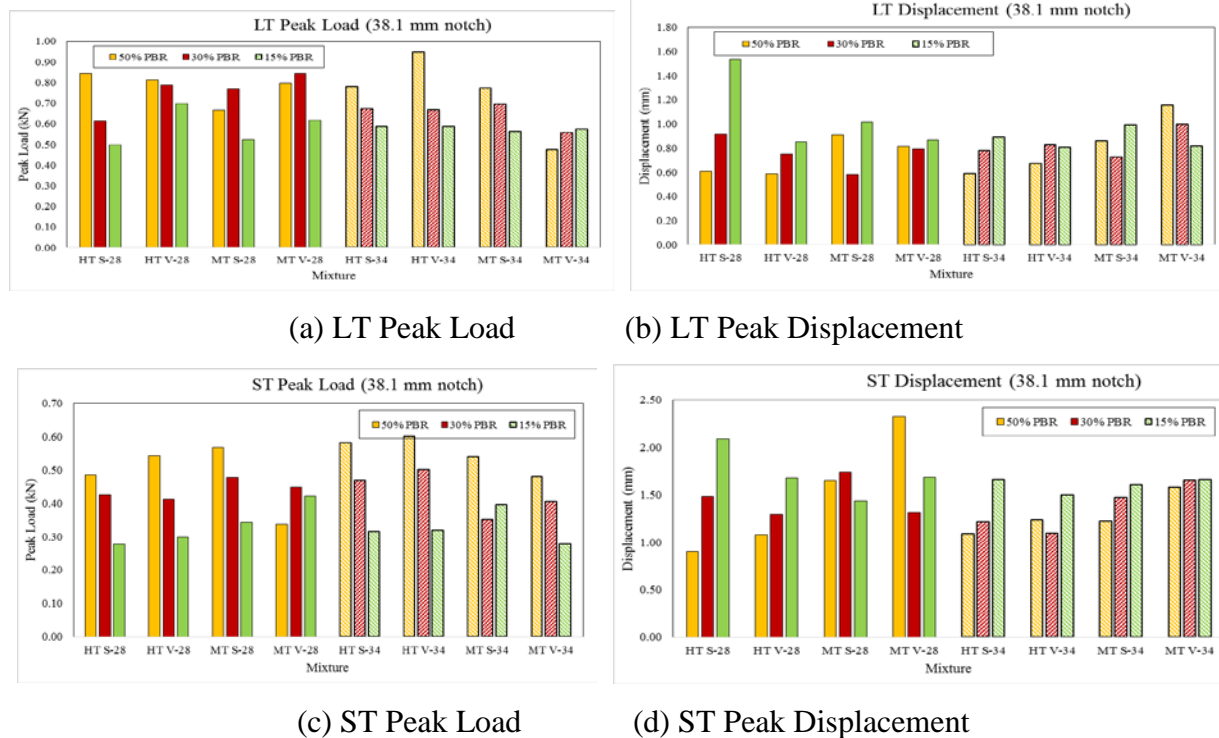


Figure 22. Peak Load and Peak Displacement for 38.1 mm Notch Length

3.1.3.1.1 SCB-LSU Statistical Analysis

ANOVA analysis is conducted to determine the statistical significance of the various controlled variables. Table 22 shows the analysis done on the SCB-LSU test results in terms of the Jc. The factors considered for this statistical analysis were: PBR, aging, traffic design level, and binder modification. The analysis is done separately for each test temperature (19 °C for the PG xx-28 grade, and 16 °C for the PG xx-34 grade).

Table 22. ANOVA Analysis of the SCB- Jc Test Results.

Factors	Df	F Value	Pr(>F)	Significance
XX-28 Binders (R² = 0.03)				
<i>PBR</i>	2	0.283	0.757	-
<i>Aging</i>	1	0.273	0.607	-
<i>Traffic Level</i>	1	0.241	0.629	-
<i>Binder Modification</i>	1	4.623	0.045	*
XX-34 Binders (R² = 0.32)				
<i>PBR</i>	2	2.817	0.087	-
<i>Aging</i>	1	1.048	0.319	-
<i>Traffic Level</i>	1	2.911	0.105	-
<i>Binder Modification</i>	1	5.994	0.025	*

*** Most significance, ** Significance, * Less significance, - No significance
 Note: F value: F statistic, Pr: Probability of Significance

Overall it can be seen that for the response J_c , ANOVA analysis cannot find any of the main factors controlled to show highly significant effects on the J_c values. It should also be mentioned that the overall model level of determination was very low (R^2 of 0.03 and 0.32). Hence, the ANOVA analysis was conducted on the detailed responses: peak load, peak displacement, and fracture energy with the factors: PBR, aging, traffic design level, binder modification, test temperature, and notch depth.

Table 23 shows the results of this ANOVA analysis, which shows that the variation of Peak Load due to the changes in mixture variables can be well explained ($R^2 = 0.80$) by the four factors used in the experimental design. In addition the fracture energy values are also sensitive to all of the design variables ($R^2 = 0.65$).

Table 23. ANOVA Analysis of the SCB Test Results for Peak Load, Peak Displacement, and Fracture Energy.

Factors	Df	F Value	Pr(>F)	Significance
Peak Load (R^2: 0.80)				
<i>PBR</i>	2	118.2	< 2.2e-16	***
<i>Aging</i>	1	632.7	< 2.2e-16	***
<i>Traffic Level</i>	1	11.4	0.000823	***
<i>Binder Replacement</i>	3	8.8	1.16E-05	***
<i>Notch Depth</i>	2	411.8	< 2.2e-16	***
<i>Residuals</i>	414			
Peak Displacement (R^2: 0.57)				
<i>PBR</i>	2	24.0	1.36E-10	***
<i>Aging</i>	1	424.3	< 2.2e-16	***
<i>Traffic Level</i>	1	28.8	1.31E-07	***
<i>Binder Replacement</i>	3	5.8	0.000674	***
<i>Notch Depth</i>	2	27.7	4.92E-12	***
<i>Residuals</i>	414			
Fracture Energy (R^2: 0.65)				
<i>PBR</i>	2	12.9	3.74E-06	***
<i>Aging</i>	1	21.79	4.23E-06	***
<i>Traffic Level</i>	1	21.69	4.42E-06	***
<i>Binder Replacement</i>	3	3.4	0.01828	*
<i>Notch Depth</i>	2	364.5	< 2.2e-16	***
<i>Residuals</i>	414			

*** Most significance, ** Significance, * Less significance, - No significance

Note: F value: F statistic, Pr: Probability of Significance

To further evaluate what factors could be controlling the J_c , a multi-linear regression analysis was done to include more specific mixture properties, including voids in mineral aggregate (VMA), effective binder content (Pbe) and the Dust to Binder (D/B) ratio. The stepwise regression and the best subset model is shown in Figure 3-24, which shows that the best fit model has a very low R^2_{adj} value of 25.1%. This indicates that the J_c is not well related to the factors controlled in the experiment even with the addition of

the mix design factors. The regression model shows that there is some level of significance of the factors but these factors are not sufficient to explain the range in Jc values for the various mixtures.

Statistical Indicators of model						Variables included in the model									
Vars	R-Sq	R-Sq (adj)	R-Sq (pred)	Mallows Cp	S	Actual PBR	Aging	FAA	Binder Jnr	Test temperature	LAS @2.5 %	Notch depth	VM A	Pbe	D/B Ratio
1	17.6	17.5	16.9	43.7	0.1369				X						
1	8.8	8.6	7.9	93.7	0.1441						X				
2	19.6	19.2	18.4	34.8	0.1354				X		X				
2	19.6	19.2	18.3	34.9	0.1355	X			X						
3	22.2	21.6	20.5	22.3	0.1334	X			X					X	
3	21.5	20.9	19.9	26.3	0.134				X		X				X
4	24.3	23.6	22.4	12.2	0.1317	X			X					X	X
4	23.8	23	21.8	15.2	0.1322	X			X		X			X	
5	26	25.1	23.7	4.8	0.1304	X			X		X			X	X
5	25.4	24.5	23.2	8.2	0.1309	X			X	X				X	X
6	26.2	25.2	23.6	5.3	0.1303	X	X		X		X			X	X
6	26.1	25.1	23.5	5.9	0.1304	X		X	X		X			X	X
7	26.4	25.2	23.4	6.5	0.1304	X	X	X	X		X			X	X
7	26.4	25.1	23.5	6.6	0.1304	X	X		X	X	X			X	X
8	26.5	25.1	23.2	7.7	0.1304	X	X	X	X	X	X			X	X
8	26.5	25	23.1	8.1	0.1304	X	X	X	X		X		X	X	X
9	26.7	25.1	23	9	0.1304	X	X	X	X	X	X		X	X	X
9	26.5	24.9	22.8	9.7	0.1305	X	X	X	X	X	X	X		X	X
10	26.7	24.9	22.6	11	0.1306	X	X	X	X	X	X	X	X	X	X

Best fit model

$$Jc = -0.650 + 0.3691 \text{ Actual PBR} + 0.05425 \text{ Binder Jnr} + 0.000003 \text{ LAS@2.5\%} + 0.1555 \text{ Pbe} + 0.2632 \text{ D/B Ratio}$$

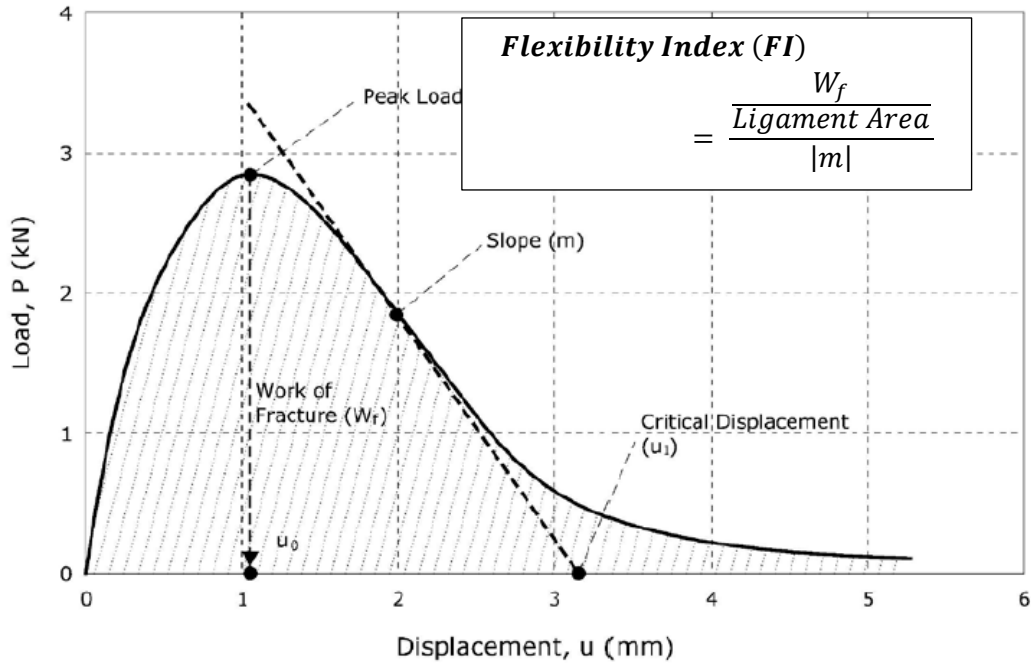
Term	Coef	SE Coef	T-Value	P-Value	VIF
Constant	-0.65	0.216	-3.01	0.003	
Actual PBR	0.3691	0.0746	4.95	0	4.15
Binder Jnr	0.05425	0.00675	8.03	0	1.2
LAS@2.5%	0.000003	0.000001	3.08	0.002	1.2
Pbe	0.1555	0.0332	4.68	0	4.8
D/B Ratio	0.2632	0.0745	3.53	0	1.51

Figure 23. Stepwise regression and Multi-linear Regression model for the Jc estimated from the SCB-LSU procedure.

3.1.3.1.2 Using the SCB-LSU to Determine the Flexibility Index

Due to the lack of the relationship between the Jc and the mixture variables, new ideas for analysis were considered. In a previous study for the WHRP, the same challenges were faced using the SCB-LSU

procedure and a proposed analysis of the SCB-LSU results by following the IFIT method for one of the notch sizes was proposed (WHRP 14-06 Draft Report). The Flexibility Index (FI) was calculated using the work of fracture and the slope at the inflection point (m). It was found the FI related very well to the mixture variables in that study, as shown in the model.



$$FI_{STOA} = -18.759 + 1.368 \times VBE - 0.3905 \times (T_{Virgin})_{Low} - 10.181 \times RBR_{EFF} + 3.100 \times \left(\frac{R\%}{100}\right)^2 \quad (11)$$

Where:

FI_{STOA} = short-term oven conditioned flexibility index

VBE = effective volume of binder, vol %

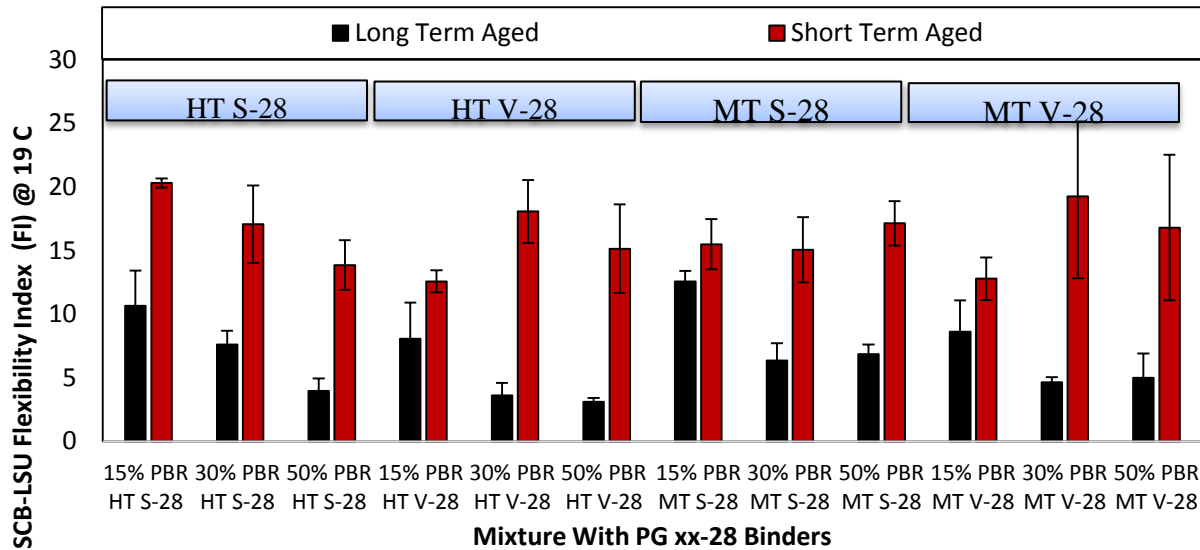
$(T_{Virgin})_{Low}$ = continuous low temperature grade of the virgin binder, °C

RBR_{EFF} = effective RAP binder ratio (see Equation 8)

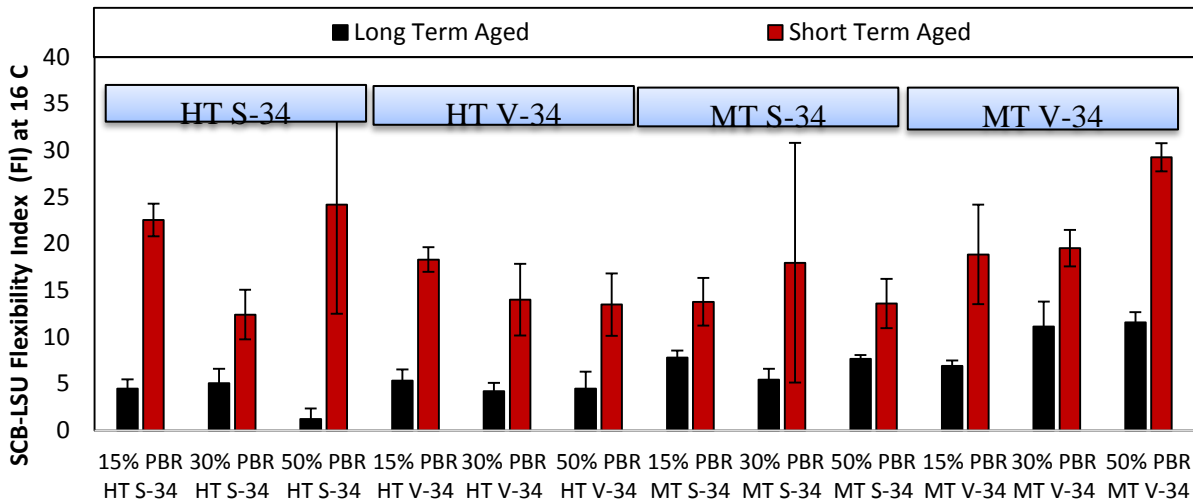
R% = percent recovery from AASHTO M332

Figure 24. Regression Model from WHRP 14-06 Draft Report

The same procedure was used with the data collected in this study. Figure 25 shows bar charts for the FI calculated from the SCB-LSU procedure. The results show clearly that this parameter is sensitive to aging and that for all mixtures, the Long Term (LT) aged mixtures have lower FI values than the Short Term (ST) aged mixtures. The plots also show, for the Mixtures made with PG xx-28, there are logical trends for the change in FI values with amount of RAP in the mixtures as measured by the PBR (i.e. the FI decreases with increasing PBR). The trends are however not the same for the mixtures utilizing PG xx-34 binders, for which no clear trends for change in PBR could be defined.



(a) Mixtures with PG xx-28 Binders



(b) Mixtures with PG xx-34 Binders

Figure 25. SCB-LSU Flexibility Index of Short and Long Term aged Mixtures for (a) Mixtures with PGxx-28 binders and (b) Mixtures with PG xx-34 binders

Since the results of using the FI parameter from the SCB-LSU procedure is more promising, statistical analysis was carried out to determine if there is a relationship between the FI values and the variables controlled in this study.

Figure 26 shows the stepwise regression outcome and the best subset multi-linear regression that could be derived. The best subset is showing fair values of R^2 (adj) of more than 60% and the best set model includes PBR, Aging, and VMA, which are logical parameters that are known to affect cracking resistance. For example PBR and aging will results in hardening of binder and embrittlement, while VMA controls the binder content which is known to affect aging rate. However, the model shows illogical relationship with PBR and no relationship to properties of binders such as the Jnr and the LAS Number of Cycles to Failure at 5 % strain.

Statistical Indicators of model						Variables included in the model								
Vars	R-Sq	R-Sq (adj)	R-Sq (pred)	Mallows Cp	S	Actual PBR	Aging	F A A	Binder Jnr	Test temperature	LAS @2.5%	VMA	Pbe	D/B Ratio
1	58.3	58	57.1	21	4.4188		X							
1	1.7	1	0	235.6	6.7848							X		
2	60	59.4	58.2	16.6	4.343		X					X		
2	59.6	59.1	58	18	4.363		X							X
3	62.3	61.5	59.9	9.9	4.2319	X	X					X		
3	61.3	60.5	58.7	13.7	4.2882	X	X						X	
4	62.9	61.8	59.7	9.7	4.2146	X	X					X	X	
4	62.8	61.7	59.9	10	4.22	X	X	X				X		

Best fit model

$$FI = -22.2 + 10.35 \text{ Actual PBR} - 1.2974 \text{ Aging} + 2.666 \text{ VMA}$$

Term	Coef	SE Coef	T-Value	P-Value	VIF
Constant	-22.2	11.8	-1.87	0.063	
Actual PBR	10.35	3.58	2.89	0.005	3.01
Aging	-1.2974	0.0891	-14.56	0	1
VMA	2.666	0.702	3.8	0	3.01

Figure 26. Results of Stepwise Regression for the FI calculated from the SCB-LSU testing at 25-mm notch depth.

To further understand the relationship between the FI parameter and mixture design variables, the response of fracture energy and post peak slope (m) were used as the responses for the statistical regressions. The fracture energy best set gave very low R² values of less than 25%, however the (m) slope showed a fair relationship with mixture parameters of 62%. The best set model is shown in Figure 27 (a), and it includes the factors of aging, percent effective asphalt (Pbe) and the Fine Aggregate Angularity (FAA). It should be noted that lower values of the slope are favorable they are inversely proportional to the FI parameter. Further analysis of the other key indicators of the SCB test indicated that the main factors of aging and PBR have major effects on increasing the Peak Load as shown in Figure 27 (b). The model with Peak Load as the response shows the best R²_{ADJ} value of approximately 70%. The model shows that increasing the aging, the PBR and Dust to Binder ratio (D/B) all result in higher Peak Load values, which is logical.

Term	Coef	SE Coef	T-Value	P-Value	VIF
Constant	0.078	0.88	0.09	0.93	
Aging	0.08179	0.00615	13.31	0	1
FAA	0.0474	0.0192	2.47	0.015	1.02
Pbe	-0.4383	0.0607	-7.22	0	1.02

$$\text{Slope} = 0.078 + 0.08179 \text{ Aging} + 0.0474 \text{ FAA} - 0.4383 \text{ Pbe}$$

- Best set model for Slope value (m) – R² adjusted= 62%

Term	Coef	SE Coef	T-Value	P-Value	VIF
Constant	0.1	0.116	0.86	0.391	
Actual PBR	0.5828	0.0885	6.58	0	1.29
Aging	0.05221	0.00337	15.5	0	1
D/B Ratio	0.382	0.146	2.61	0.01	1.29

$$\text{Peak Load} = 0.100 + 0.5828 \text{ Actual PBR} + 0.05221 \text{ Aging} + 0.382 \text{ D/B Ratio}$$

- Best set model for Peak Load – R² adjusted= 70%

Figure 27. Best set models for (a) Slope value (m), and (b) Peak Load for the SCB-LSU testing at 25-mm notch.

In summary, the SCB-LSU procedure appears to give useful indicators of the effects of mixture design variables and aging on cracking parameters. The best indicator for effects of aging is the FI parameter that is calculated from the fracture energy (area under the curve) and the post peak slope (m). However, the relationship of this parameter to the mixture variables is not very strong and does not show logical trends with some of the mixture variables. The detailed analysis of the various test indicators show that the Peak Load and the post peak slope are the two parameters that are most sensitive to aging and to mixture variables.

3.1.3.1.3 Comparison to Previously Proposed Models of the FI

In the WHRP 14-06 study in which the use of the FI for the analysis of the SCB-LSU was suggested, a model relating the FI to specific mixture and binder parameters was introduced. The model is shown in the following equations which cover the FI at short term aging as well as the relationship of long term aging with short term aging.

$$FI_{STOA} = -18.759 + 1.368 \times VBE - 0.3905 \times (T_{Virgin})_{Low} - 10.181 \times RBR_{EFF} + 3.100 \times \left(\frac{R\%}{100} \right)^2$$

Where:

FI_{STOA} = short-term oven conditioned flexibility index

VBE = effective volume of binder, vol %

$(T_{Virgin})_{Low}$ = continuous low temperature grade of the virgin binder, °C

RBR_{EFF} = effective RAP binder ratio (see Equation 8)

$$\text{RBR}_{\text{EFF}} = \frac{\% \text{RAPBinder}}{\% \text{TotalBinder}} + 1.3 \left(\frac{\% \text{RASBinder}}{\% \text{TotalBinder}} \right)$$

$$\text{FI}_{\text{LTOA}} = 0.6550 \times \text{FI}_{\text{STOA}} - 0.7019$$

Where:

FI_{LTOA} = long-term oven conditioned flexibility index

FI_{STOA} = short-term oven conditioned flexibility index

The models were used to estimate the FI values for the mixtures of this study and to compare the measured with the estimated FI values, as shown in Figure 28. Unfortunately the measured and the predicted values of the FI do not show a strong correlation, but they show the correct trend of the change in values.

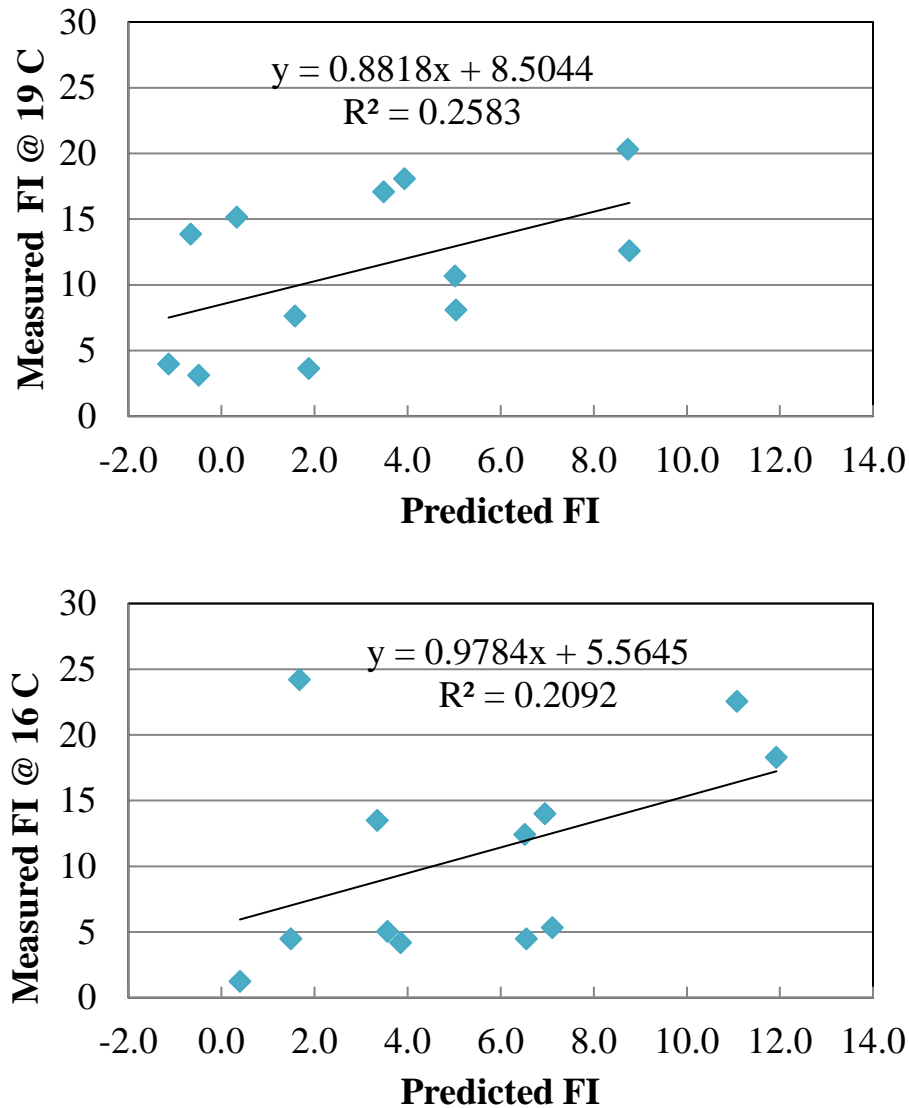


Figure 28. Comparison of Measured Values of FI from the SCB-LSU with values predicted using the model proposed by WHRP 14-06 study

3.1.3.1.4 Sensitivity analysis of the FI model

To estimate which of the factors have the most influence on critical response variables, a sensitivity analysis can be used. In table 24 the mix design and aging factors are listed in the first column and the percent change in the responses are estimated using the best fit models explained earlier. The percent of average values are calculated from using the models and changing the value of the factor between the minimum and maximum values shown. The change in the response calculated is then divided by the average and taken as percentage. For example, for the FI response, changing the actual PBR between 8% and 60% in the best fit model resulted in a change in FI of 5.4, which is 45% of the average of 11.9. These percentages are therefore the indicators of sensitivity of response to the specific factor.

Table 24. Sensitivity Analysis of the SCB-LSU response to Mixture Design and Conditioning Factors

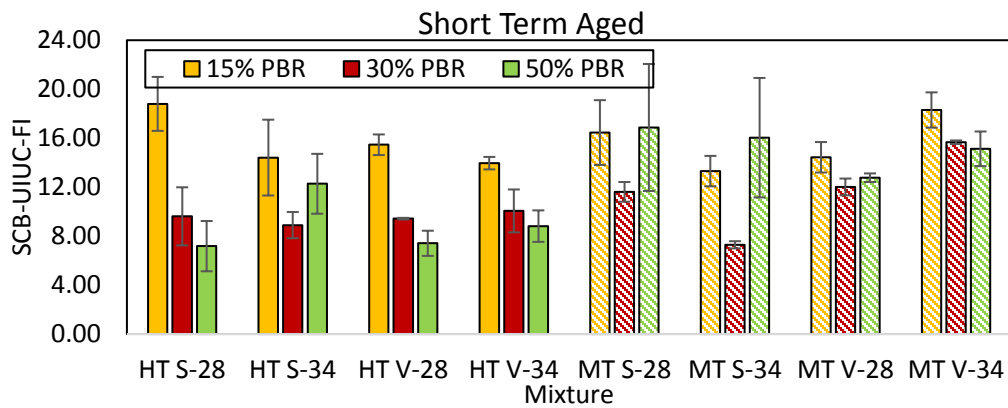
Responses Measured			FI		Slope		Fracture Energy		Peak Load		Displacement at Peak Load	
Factors	Ranges in Values		Change	% of Average	Change	% of Average	Change	% of Average	Change	% of Average	Change	% of Average
Actual PBR	Min	8%	5.4	45%			264.2	44%	0.3	29%		
	Max	60%										
Aging (hours)	Min	4	-10.4	-87%	0.7	93%			0.4	40%	-0.7	-37%
	Max	12										
FAA (%)	Min	42.9			0.2	26%					-0.5	-24%
	Max	46.7										
Binder Jnr (1/kPa)	Min	0.5										
	Max	2.7										
Test Temperature (°C)	Min	16					36.7	6%				
	Max	19										
LAS@2.5% (Cycles)	Min	7162										
	Max	26755										
Pbe (%)	Min	4.1			-0.7	-94%	149.3	25%			1.2	60%
	Max	5.6										
VMA (%)	Min	14.0	9.4	79%								
	Max	17.5										
D/B Ratio	Min	0.71							0.1	11%		
	Max	1.02										
AVERAGE			11.9		0.7		606.6		1.0		2.0	
STD			6.8		0.5		123.4		0.3		0.9	
MIN			1.6		0.2		349.0		0.5		0.6	
MAX			32.5		3.3		1074.0		1.9		6.8	

As shown in the table, the FI is very sensitive to aging and to VMA, while the slope (m) is sensitive to the aging and the effective binder content. What is not logical is the lack of effects of the binder parameters (Jnr and LAS at 2.5% strain) as none of the models actually identified these variables as important although the parameters had relatively wide ranges of 0.5 to 2.7 for the Jnr and 7,000 to 26,000 cycles for the LAS fatigue life. It appears that the SCB-LSU test is not highly affected by the binder properties.

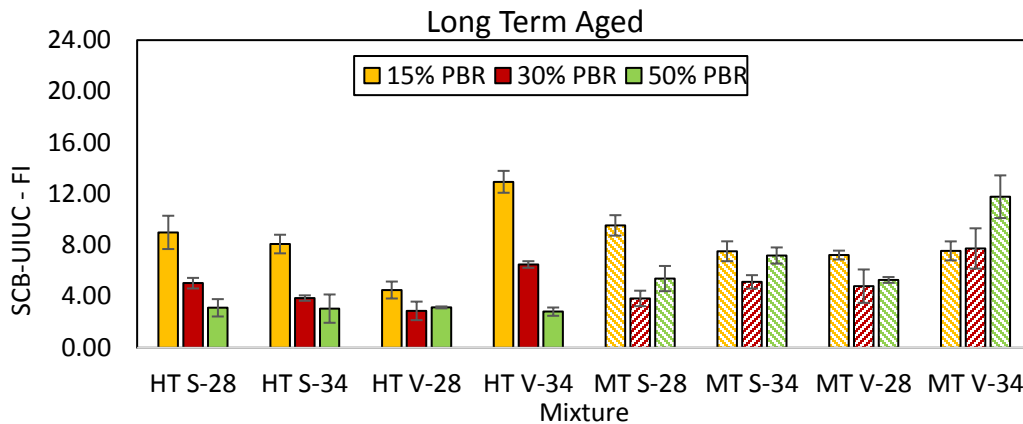
3.1.3.2 SCB-IFIT procedure

As described earlier the SCB-IFIT procedure involves using the same testing geometry (with a single notch depth) as the SCB-LSU but requires running the test at 25 °C and includes a faster testing rate of loading of 50 mm/min as compared to 0.5 mm/min for the SCB-LSU. This section includes the complete graphical and statistical analyses of the results from this procedure.

The same set of mixtures tested for the SCB-LSU was tested also with the SCB-IFIT procedure. Results for all mixtures in terms of the Flexibility Index (FI), which is the main output recommended in the AASHTO TP105 standard, are shown in Figure 29. For the complete dataset, the FI, which accounts for fracture energy and post-peak behavior, varied between 2 and 16. This range is considered wide and thus can be considered suitable for differentiating between mixture variables. The fracture energy values for all mixtures varied between 1,400 and 1,900 J/m², which given the wide variety of mix designs used in this study, is not considered significantly wide. This observation is in agreement with previous literature showing the FI typically shows a higher sensitivity than the fracture energy to mixtures variables. It should also be noted that the COV for fracture energy the mixtures was generally in the range of 5-15% with an average of 11%, while the COV for FI was between 8-20%, with an average of 13%.



(a) SCB-UIUC Results for Short Term Aged Mixtures



(b) SCB-UIUC Results for Long Term Aged Mixtures

Figure 29. Summary of Flexibility Index for all mixtures: (a) Short Term aged (b) Long Term aged

Analysis of the trends shown in Figure 29 suggests that aging significantly affects the FI parameter, but it is not clear if there are clear effects on post-peak slope and, hence, trend with a change in Percent Binder Replacement (PBR) or the change in binder grade from PG xx-28 to a PG xx-34 grade. Therefore, the effects of binder modification and mixture design level are not immediately clear from the data, although modified binders (V grades) appear to show a higher FI, which is logical.

3.1.3.2.1 Statistical Analysis of the SCB-IFIT Results

In order to better understand the significance and trends in the data, a statistical analysis was employed to determine the best subset of factors that can explain the variation in the Peak Load, Post-Peak Slope, Fracture Energy and the FI parameter. The results for the FI is shown in Figure 30, which indicates that the most important factors controlling the FI are Aging, binder fatigue (LAS 2.5%), Percent Effective Binder, and Dust to Binder ratio. The R^2_{ADJ} is 68.9%, which is considered a fair value.

Vars	R-Sq	R-Sq (adj)	R-Sq (pred)	Mallows Cp	S	Actual PBR	Aging	FAA	Binder Jnr	Binder IT	LAS @2.5%	VMA	Pbe
1	45.7	45.4	44.5	146.5	3.773		X						
1	19.1	18.7	17.5	307.7	4.604								
2	64.8	64.4	63.7	32.8	3.048		X						
2	60.3	59.8	59.1	60.1	3.236		X						X
3	67.4	66.9	66.1	18.6	2.938		X				X		
3	67.2	66.7	65.9	20.0	2.948		X						X
4	69.6	68.9	68	7.7	2.848		X				X		X
4	68.7	68	67.1	13.2	2.89		X				X	X	
5	70.1	69.2	68.1	6.6	2.832	X	X				X		X
5	69.7	68.8	67.8	9.0	2.85		X	X			X		X
6	70.3	69.4	68.1	6.9	2.827	X	X	X			X	X	X

Best fit model

$$FI = 20.68 - 0.8636 \text{ Aging} - 0.000034 \text{ LAS@2.5\%} + 2.223 \text{ Pbe} - 15.62 \text{ D/B Ratio}$$

Term	Coef	SE Coef	T-Value	P-Value	VIF
Constant	20.68	4.65	4.45	0	
Aging	-0.8636	0.0521	-16.59	0	1
LAS@2.5%	-3.4E-05	0.000009	-3.76	0	1.01
Pbe	2.223	0.621	3.58	0	1.52
D/B Ratio	-15.62	2.44	-6.41	0	1.51

Figure 30. Best Sub-set Model for FI from the IFIT procedure

The regression model shows that the FI decreases with Aging, with LAS 2.5% cycles to failure, and with Dust to Binder Ratio, while it increases with Percent of Effective Binder. These trends are logical

with the exception of the LAS cycles to failure at 2.5% as it is expected that binders with higher fatigue life should give better FI values. It is important to note, however, that the role of the binder parameter is very small as the model without it can give an R^2_{ADJ} of 66.7% which is close to the value of 68.9% for the model with this parameter.

To further understand which of the SCB-IFIT engineering parameters are most sensitive to the mixture design factors, the results of the statistical analysis for the other parameters are shown in Figure 31.

Term	Coef	SE Coef	T-Value	P-Value	VIF
Constant	1230	160	7.71	0	
Actual PBR	706	108	6.51	0	1.31
Binder IT	46.79	6.35	7.36	0	1.09
LAS@2.5%	0.001883	0.000724	2.6	0.01	1.08
D/B Ratio	-700	178	-3.94	0	1.32

Best fit model

R-Sq (adj)= 37.1%

Fracture Energy = 1230 + 706 Actual PBR + 46.79 Binder IT + 0.001883 LAS@2.5% - 700 D/B Ratio

Term	Coef	SE Coef	T-Value	P-Value	VIF
Constant	0.63	2.57	0.25	0.807	
Aging	0.2341	0.0179	13.1	0	1
FAA	0.1831	0.0555	3.3	0.001	1.02
Binder IT	0.1107	0.0268	4.13	0	1
Pbe	-2.042	0.175	-11.67	0	1.02

Best fit model

R-Sq (adj)= 63.9%

Slope = 0.63 + 0.2341 Aging + 0.1831 FAA + 0.1107 Binder IT - 2.042 Pbe

Term	Coef	SE Coef	T-Value	P-Value	VIF
Constant	1.175	0.833	1.41	0.16	
Aging	0.1107	0.00578	19.16	0	1
FAA	0.0823	0.0179	4.59	0	1.02
Binder IT	0.08171	0.009	9.08	0	1.08
LAS@2.5%	0.000006	0.000001	5.52	0	1.09
Pbe	-0.926	0.0568	-16.32	0	1.03

Best fit model

R-Sq (adj)= 81.5%

Peak Load = 1.175 + 0.11070 Aging + 0.0823 FAA + 0.08171 Binder IT + 0.000006 LAS@2.5% - 0.9260 Pbe

Figure 31. Results of Statistical Models for the Fracture Energy, Post Peak Slope, and Peak Load for the UIUC-IFIT results

The additional statistical analysis shows that the Fracture Energy model has an R² value of only 37.1%, which indicates it is not sensitive to the mixture design variables or to aging, while the post-peak slope model has an R² value of 63.9%. It is therefore clear that the post-peak slope is sensitive to mixture variables and it appears to be the parameter resulting in variation of the FI values. The most interesting observation is that the Peak Load is shown as the most sensitive with the highest R² value of 81.5%.

3.1.3.2.2 Sensitivity Analysis of the UIUC-IFIT responses to Mixture Variables

Table 25 provides a summary of all the responses discussed and shows the change in their values due to varying the mixture design and aging factors. It also provides the change as a percentage of the average value of each response. The first important observation is that the main response parameter (FI) is not sensitive to the Percentage of Binder Replacement (PBR), which raises serious concerns about this test procedure. The analysis shows that only the Fracture energy is somewhat sensitive (22% change with respect to the average) but all other parameters are not. Another concern is the high sensitivity of the post peak slope to Percent Effective Binder which shows that a 1.5% change in binder content results in more than 100% change in average slope value.

Table 25. Sensitivity Analysis of the SCB-IFIT Responses to the Mixture and Aging Variables

Responses Measured			FI		Slope		Fracture Energy		Peak Load		Displacement at Peak Load	
Factors	Ranges in Values		Change	% of Average	Change	% of Average	Change	% of Average	Change	% of Average	Change	% of Average
Actual PBR	Min	8%					367.12	22%				
	Max	60%										
Aging (hours)	Min	4	-7	-70%	2	78%			1	32%	-0.23	-19%
	Max	12										
FAA (%)	Min	42.9			0.70	29%			0.31	11%		
	Max	46.7										
Binder Jnr (1/kPa)	Min	0.5										
	Max	2.7										
Binder IT (°C)	Min	12.0			1	29%	290.10	17%	1	19%		
	Max	18.2										
LAS@2.5% (Cycles)	Min	21416	-2	-21%			112.80	7%	0.36	13%		
	Max	81318										
Pbe (%)	Min	4.1	3	34%	-3	-128%			-1	-51%		
	Max	5.6										
VMA (%)	Min	14.0										
	Max	17.5										
D/B Ratio	Min	0.71	-5	-49%			-217.00	-13%			-0.27	-22%
	Max	1.02										
AVERAGE			9.8		2.4		1672.4		2.7		1.2	
STD			5.1		1.6		280.9		0.7		0.3	
MIN			1.3		0.6		1054.2		1.3		0.7	
MAX			26.5		10.5		2566.7		4.9		2.3	

In summary, two criteria were used to select the best subset of factors in the regression, a high R^2_{ADJ} value and a low Mallow's C_p value. Based on the regression analysis, the SCB-IFIT procedure does not appear to be the best approach due to the lack of sensitivity to the Percent Binder Replacement, an illogical trend with binder fatigue properties, and the over sensitivity to the effective binder content.

3.1.3.3 Intermediate Temperature Specification Framework based on the SCB-LSU Test

In previous sections the results of the SCB-LSU test and the SCB-IFIT test were presented and discussed to explain the sensitivity of the test outputs to the mixture design and aging conditions that were controlled. The analyses indicated that the best test is the SCB-LSU but that the J_c parameter, which is recommended as the output of this test, was not found to be reliably able to discriminate between mix design factors known to influence cracking. Instead, using only one notch size and using the analysis described in the SCB-FIT is the best parameter to be used for controlling intermediate temperature cracking resistance. An important advantage of the SCB-LSU is it requires the test to be done at the PG intermediate temperature, which allows a direct consideration of the climate at which the project is constructed.

The possibilities for the framework for specifications include considering the following three variables:

- Climate, since it is known that PG grades vary across the state and that fatigue is sensitive to temperature of test.
- Traffic level (LT, MT, HT), since it is expected that fatigue cracking is dependent on the number of loading passes applied on the pavement, and
- The type of construction: whether the project is an overlay or new construction. It is well established that overlay mixtures need to be designed to a higher reliability (in terms of fatigue resistance) to ensure performance.

The options that can therefore be considered for the framework are:

- One test temperature and one limit: this option is not deemed acceptable since two base binders (each with a different intermediate temperature grade) are used in Wisconsin. The result could bias the results for one binder versus another of a difference grade (e.g. PG 58-34 versus PG 58-28).
- One temperature and multiple limits: Again, this option is not deemed acceptable given the two base binders.
- Two temperatures and multiple limits: This appears to be the best option to account for (1) differences in the base binder grades used, and (2) to increase the reliability of the design for MT and HT designs. In addition, increased limits for overlay designs can also be considered in this framework.

Using the third alternative, a framework for the specification is offered. The values for short term aging are based on the average for the MT and HT mixes tested. These averages are used for the HT column (18.0), and then assuming MT is for 7 million ESALs, as compared to 35 million ESALs for HT, the log of 35/7 was used to determine the MT limit (12.0). Similarly, assuming LT is used for 2 million design ESALs maximum, the log of 7/2 was used to determine the limit for LT mixes (6.0). To consider aging effects, the average of FI values for short term aging (4 hours) was divided by the FI average for long term aging (12

hours). The ratio was used to determine the values for long term aging (2.5, 5.0 and 7.5). It should be noted that rounding of the numbers was used to define the limits.

Table 26. Proposed Intermediate Temperature Cracking Framework

Traffic	LT			MT			HT		
	Overlay	Other Construction		Overlay	Other Construction		Overlay	Other Construction	
PG-LT	-28	-28	-34	-28	-28	-34	-28	-28	-34
Test Temp	19	19	16	19	19	16	19	19	16
Minimum FI (Short-Term Aged 4hrs)	*	6.0		*	12.0		*	18.0	
Minimum FI (Long-Term Aged 12hrs)	*	2.5		*	5.0		*	7.5	

* The limits for Overlay should be increased by 50% to account for the excessive movements at the pavement joints or cracks. This increase should be left to the discretion of the material engineer of the project.

3.1.3.4 Performance Tests to Evaluate Low Temperature Cracking Resistance

The Disc-Shaped Compact Tension (DCT) test, as specified in ASTM D7313 and the low temperature SCB (SCB-UMN) test, as specified in AASHTO TP105 were selected as candidate tests for thermal cracking under Experiment 1-b. The objective of this experiment was to evaluate numerous test methods for fatigue and thermal cracking by varying factors known to influence intermediate and low temperature performance. The specific factors evaluated were: percent binder replacement (15%, 30%, 50%), mix traffic level (MT, HT), polymer loading (S, V), and aging (short term, long term), detailed justification for selection of these factors was presented previously in Table 7. Asphalt binder low temperature grades of -28°C and -34°C were used to represent the two climatic zones in Wisconsin.

For both tests, test temperature was defined as low temperature PG + 10°C, consistent with the concept of linking performance test temperature to climate. The main output of these tests is fracture energy (kJ/m²). The DCT test is used in existing specifications in neighboring states including Minnesota and Iowa; a minimum value is specified in an effort to reduce risk of thermal cracking. A summary of these specifications and the specification used in WisDOT High RAM pilot project are provided in Table 27. As shown in the table, specification targets and aging methods used vary by state. In addition both MN and the WI high RAM project required production verification of DCT results.

Table 27. Summary of Existing Specifications for the DCT test

State	Aging Condition	Traffic Level	Test Temp (°C)	Test Requirements	Minimum Fracture Energy (J/m ²)
WI – High RAM Pilot Project	Long Term AASHTO R30 or 12 hr loose mix @ 135°C	Applies to all traffic levels	LT PG + 10°C	Mix Design Production	400
MN	Short Term AASHTO R30	Traffic Levels 2&3 (up to 3 million ESALS)	LTPBind 98% Reliability Low Temp +10°C	Mix Design Production	450 (Mix Design) 400 (Production)
		Traffic Levels 4&5 (up to 30 million ESALS)	LTPBind 98% Reliability Low Temp +10°C	Mix Design Production	500 (Mix Design) 450 (Production)
IA	Short Term AASHTO R30	<10 million ESALs	LT PG + 10°C	Mix Design	400
		10 -30 million ESALs	LT PG + 10°C	Mix Design	460
		> 30 million ESALs	LT PG + 10°C	Mix Design	690

3.1.3.4.1 DCT Results and Analysis

The DCT test was conducted according to ASTM D7313, the main output of the test is fracture energy, secondary outputs are peak load and time to peak load. Conceptually, peak load can be considered measure of stiffness, as the mix becomes stiffer the peak load should increase. The time to peak load is an indicator of flexibility. Figure 32 and Figure 33 present the fracture energy for the mixtures tested in this study for the low temperature grades of binder -28 and -34, respectively. At least two replicates were tested for each mixture. Two additional tests were conducted for mixtures that had a difference in fracture energy greater than 78.5 J/m², the same procedure that was used in the WisDOT High RAM pilot specification. The error bars show the standard deviation of the replicates. The peak load for all the mixtures ranged from 2.6 to 3.8 kN; whereas, the fracture energy ranged from 436 to 708 J/m² and the standard deviation was 75 J/m², which is similar to the 78.5 J/m² error associated with the test.

For the results shown in Figure 32 and Figure 33, test temperatures were the PG LT grade + 10°C, so tests were conducted at -18°C and -24°C for the -28°C and -34°C grades, respectively. In the figures

mixes are grouped by percent binder replacement in a set of three bars. Moving from left to right, the first data set represents the high traffic mix after short term aging (ST) using a standard (S) graded binder. The next data set is the same mix design after long term aging (LT). The third and fourth data sets are the same mix design with modified binder (V) after short and long term aging. The sequence is then repeated for the MT mixes in data sets 5-8.

From the graphical representation of the data, it is very difficult to find consistent trends with the variation of any of the mixture factors controlled in the experiment. For example the variation of PBR between 15% and 50% sometimes show a decreasing trend of peak load (Mixes HT S-28 LT and HT V-28 LT), but for others (MT V-28 LT and MT V-28 ST) the opposite trend is observed. Furthermore, no discernable effects of aging, binder modification, or mix traffic level are observed. Related to the specification criteria presented in Table 27, three of the 24 short term aged mixes (12.5%) exceeded the 500 J/m² threshold used for high traffic mixes in the MnDOT specification and all of the mixes exceed the 400 J/m² threshold used for all mixes under the WisDOT high RAM specification.

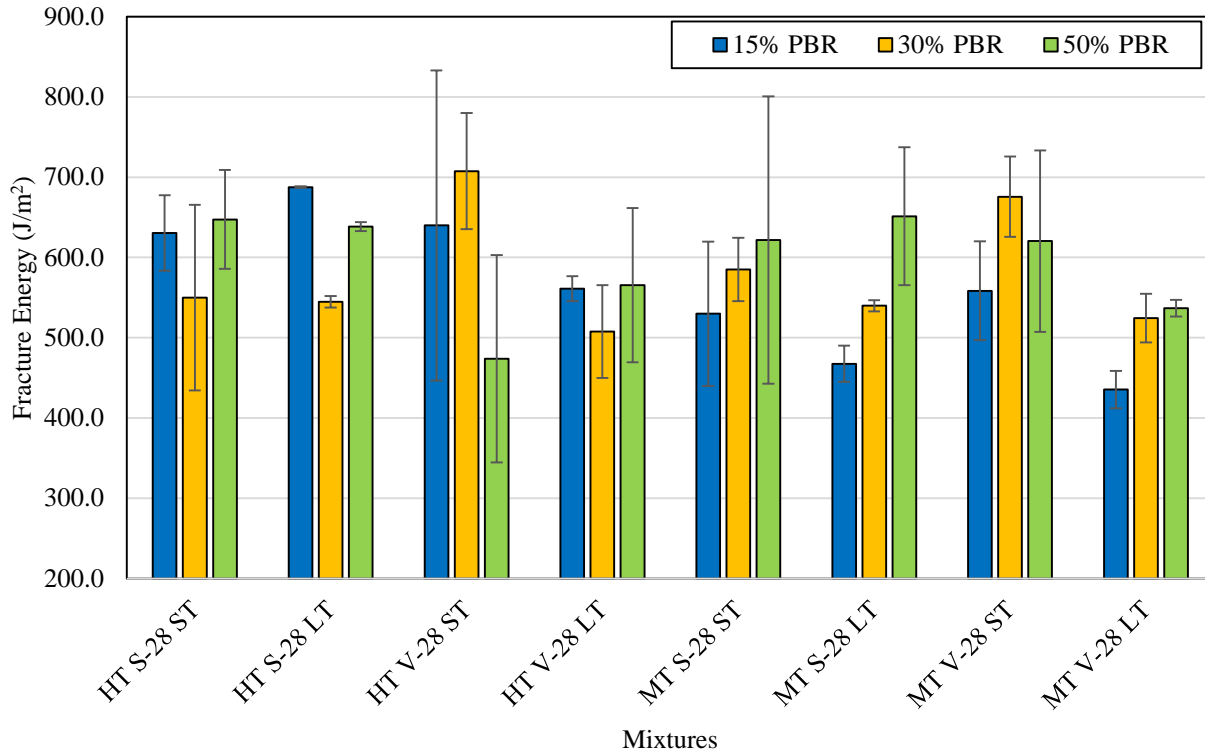


Figure 32. Summary of DCT Results @ -18°C (LT PG = -28°C)

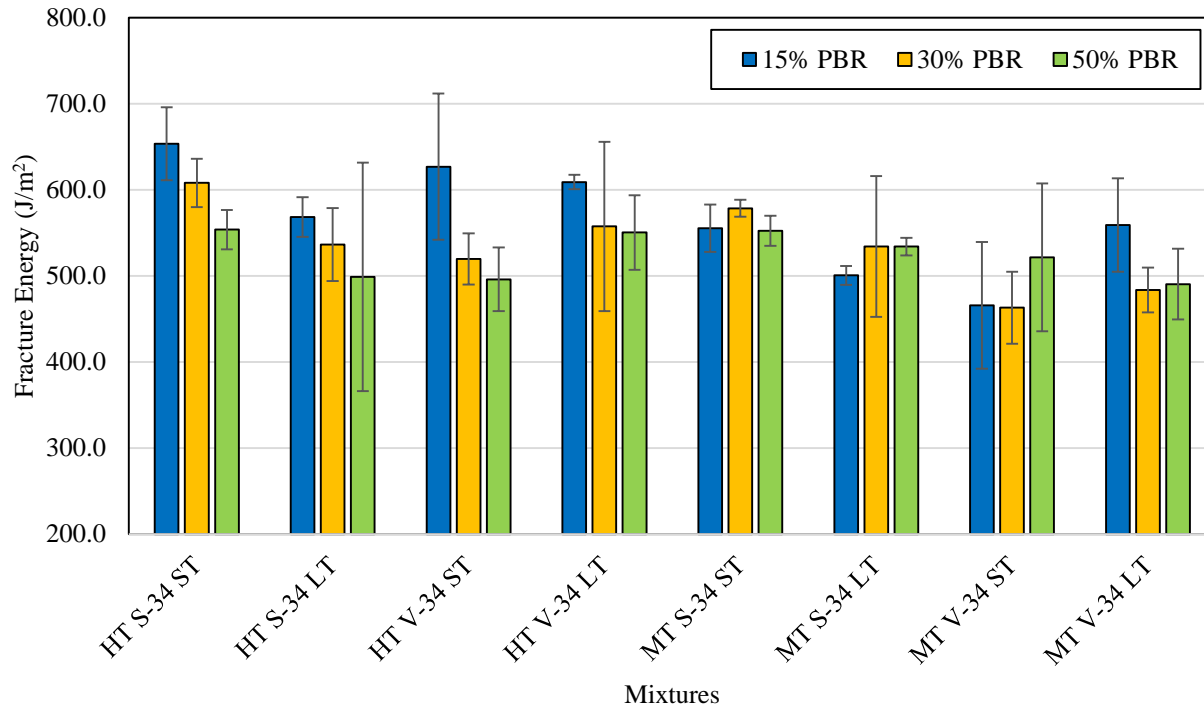


Figure 33. Summary of DCT Results @ -24°C (LT PG =-34°C)

The blending chart analysis detailed in subsequent sections of this report was used to estimate the effect of binder replacement on mixture low temperature binder grade, with results are presented in Table 28. The low temperature grade of the RAP was -20.4 °C.

Table 28. Estimated Effect of Binder Replacement on LT PG

Percent Binder Replacement	PG 58-28 (LT Continuous Grade -30°C)	PG 58-34 (LT Continuous Grade -34.9)
15	-28.6	-32.7
30	-27.1	-30.6
50	-25.2	-27.7
Max Deviation from Plan Grade (°C)	2.8	6.3

As shown in Table 28, due to the low temperature properties of the RAP used, binder replacement caused deviations of approximately 3 °C (1/2 PG) and 6 °C (full PG) for the PG 58-28 and PG 58-34 binders respectively. For the PG 58-28 DCT results, the estimated low temperature PG data provides some insight into the relative insensitivity of fracture energy to percent binder replacement observed. However, the increase of one PG grade caused by binder replacement observed in the PG 58-34 did not result in a significant reduction in mixture fracture energy.

To provide a broader perspective of the data collected, the average values calculated for the main factors controlled are shown in Table 29 for the PG xx-28 binders and Table 30 for PG xx-34 binders.

Table 29. Analysis of Trends of Mixtures' Main Variables with DCT Average Values of Response Parameters for the PG xxx-28 Binder

Parameter	Level	Peak Load (kN)	Time at Peak Load (secs)	Fracture Energy (J/m ²)
Percent Binder Replacement (PBR)	15%	3.12	8.41	564
	30%	3.27	8.21	579
	50%	3.15	7.76	594
Oxidative Aging	ST	3.15	8.05	603
	LT	3.21	8.20	555
Modification	PG S - 28	3.05	8.43	591
	PG V - 28	3.31	7.83	567
Average		3.18	8.13	579
Range		0.26	0.67	48
Std Dev		0.09	0.26	17.89
COV		2.8%	3.2%	3.1%

Table 30. Analysis of Trends of Mixtures' Main Variables with DCT Average Values of Response Parameters for the PG xxx-34 Binder

Parameter	Level	Peak Load (kN)	Time at Peak Load (secs)	Fracture Energy (J/m ²)
Percent Binder Replacement (PBR)	15%	3.18	7.77	567
	30%	3.41	7.52	535
	50%	3.22	7.44	525
Oxidative Aging	ST	3.29	7.76	550
	LT	3.24	7.39	535
Modification	PG S - 34	3.21	7.63	556
	PG V - 34	3.33	7.52	529
Average		3.27	7.58	542
Range		0.23	0.38	43
Std Dev		0.08	0.15	15.67
COV		2.5%	2.0%	2.9%

Analysis of the main effects highlights the insensitivity of the DCT test parameters to the mix design variables evaluated in this study. The coefficient of variation between all main effects is 3.0%, making it difficult to discern between the factors studied and the variability of the test. For example, the accepted standard deviation of the test is 78.5 J/m², whereas the deviation observed in the test results was approximately 45 J/m².

Some directional trends can be identified when experimental factors are isolated, a summary of the observations for each parameter and each binder grade is provided in Table 31. In addition, combinations of factors and test outputs that did not have consistent trends for PG 58-28 and PG 58-34 are highlighted.

Table 31. Trends Observed in Main Effects – DCT

Factor	General Trend		
	Peak Load	Time to Peak Load	Fracture Energy
Increase PBR	PG 58-28: No trend. PG 58-34: No trend.	PG 58-28: Decrease (0.70s) PG 58-34: Decrease (0.33s)	PG 58-28: Increase (31 J/m ²) PG 58-34: Decrease (42 J/m ²)
Increase Aging	PG 58-28: Increase (0.06 kN) PG 58-34: Decrease (0.05 kN)	PG 58-28: Decrease (0.15s) PG 58-34: Decrease (0.37s)	PG 58-28: Decrease (48 J/m ²) PG 58-34: Decrease (14 J/m ²)
Use of Modification	PG 58-28: Increase (0.26 kN) PG 58-34: Increase (0.08 kN)	PG 58-28: Decrease (0.60s) PG 58-34: Decrease (0.11s)	PG 58-28: Decrease (24 J/m ²) PG 58-34: Decrease (28 J/m ²)

As shown in Table 31, time to peak load is the most consistent test parameter in that similar trends were observed for both PG 58-34 and PG 58-28 binders. The direction of these trends also shows potential for use of time to peak load as an indicator of mix embrittlement. Increasing PBR and aging both resulted in decreases in time to peak load, which is consistent with expectations. Use of polymer modification also caused a decrease in time to peak load, which was not expected. In this study, polymer modification as defined by the “S” and “V” grades in AASHTO M332 most benefits the high and intermediate temperature properties, with minor effects on low temperature performance. This study is also limited to one modification system, different modifiers may show different performance. There is also potential that effects on mix performance would be observed if a modifier specifically intended to alter low temperature properties was used and the mix test was conducted at the same temperature. Inconsistent trends were observed for the peak load parameter specifically for increasing PBR and increasing aging. Modification resulted in an increase in peak load, particularly for -28 grades. Variations in fracture energy were in most cases less than half of the accepted standard deviation of the test (78.5 kJ/m²)

The insensitivity of the DCT test to mix design factors observed in this study is consistent with findings of previous research. A similar study was recently completed in Illinois that had similar conclusions with regard to the effects of binder replacement on fracture energy being inconsistent between different mixes. In some mixes an increase in fracture energy was observed, in others there was a decrease. The research also observed a very narrow range of DCT results for eight plant produced mixes that varied by traffic level, binder replacement and aggregate source (Al-Qadi, et al., 2015). However recent research presented at the 2016 AAPT meeting presented that for a given aggregate source the DCT test was found sensitive to use of both RAP and RAS as decreasing fracture energy was observed in both cases with increasing recycled contents. Furthermore, when RAP was held constant at 45% improvements in DCT fracture energy were observed with decreasing binder grade. In that data set use of a PG 46-34 with 45% RAP resulted in equivalent fracture energy to the virgin mix prepared with PG 64-22 (Buttlar, et al., 2016).

In both these studies the DCT test temperature was -12°C which was selected based on the climate of Illinois.

Results with respect to the effects of aging are also consistent with the literature, as no effect on fracture energy was observed for samples tested after short term and long term aged mixes according to the AASHTO R30 (Dave, et al., 2011). The short term aging protocol in AASHTO R30 is 4 hours loose mix aging at 135°C, the long term aging protocol is 5 days compacted mix aging at 85°C.

A different study evaluated the effect of loose mix aging at 135°C for aging times from 2 to 50 hours and found that up to 8 hours loose mix aging fracture energy increased, then decreased at subsequent aging times (Braham, et al., 2009). The varying effects of aging with time were attributed to the stiffening and embrittlement caused by aging having competing influences on fracture energy. Stiffening causes an increase in peak load, and a corresponding increase in fracture energy. Embrittlement reduces fracture energy because the softening slope becomes steeper. At longer aging times, the reduction in fracture energy caused by embrittlement exceeds the increase caused by stiffening and overall fracture energy is reduced. This work was only done on one mix design, but the implications of this finding is that if the mix is not sufficiently aged a substantial drop in fracture energy will not be observed. Research related to the WisDOT High RAM pilot project reported similar fracture energy results for mixes long term aged according to AASHTO R30, and loose mix aged at 135°C for 12 and 24 hours (Hanz, et al., 2016). Finally, regarding the effects of polymer previous research found a slight improvement in fracture energy due to polymer modification (Dave, et al., 2011). Whereas, Data generated in this study found no significant effect of modification.

Statistical analysis using Analysis of Variance (ANOVA) was applied to quantify the trends observed in the data and to determine how well the experimental factors selected for this study can explain the variation in DCT fracture energy. The ANOVA was evaluated at a confidence level of 95% ($\alpha = 0.05$), the factors considered include: percent binder replacement (PBR), aging, traffic design level, and binder modification. The binder low temperature PG grade was included as a blocking factor because the PG grade was the basis used for selecting test temperature. Results are presented in Table 32.

Table 32. ANOVA Results for DCT Fracture Energy ($\alpha = 0.05$)

Factor	Degrees of Freedom	Sum of Squares	Mean Sum of Squares	F Value	Pr(>F)	Significance
PBR	2	1188	594	0.103	0.902	-
Aging	1	23533	23533	4.092	0.046	*
Traffic Level	1	37345	37345	6.493	0.013	*
Binder Modification	1	15918	15918	2.768	0.100	-
LT Grade (Block)	1	32366	32366	5.627	0.020	*
Residuals	89	511888	5752			
Adjusted R²= 12%						

*** Most significance, ** Significance, * Less significance, - No significance

The statistical analysis presented in Table 32 corroborates the observation that the DCT fracture energy parameter was not sensitive to the factors varied in this study. The adjusted R² of the model of 12%

indicates that a majority of the variation observed cannot be explained by the factors selected. Therefore, while the analysis identified aging and mix traffic level as statistically significant factors, they are not practically significant. The blocking factor of low temperature grade was also identified as significant, meaning that for the same set of mixes the response is different for mixes -34°C grades tested at -24°C and -28°C grades tested -18°C. No conclusions can be drawn from this particular model, but the identification of the blocking effect as a significant factor should be of interest to future development of the test as this experiment was designed to mirror the approach many states are taking to implement the test.

As a final attempt to further evaluate the variation in DCT fracture energy values reported multi-linear regression was applied to allow for inclusion of mixture specific properties in the analysis. Specifically, VMA, Pbe, and D/B ratio were used to represent mixture volumetric properties; and the percent aggregate passing the #8 sieve (P8) was used to represent gradation. The marker values for percent binder replacement of 15%, 30%, and 50% used in the ANOVA were replaced with the actual PBR of the mix designs and the general description of traffic level (MT or HT) was replaced by values of FAA. Binder modification and aging were also included in the analysis. Results presented in Table 33 indicate that inclusion of these additional effects resulted in a marginal improvement in the R² value from 12% to 19%. However, the practical interpretation of this result is that that 80% of the variation in test results observed remains unexplained by the factors selected. Based on this result the linear regression equation does not have the ability to assess the effect of mix composition, binder formulation, aging, or other factors on DCT fracture energy.

Table 33. Results of Multi-Linear Regression Analysis Including Main Effects and Mixture Properties

Factor	Significance	Coeff
Actual PBR	x	-209.4
Aging	x	-3.91
FAA	x	32.78
Binder Modification	x	11.24
VMA	-	0
Pbe	x	-123.7
D/B Ratio	x	-294
R² for the model	19%	

3.1.3.4.1.1 Effect of Aggregate Quality on DCT Fracture Energy

The work plan developed for Task 1-b in the work plan did not include the effects of aggregate quality in the experimental design on the basis that aggregate source would be dictated by proximity to the project location rather than meeting the requirements of a performance test. The average DCT fracture energy observed across all mixtures was approximately 550 J/m², approximately 25% to 40% higher than the specification limits summarized previously. The mixes studied were not designed to be superior performing and 66% of the designs would require a binder grade adjustment based on binder replacement maximums in WisDOT specifications. Numerous studies including internal testing at MTE, results of the WisDOT pilot projects and published literature have noted that there is a significant effect of aggregate properties on

DCT fracture energy. A qualitative example of how aggregate quality potentially changes the manner in which mixtures fail is presented in Figure 34. The mix on the left is aggregate from the same granite source used in this study, the mix on the right used aggregate sourced from SE Minnesota. As shown the failure surface of the granite mix has very few exposed aggregates indicating a majority of the failure occurred in the asphalt mastic. The failure surface of the limestone mix includes many fractured coarse aggregates. As shown at the bottom of the figure, the manner in which the samples failed significantly impacted fracture energy.

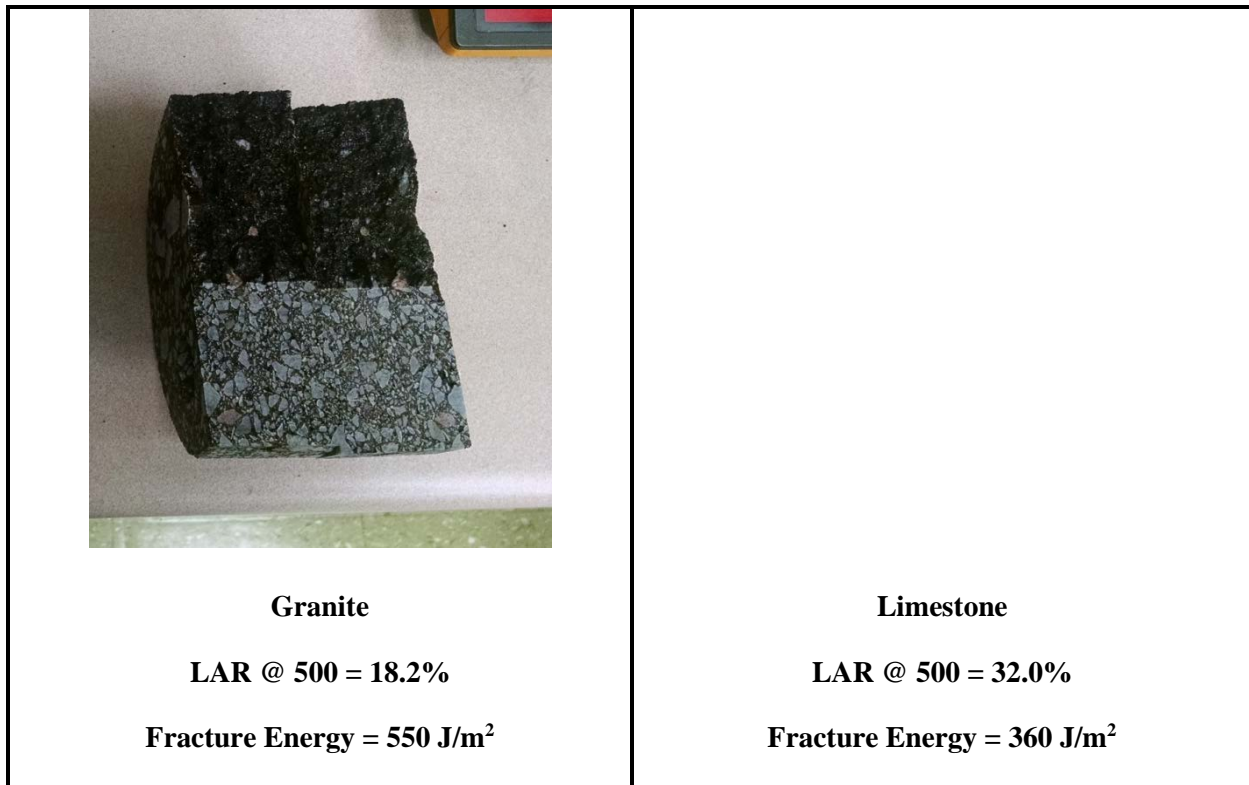


Figure 34. Cross Section of Failed DCT samples for Different Aggregate Types

The effect of aggregate type shown in Figure 34 was also observed in previous research when the DCT test was run at PG low temperature - 2°C, the granite aggregate remained intact and the limestone aggregate fractured. When test temperature was increased to 22°C above the low temperature grade no fracture was observed with either aggregate type (Braham, et al., 2007). The research confirmed that for the mixes tested in the low temperature PG grade range granite aggregates gave significantly higher fracture energy values, ranging from 400 J/m² to 1100 J/m² than limestone aggregates (200 J/m² – 700 J/m²). At much higher test temperatures (LT PG + 22°C) the aggregate effect was much less, with the limestone performing better than the granite in some cases. The differing influence of aggregate was explained by mastic stiffness, at lower temperatures the stiffness of the mastic is sufficiently high for the strength of the aggregate to influence the crack path, if the aggregate is of lower strength the crack will go through the aggregate leading to lower fracture energy. At higher test temperatures the crack path travels around the aggregates, indicating that the mix is failing within the mastic. Furthermore, statistical analysis identified aggregate type as the third most influential factor on the response. Changes in test temperature were most significant, followed by aggregate type which was more significant (based on p-value) than asphalt content

or air voids (Braham, et al., 2007). This data confirms that the aggregate type influences the manner in which samples fail when tested at the temperature range used in current specifications.

Further research related to the factors influencing the DCT test and specifically the contribution of aggregate was presented the 2016 AAPT meeting. The paper investigated the use of space diagrams to relate high temperature and low temperature performance using the Hamburg Wheel Tracking and DCT tests. Numerous factors were studied including the effects of RAP, RAS, binder PG, rejuvenators, and aggregate source. Based on the climate of Illinois, all tests were conducted at -12°C. Data comparing the effect of changing aggregate source to changing binder grade is summarized in Table 34. Results provide another example of the significant influence of aggregate source on DCT fracture energy, as similar increases in fracture energy were observed when changing aggregate source from granite to limestone and reducing low temperature PG for the same aggregate source.

Table 34. Effect of Aggregate Source and PG Selection on DCT Fracture Energy at -12°C (Buttler, et al., 2016)

Aggregate Source	Binder Grade	DCT Fracture Energy (J/m ²)	Change in Fracture Energy
Virgin Limestone	PG 64-22	411.2	
Virgin Limestone	PG 58-28	609.1	+197.9
Crushed Gravel	PG 64-22	551.0	+140.0

Internal research at MTE has generated DCT fracture energy data for aggregate sources in areas including NW WI, Central WI, and SE MN. Two of the aggregates used in the current WHRP study are from sources located in Central WI (Cisler and Wimmie). A brief description of the mixes studied is provided in Table 35 and the fracture energy is plotted in Figure 35. The descriptions in the table follow the mixes from left to right in Figure 35.

Table 35. Summary of Mixes Used to Evaluate Effects of Aggregate Source on DCT Fracture Energy

Mix Description	LAR at 500 (%)	Binder Grade	Notes
Gravel Pit #1	24.3	PG 52-34	E1 (12.5 mm) 32% PBR, 18% from RAP, 14% from RAS
Gravel Pit #1	24.3	PG 58-28	E1 (12.5 mm) 24% PBR, 9% from RAP, 13% from RAS
Granite Quarry	18.2	PG 64-34P	E10 (12.5mm) 16% PBR from RAP. 3.0% Design Air Voids
Granite Quarry	18.2	PG 58-28	E1 (12.5 mm) 22% PBR, 12% from RAP, 10% from RAS
Gravel Pit #2	15.0	PG 64-34P	E3 (12.5mm) 14% PBR from RAP
Gravel Pit #3	21.6	PG 58-34P	E1 (19.0mm) 15% PBR from RAP
Limestone Quarry	32.0	PG 58-34	E1 (12.5mm) 15% PBR from RAP

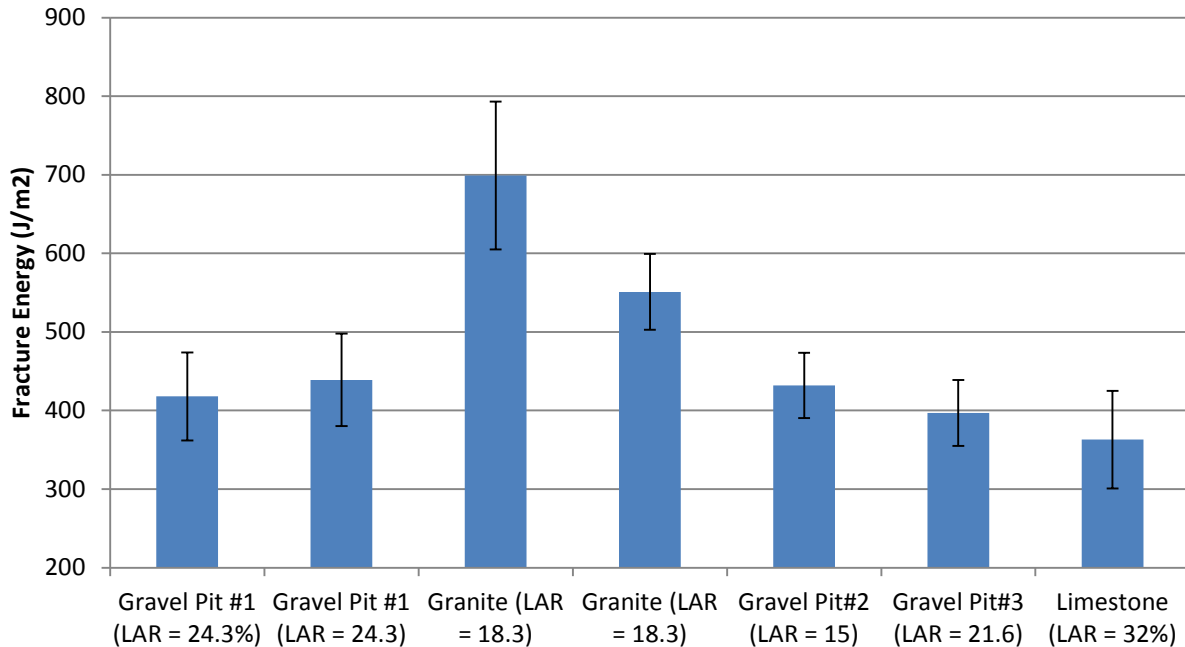


Figure 35. DCT Fracture Energy Results for Mixes from Various Aggregate Sources

For the data presented in Figure 4 Gravel Pit#1 and Granite represent results from the Wimmie and Cisler sources respectively, Gravel Pit #2 is a source in NW WI and the final two sources (Gravel Pit #3 and Limestone) are from SE MN. All mixes were plant produced and aged for 12 hours at 135°C. All mixes were tested at the PG low temperature grade + 10°C, the same procedure used in the current WHRP research. Significantly higher values of DCT fracture energy are observed for the granite mixes, particularly when asphalt was added to meet the 3.0% design air voids. The mix from Gravel Pit #2 had the lowest level of binder replacement and used a heavily modified binder PG 64-28P. With these factors DCT fracture energy could still not approach results observed for the granite aggregate indicating that both aggregate wear resistance and shape could have an impact on fracture energy. The limestone mix, had a DCT fracture energy lower by a factor of 1.5 than the granite mix designed for the same traffic level.

Limited research on the interactive effects of aging and aggregate source was also conducted. In this study three plant produced mixtures, two from a limestone aggregate source (LAR = 32%) and one from a gravel source (LAR = 15%) were evaluated after various levels of aging. The aging levels selected were reheat, 12 hours loose mix aging at 135°C, and 24 hours loose mix aging at 135°C. Results presented in Figure 36 show that the limestone aggregate is insensitive to aging across all aging conditions, whereas a significant decrease in fracture energy is observed for the gravel mix between reheat test results and results after 12 hours loose mix aging. The limestone aggregate the DCT fracture energy parameter is insensitive to significant changes in binder stiffness, a preliminary indication that the aggregate rather than the properties of the asphalt mastic is controlling DCT performance.

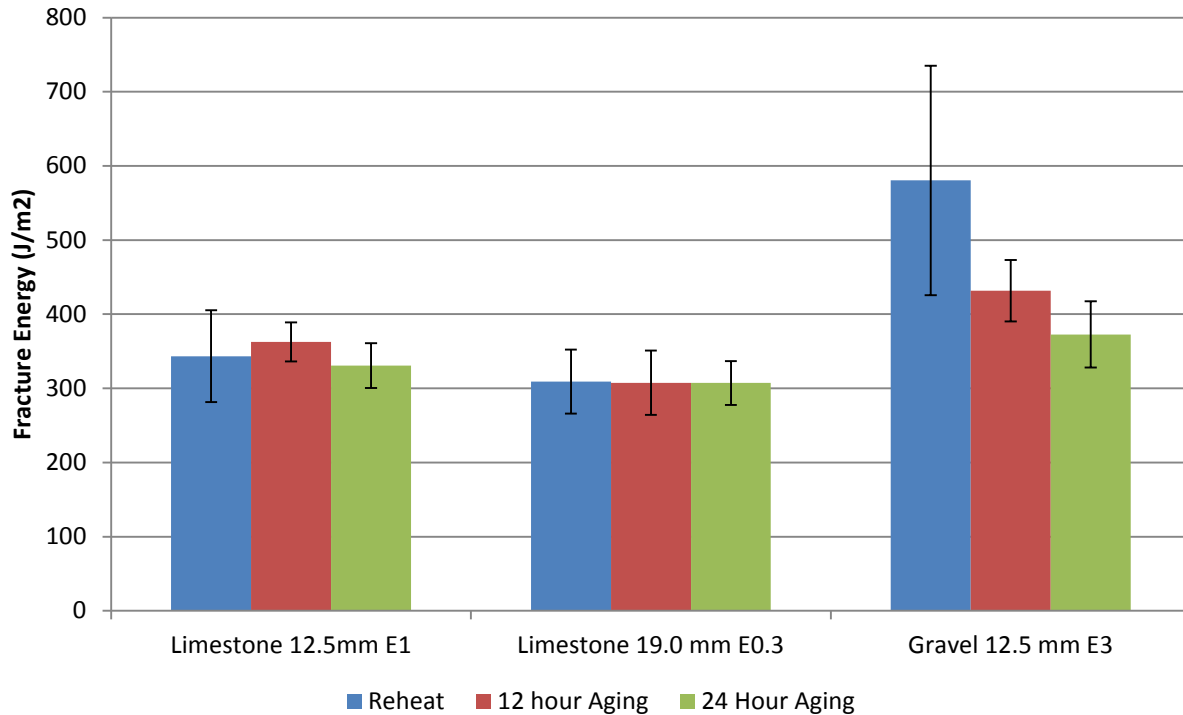


Figure 36. Effect of Aggregate Source and Aging on DCT Fracture Energy

In anticipation of MnDOT implementation of a DCT pilot program for the 2016 construction season a survey of mixes designed using aggregate sources in SE MN were evaluated using the DCT test. The pilot specification tests mixes after short term aging at a test temperature specific to the climate the mix will be placed in. Temperatures are defined as the 98% reliability low temperature grade provided by the LTTTPBind software, for this data set all test temperatures were 21.1°C. All mixes were laboratory produced. Results are presented in Figure 37. The labels at the bottom of the figure include mix traffic level (E0.3 to E3), binder PG, and the aggregate source used for the coarse and fine aggregate portions of the mix. Three different sources of dolomitic limestone and one gravel source were used. For identifying source L1 (LAR 32%/Abs 2.2%), L2 (LAR 31%/Abs 1.0), and L3 (LAR 31%/Abs 1.9%) are limestone sources, G1 (LAR 26%/Abs 1.2%). The fine and coarse portions of the aggregate blends were varied to assess the ability to improve DCT fracture energy by changing aggregate quality and structure. As shown in Figure 37, DCT fracture energy values were insensitive to changes in PG grade and to changes in both the coarse and fine portions of the aggregate structure when the different combinations of limestone are used. The only mix that had a substantial increase in fracture energy was the E3 surface mix made from using a gravel source in the coarse aggregate fraction (far right data point).

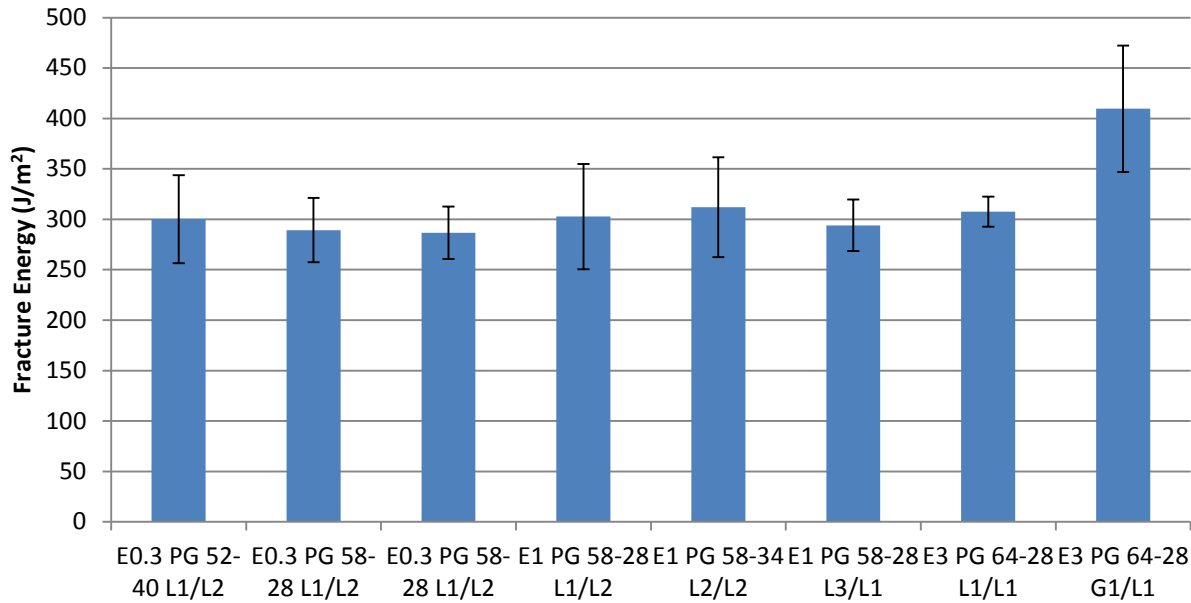


Figure 37: DCT Fracture Energy Results for Mix Designs Produced Using Various Aggregate Sources in SE MN

Minimum fracture energy values in the MnDOT pilot study were 450 J/m² for the E0.3 and E1 mixes and 500 J/m² for the E3 mixes, so none of the designs evaluated met specification. The pilot program selected a high recycle mix for the MnDOT district this mix was placed in. As a result of this data set the project special provision was modified to require the high RAM mix to meet or exceed the DCT fracture energy of a conventional mix from the same aggregate source.

The MnDOT pilot program was a result of a study conducted in the 2013 construction season on five paving projects located throughout the state. The location of these projects is provided in Figure 38. The study required the contractor to submit DCT fracture energy results as part of the mix design, if the mix passed specification limits it was approved, if the mix failed adjustments were recommended and the mix was re-tested. Samples were also taken during production to compare lab vs. field produced DCT results (Johanneck, et al., 2015). A summary of the results of mix design, adjustments (if needed), and production testing is provided in Figure 39, in the figure the red line represents the specification target.

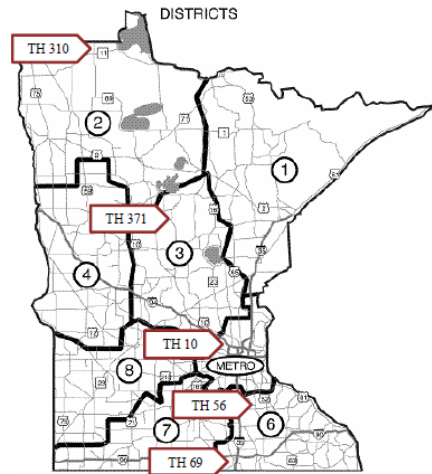


Figure 2.1: Map of project locations across Minnesota.

Figure 38. Location of 2013 Construction MnDOT DCT Pilot Study (Johanneck, et al., 2015)

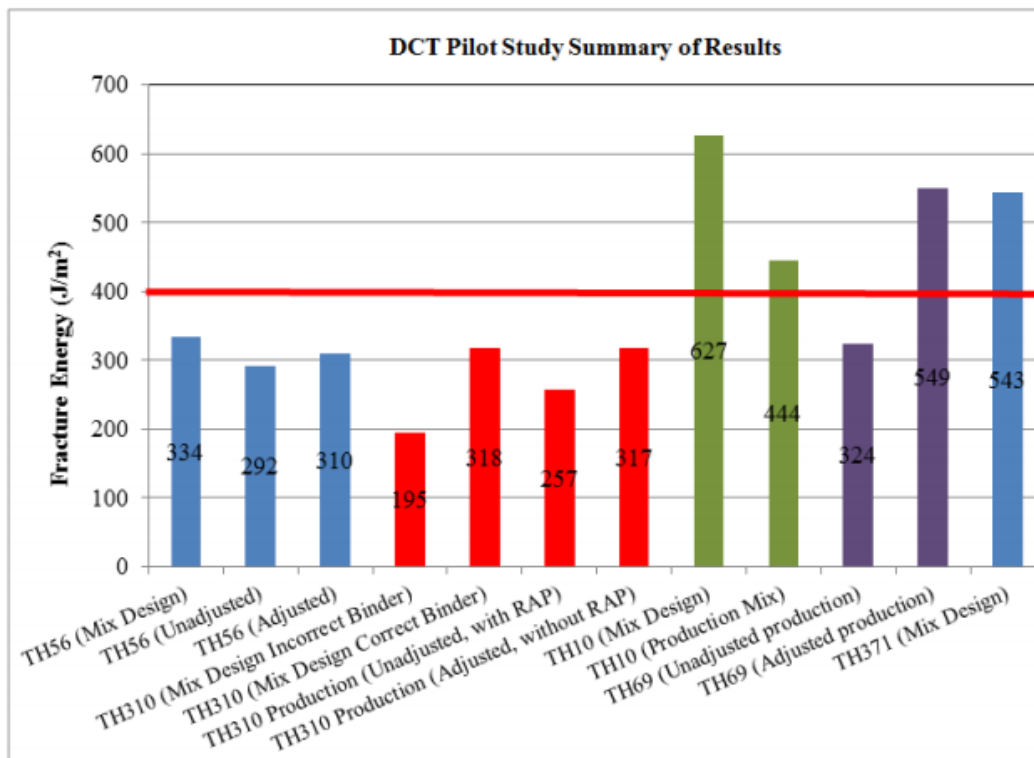


Figure 39. Summary of DCT Fracture Energy Results for Mix Design, Adjustment, and Production MNDOT DCT Pilot Study (Johanneck, et al., 2015)

As shown in Figure 39, two of the five projects selected were able to meet DCT fracture energy limits during mix design. Mix design adjustment was successful in only one of the three projects (TH69). The TH69 project is located near the Minnesota/Iowa border and according to the LTTBind program the 98% reliability low temperature PG grade is -28°C , so the DCT testing was conducted at -18°C and the

initial binder used was a PG 58-28. Based on mix design results the adjustment recommended was to decrease the RAP content from 30% to 20% and reduce the binder grade to PG 58-34, the test temperature remained at -18°C. The adjustments made to TH56 and TH 310 were to increase binder content by 0.1% and decrease RAP content from 20% to 0% respectively. Both adjustments had a marginal effect on DCT fracture energy (Johanneck, et al., 2015). The test section in TH56 is represents the mix design test data generated by MTE presented in Figure 37, in comparing the two data sets, there is very good agreement between the MnDOT and MTE. Both data sets demonstrate that meeting the 400 J/m² or 450 J/m² minimum fracture energy requirement using conventional mix designs under the testing conditions established in the pilot program is unlikely. Crack surveys were conducted nine months after construction and no significant thermal cracking was observed in the sections with DCT fracture energy values well below the 400 J/m² minimum established in the pilot project.

3.1.3.4.1.2 Sensitivity Analysis of the DCT Responses to Mixture Variables

Table 36 provides a summary of the responses discussed for the DCT test and shows the change in their values due to varying the mixture design and aging factors using a best subsets regression model. It also provides the change as a percentage of the average value of each response. Care should be taken in interpreting the results of the table since all regression models generated for the DCT test in this experiment had low explained variance for the reasons outlined in previous sections.

Table 36. Sensitivity Analysis for the DCT Test

Responses Measured			Peak Load		Time at Peak Load		Fracture Energy	
Factors	Ranges in Values		Change	% of Average	Change	% of Average	Change	% of Average
Actual PBR	Min	8%	-0.88	-27%			-250.64	45%
	Max	60%						
Aging Condition	Min	1					-31.30	6%
	Max	2						
Traffic	Min	1			1.07	14%		
	Max	2						
Test Temperature (°C)	Min	-24	-0.12	-4%	0.53	7%	32.94	-6%
	Max	-18						
Binder Jnr (1/kPa)	Min	0.5	-0.23	-7%	0.37	5%	24.33	-4%
	Max	2.7						
Total AC (%)	Min	5.3	0.17	5%	1.52	19%		
	Max	5.8						
P8 (%)	Min	36.5	-0.57	-18%			-172.37	31%
	Max	50.9						
D/B Ratio	Min	0.72	0.75	23%			123.22	-22%
	Max	1.02						
AVERAGE			3.22		7.85		560.8	
STD			0.27		1.21		80.9	
MIN			2.61		5.01		382.5	
MAX			3.91		11.32		776.4	

3.1.3.4.2 SCB-UMN Results and Analysis

The other test used for measuring thermal cracking resistance is the SCB-UMN developed by the University of Minnesota and is described in AASHTP TP105. Similar to the DCT, the test is conducted at the low temperature grade of the binder used in the mixture but it applies the load at much slower rate as controlled by the Crack Opening Mouth Deformation (COMD).

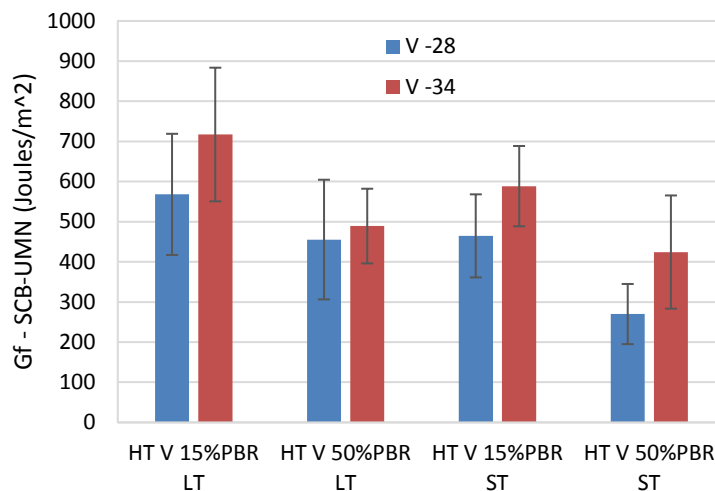
The output of the test is similar to the other SCB tests in terms of providing a stress-strain curve from which the fracture energy is calculated from the area under the curve, but it also allows determining the initial stiffness and the K1 fracture parameter. The fracture energy has been used before in a few studies to relate to the cracking of pavements in the field.

For this test, although a complete set of samples for all combinations were prepared, only a subset of the results could be analyzed due to the difficulty of setting up the test and the loss of many samples during the trial testing to establish the stability of the rate of the CMOD. A complete set of the HT mixes made with Cislser aggregates for the V-28 and V-34 grades is analyzed, in addition to a set of mixtures with S-28 binder grade.

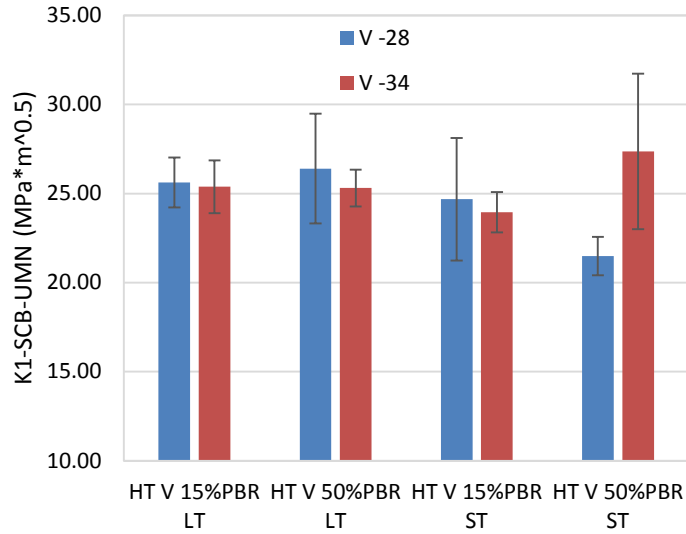
Figure 40 depicts the values of Gf, K1 and Stiffness for the V-28 and V-34 mixtures. The results are organized to show the effects of PBR and the effect of Short Term (ST) versus Long Term (LT) aging. For the Gf results, it can be observed that all mixtures with V-34 binder give on average marginally higher Gf values than the mixtures with V-28 grade binder. It should be mentioned that the mixtures with V-34 grade are tested at -24 °C while the others are tested at -18 °C. The effect of PBR is also observed as the mixtures with 50% PBR give lower values of Gf than those with 15% PBR. In addition, the effect of aging can also be observed with the mixtures that are Long-term (LT) aged giving slightly higher Gf values than those that are Short-Term (ST) aged.

The effects of the binder grade and the PBR are logical; however, the increase in Gf with aging was not expected as aging is expected to make mixtures more brittle. This illogical trend has been reported before and the only explanation that could be offered is that the 12 hours aging at 135 °C is not getting the mixtures to the brittle behavior commonly expected from oxidative aging.

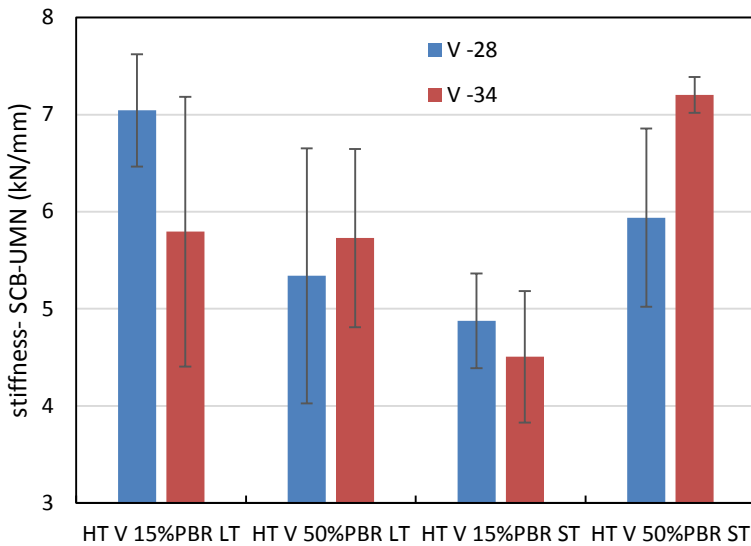
The results for the K1 and initial stiffness shown in Figure 341 do not show useful trends; the K1 values are almost the same for all mixtures and the stiffness values are highly variable and inconsistent.



(a) Fracture Energy, Gf



(b) K1 Parameter



(c) Stiffness

Figure 40. Results of the SCB-UMN cracking test for mixtures with HT designs and V grade binders. Mixtures with V-28 binders are tested at -18 C and mixtures with V-34 binders are tested at -24 C.

Figure 41 depicts the values of the Gf for the mixtures produced with the S-28 binders as compared to mixtures with the V-28 binders for the 15% PBR. As shown the V-28 mixtures give marginally higher values of Gf than the S-28. This could be due to the effect of modification used in the V-28 binders. It is also observed that the Short Term aged mixtures (ST) give lower Gf values than the Long Term aged with the same composition. This is consistent with the results shown in the previous figure.

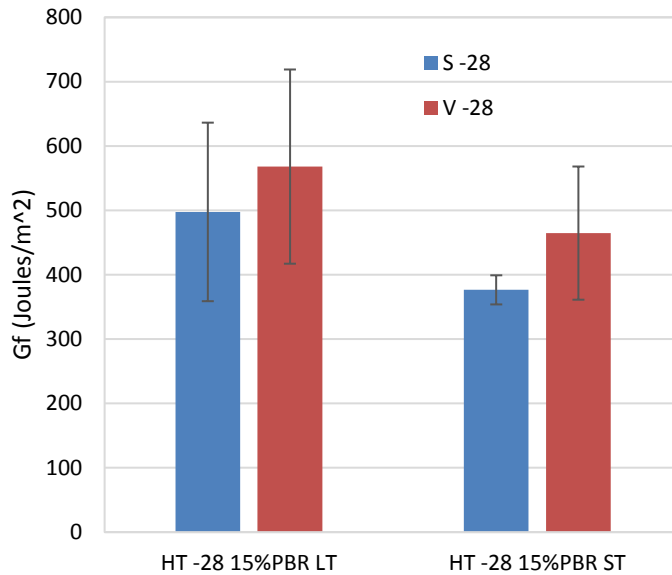


Figure 41. Gf for the mixtures produced with the S-28 binders as compared to mixtures with the V-28 binders for the 15% PBR

3.1.3.5 Low Temperature Performance Specification Framework

The approach used in developing DCT specifications in other states establishes a minimum fracture energy that increases for higher traffic mixes. In general, specification limits range from 400 to 690 J/m² based on aging condition and traffic level. Climate is accounted for by referencing the test temperature to the low temperature PG of the asphalt binder. The data generated in this study and summarized in the literature do not support this type of approach due to the insensitivity of the test to factors known to affect cracking resistance and the influence of aggregate type on fracture energy.

There are two different avenues of research recommended prior to DCT test implementation. The first is expanded use of the DCT test procedure to evaluate the effect of aggregate source using mixes that meet current WisDOT standards. This work will provide supporting information to evaluate the need to adjust specification limits implemented by Iowa or MnDOT or identify the need to go in another direction with the specification. One of the risks of applying one limit to the entire state is that it has potential to cause two extreme cases, one in which use of a hard aggregate results in the mix passing DCT fracture energy regardless of mix composition, and the second in which a soft aggregate is used and the mix cannot pass the specification limit. This issue is well recognized in the literature where it is acknowledged that current specifications will require importing harder aggregates in areas where they are not locally available and the economic tradeoff associated with this cost compared to better performance (via higher fracture energy) should be considered in project selection (Buttler, et al., 2016). The potential impact of this approach is that well established aggregate sources used to construct HMA pavements will be eliminated, causing increased costs associated with importing aggregates and consumption of certain aggregate sources at a higher rate. Using the current test procedure, a possible solution is to establish allow the fracture energy target values to change with regionally or with different aggregate sources.

The second research is a more thorough evaluation of the test procedure as it relates to implementing a specification. Due to the test temperature used, the current specification uses the same limit to evaluate materials with completely different failure behavior. As stated in the literature at this

temperature the fracture energy values vary because the crack path goes through the mastic for mixes prepared with hard aggregate and travels through the coarse aggregate for softer aggregates. At higher test temperatures the effect of aggregate type on fracture energy diminished and the test result is a better representation of the properties of the mastic. Further research is needed to investigate increasing the DCT test temperature in order to remove the confounding effect aggregate type has on interpretation of the data. Low temperature cracking is a non-load associated distress that mainly occurs through the mastic phase of the HMA mix. There is potential that application of the DCT at a higher test temperature will better isolate the behavior of the asphalt mastic, making the test more sensitive to binder replacement, PG grade, aging, and other mix volumetric factors.

These considerations notwithstanding, it may be useful to provide an interim specification framework for discussion, as shown in the table below based on the data in this project. The values for minimum fracture energies are estimated from the average values for MT and HT mixes, and reduced by 200 J/m² to account for the aggregate types in mixes. These values are used for MT mixes in the table and the standard deviation from the results was determined as 100 J/m² for Short Term aging and 50 J/m² for Long Term aging. The minimum values for HT mixes are equal to those of the MT mixes plus one standard deviation, while for LT mixes are equal to the same minus one standard deviation.

Table 37. Initial Framework for Control of Low Temperature Cracking

Traffic	LT			MT			HT		
	Overlay	Other Construction		Overlay	Other Construction		Overlay	Other Construction	
PG-LT	-28	-28	-34	-28	-28	-34	-28	-28	-34
Test Temp	-18	-18	-24	-18	-18	-24	-18	-18	-24
DCT Minimum Fracture Energy (Short-Term Aged 4hrs) J/m ²		300			400			500	
DCT Minimum Fracture Energy (Long-Term Aged 12hrs) J/m ²		250			300			350	
SCB-UMN Minimum Fracture Energy (Short-Term Aged 4hrs) J/m ²		200			350			500	
SCB-UMN Minimum Fracture Energy (Long-Term Aged 12hrs) J/m ²		TBD			TBD			TBD	

In the interim, thermal cracking is estimated in the AASHTOWare ME design method based on three mixture properties: tensile strength at -10°C , creep compliance, and the coefficient of thermal expansion. Recent research conducted by WHRP suggests that thermal cracking risk can be reduced by controlling the low temperature grade of the binder used in the mix. The study used the same three aggregate sources that were included in the current project and identified that asphalt binder PG was the only factor to influence predicted thermal cracking due to the effect of binder grade on creep compliance, the effect of aggregate source was found insignificant (Bonaquist, 2011). Based on these results the proposed interim solution to control thermal cracking until issues with the DCT are resolved is to continue with current practice for conventional mixes and require grading of extracted and recovered asphalt from mix designs that exceed binder replacement limits for RAP, RAS, or RAP/RAS.

3.2 Experiment 2: Sensitivity of Selected Performance Tests to Production Variation

During production, aggregates could degrade to different degrees as they progress through the hot mix plant. The result is typically a slight change in the dust content (P200) of the mix over time. Contractors similarly may adjust added asphalt content to counteract these and other effects in order to maintain volumetrics. An experiment was designed to determine the effects of these changes in production on the five response variables obtained during the SCB-IFIT test. An ANOVA was performed on the dataset with the results shown in Table 38. The tables separate the results in two parts, one for the HT mixes and the other for the MT mixes.

The results of the ANOVA analysis are show that the FI, the post-peak slope, and peak load have fair to good R^2_{ADJ} values with the mix and binder parameters controlled in the experiment, while the fracture energy and displacement at peak load show very low R^2_{ADJ} value.

For the FI values, it is found that the aggregate source and the asphalt content have significant effects, but not the filler content.

For the Post-Peak Slope and the Peak Load, the results show that aggregate source is a significant factor for both responses, while the filler content is only marginally significant (p-value of 0.011) for the HT mixes but not the MT mixes. The asphalt content variation is not significant for responses.

Based on this experiment it is concluded that minor changes to P200 during production would not be expected to significantly affect the FI and Post-Peak Slope; however, changes in asphalt within the tolerance limits could significantly affect FI, and changing aggregate sources could change all responses. This confirms the concern expressed earlier that the results of this procedure could be over-sensitive to the asphalt content.

Therefore, if the FI is used in the specifications, the limits should be set low enough to allow for the inherent variability in asphalt content. Also aggregate source changes should be restricted to avoid failing of the specifications.

Table 38. ANOVA Analysis for Production Variation Experiment at Confidence Level of 95%

	Responses Variables	FI		Post-Peak Slope m		Fracture Energy		Peak Load		Displacement at Peak Load	
		P-Value	Significance	P-Value	Significance	P-Value	Significance	P-Value	Significance	P-Value	Significance
HT-V-28	Aggregate Source	<2.0x10 ⁻¹⁶	Yes	<2.0x10 ⁻¹⁶	Yes	0.054	No	<2.0x10 ⁻¹⁶	Yes	1.8x10 ⁻⁹	Yes
	Asphalt Content	0.001	Yes	0.176	No	1.0x10 ⁻⁵	Yes	0.252	No	4.0x10 ⁻⁴	Yes
	Filler Content	0.124	No	0.475	No	0.001	Yes	0.011	Yes	0.166	No
	R ² _{adj}	66.0%		58.5%		27.6%		55.2%		37.4%	
MT-S-28	Aggregate Source	<2.0x10 ⁻¹⁶	Yes	9.1x10 ⁻¹⁵	Yes	0.257	No	<2.0x10 ⁻¹⁶	Yes	3.4x10 ⁻¹⁰	Yes
	Asphalt Content	0.018	Yes	0.243	No	6.2x10 ⁻⁷	Yes	0.267	No	0.010	Yes
	Filler Content	0.207	No	0.644	No	0.048	Yes	0.306	No	0.492	No
	R ² _{adj}	57.8%		46.5%		26.1%		54.3%		36.9%	

3.3 Experiment 3: Development of Supplemental Guidelines for Required Performance Testing for High Recycled Content Mixes

It is expected that the virgin binder used during the production of HMA or WMA will blend to some degree with the recycled binder used in the mixture. Several national and regional studies have investigated the efficacy of using blending charts to estimate the blended binder rheological properties in the mixture. NCHRP 09-12 investigated the use of blending charts with RAP materials and confirmed that linear blending charts can predict blended binder properties with reasonable accuracy (McDaniel & Anderson, 2001). A more recent WHRP study applied the blending chart concept to RAP and RAS materials from Wisconsin and found that linear blending charts were applicable to RAP materials, but RAS binder showed considerable non-linearity for the low temperature m-value parameter. It was recommended that linear blending be applied to RAS materials up to 30% binder replacement since in practice usage should fall below that threshold (Bonaquist, 2011).

A recently developed, non-solvent based method for estimating blended binder properties uses mortar (mixtures of virgin binder and fine RAP/RAS aggregate) testing to evaluate the effect of blending on the performance grading properties of the mix. This procedure eliminates the use of solvents and may provide a means to directly quantify the extent of blending that occurs between the recycled and virgin binders (Swiertz, Mahmoud, & Bahia, 2011). The mortar method has shown promise in other studies in accurately characterizing blended binder properties (Hajj, Salazar, & Sebaaly, 2012).

3.3.1 Overview of the Results

In this study, results from the extraction and linear blending chart procedure were compared to the results of the mortar procedure for combinations of RAP and RAS materials with two base binders. Binders were extracted using toluene and recovered with the Rotavapor method. For characterization of low and intermediate temperature properties, extracted binders were PAV aged; as-recovered binders were used to characterize the high temperature properties of the extracted binder. Mortar testing followed the methodology proposed by Swiertz and Bahia (Swiertz & Bahia, 2011). RAP materials used in this experiment are the same as used throughout this project, and the RAS materials were supplied by a contractor in Southwest Wisconsin. The experimental design for this study is shown in Table 9.

The continuous grading properties for the recovered binders are shown in the table below. The low temperature properties of the RAS are difficult to measure in the BBR since the binder is exceptionally brittle and difficult to cast. For low temperature characterization of RAS materials, estimation of BBR S(60) and m-value were made from 4 mm DSR testing. RAP materials were characterized both with the traditional BBR method as well as the 4 mm DSR testing. In general, agreement between the methods for S(60) ($R^2 = 0.97$) and m-value ($R^2 = 0.98$) was noted for this study, so 4 mm DSR data was used for all comparisons.

Table 39. Continuous Grading Properties for the Recovered Binders

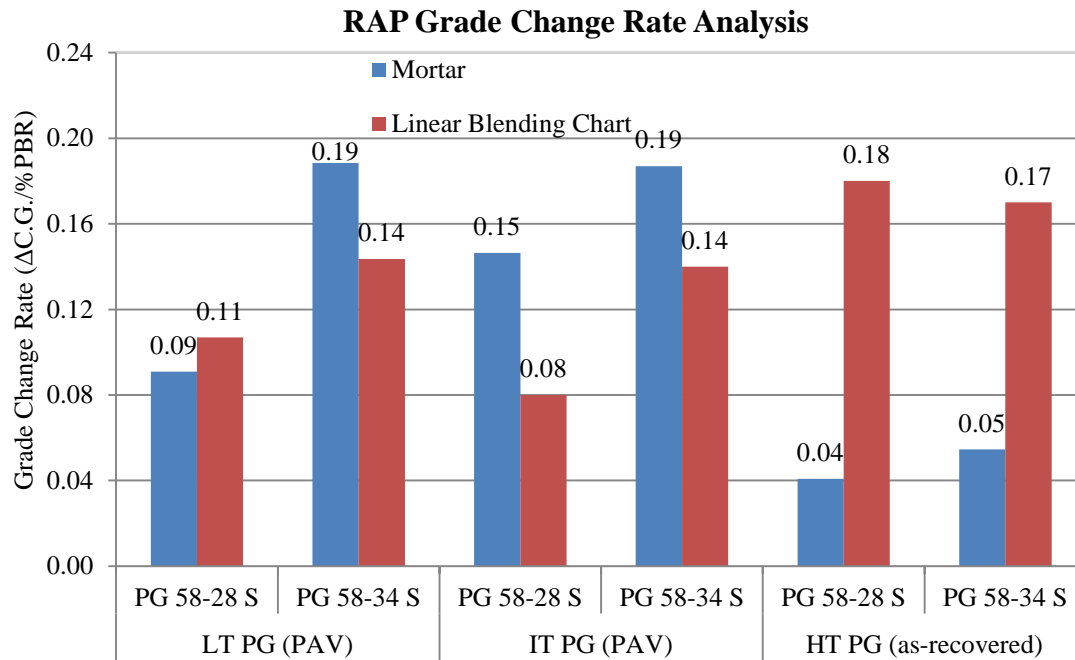
Material	As-Recovered High Temperature Continuous Grade (°C)	PAV Intermediate Temperature Continuous Grade (°C)	PAV Low Temperature Continuous Grade (°C)	ΔT_c
RAP	78.0	26.5	-19.7	-6.8
RAS	149.2	49	9.5	-29.7

To compare the results of the two methods of analysis and account for slight variations in continuous grade determination at different labs, the effect of the recycled binder on the virgin binder grade is normalized using a parameter called the “grade change rate” in this report. The grade change rate is the change in performance grade of the blended binder per one percent binder replacement. For example, a grade change rate of 0.25 °C/%PBR means that for every 4% PBR, the user can expect a 1 °C change in the binder performance continuous grade. Grade change rates are dependent on the virgin binder used, the RAP used, and are usually different at low, intermediate, and high temperatures.

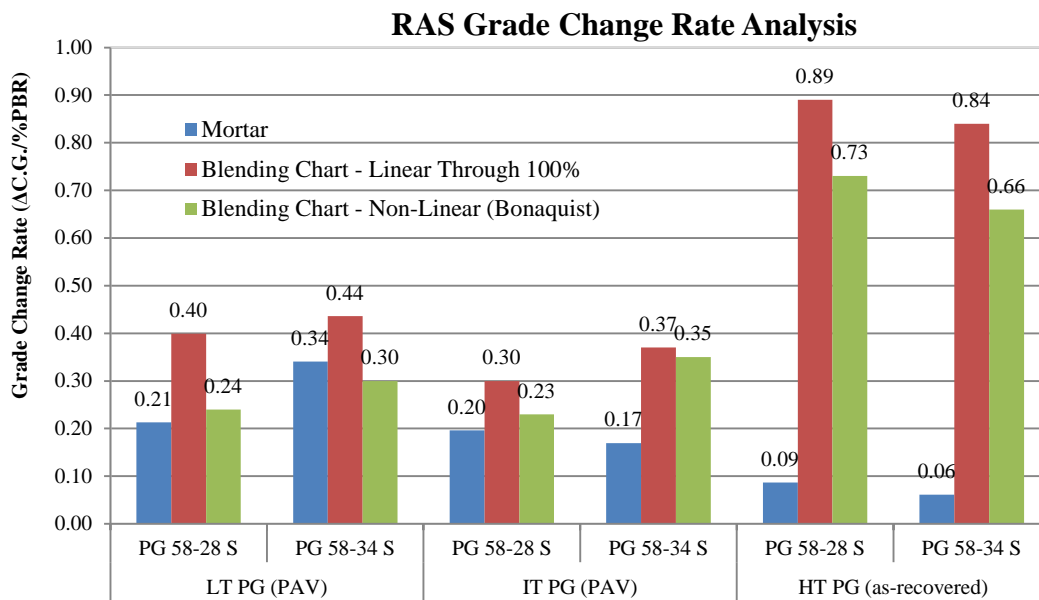
RAP and RAS Analysis

The grade change rate for both blending methods was calculated at low, intermediate, and high temperatures independently for RAP and RAS materials. A summary of this comparison is shown below. For the RAP analysis, the two methods agree well for low temperature and fairly well for intermediate temperature 58-34. At high temperature, the linear blending chart shows approximately four times the grade change rate for the mortar procedure. The differences at high temperature may suggest that either (1) a lack of blending is taking place during the mortar preparation procedure for high temperature testing, and/or (2) mortar is interfering (through particle interaction, bridging, etc.) with accurate DSR measurements. It is important to note that the effects of recycled binder are considered to be beneficial at high temperature, so an accurate characterization is not crucial. Accuracy at low temperatures is considered more critical since recycled materials are assume to be detrimental to resistance to thermal cracking.

Findings for the RAS materials are similar to those for RAP: the low and intermediate temperature characterization shows the closest comparison between linear blending and mortar methods, whereas at high temperature the differences in methods are pronounced. Since the continuous grade of the RAS materials is found to be 149.2 °C, it stands to reason that a lack of blending may be responsible for the low grade change rate for the mortar procedure. Interestingly, the approach proposed by Bonaquist (2011) of using 30% PBR for the limit of linear estimation for RAS appears to compare much more favorably with the mortar procedure, which for RAS materials was prepared at approximately 26% PBR. It should be noted that in all combinations for RAP and RAS final grade of blends are m-value controlled.



(a)



(b)

Figure 42. (a) RAP grade change rate comparative analysis, and (b) RAS grade change rate comparative analysis.

3.3.2 Comparison of RAP and RAS Blends

The grade change rates shown in Figure 42 were used to estimate the absolute change in virgin binder continuous grade at low, intermediate, and high temperature for the combinations of RAP and RAS at the two arbitrary levels of total binder replacement listed in Table 9. In all instances, the change in continuous grade is reported as a positive number, which can be applied to the virgin binder continuous grade to determine the resulting blended binder grade. For example, the 95% RAP/5% RAS blend at 15% PBR resulted in a change in low temperature grade of 1.7 °C for the PG 58-28 base binder. If the starting low temperature grade of this binder is -30 °C, the blended binder would be expected to have an effective grade of -28.3 °C. A summary of these estimates is shown in Figure 43, Figure 44 and Figure 45.

As expected, the low temperature comparison between the extraction and mortar methods is the best, with an average difference between methods of 1 °C for both binders at both PBR levels. At intermediate temperature the average difference remains at 1 °C, although the intermediate temperature grading interval is only 3 °C as opposed to 6 °C at low and high temperatures. At high temperature, however, the average difference between the methods is 7.73 °C, with much wider range. So the methods would not give different results in performance grade changes due to RAS and RAP, with the mortar procedure being more conservative than the extraction procedure.

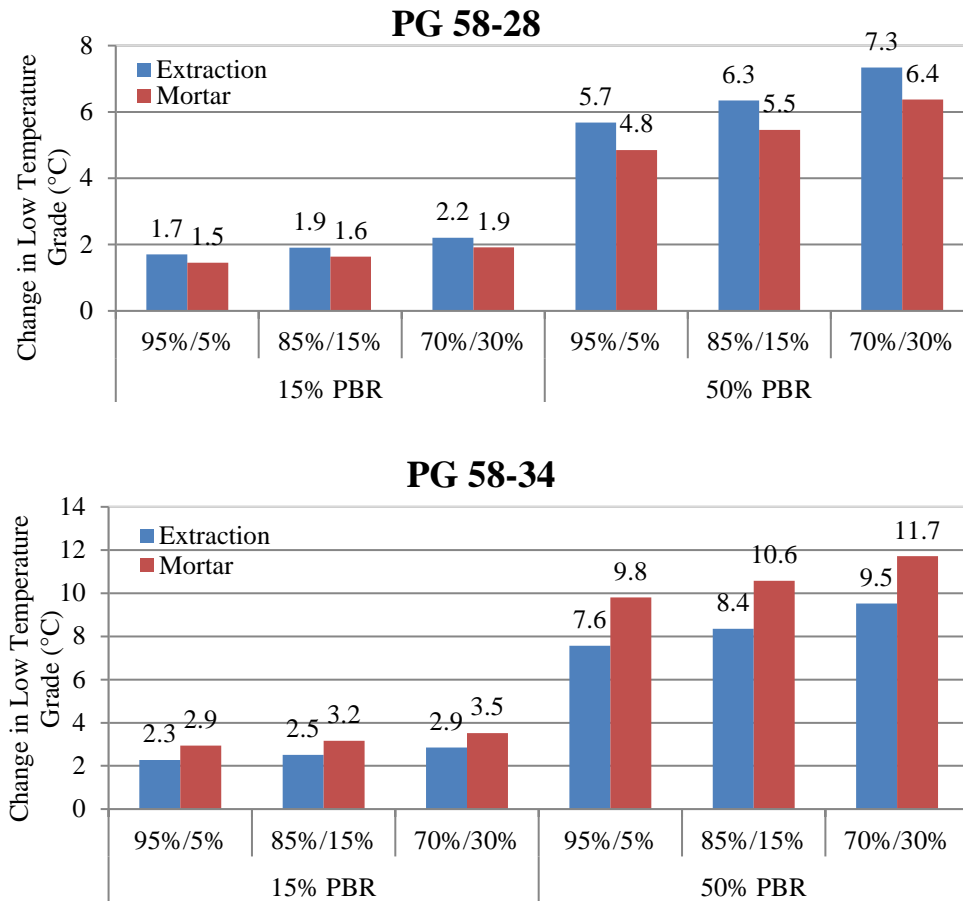


Figure 43. Low Temperature Grade Change analysis for RAP/RAS Combinations (estimated from Grade Rate Changes of Figure 2).

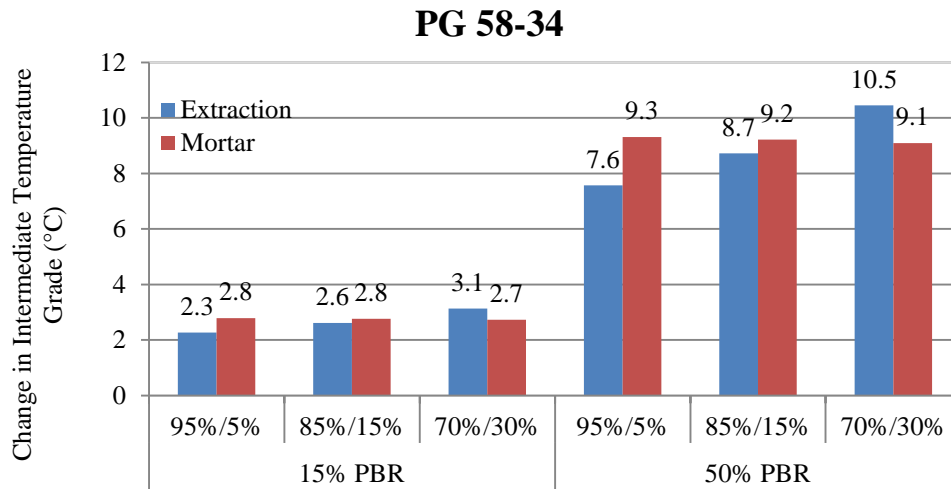
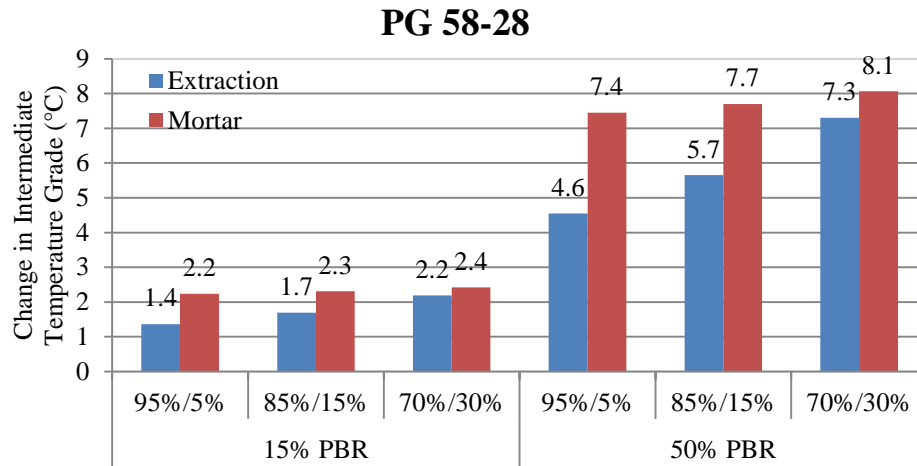


Figure 44. Intermediate Temperature Grade Change analysis for RAP/RAS Combinations (estimated from Grade Rate Changes of Figure 2).

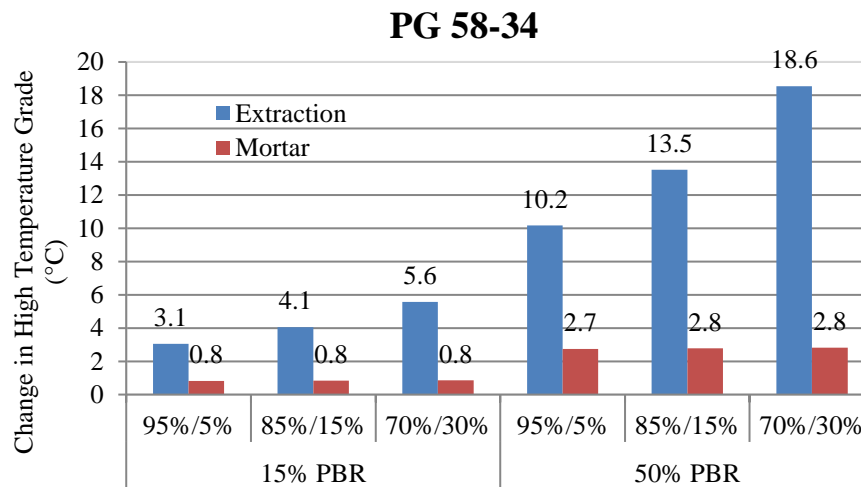
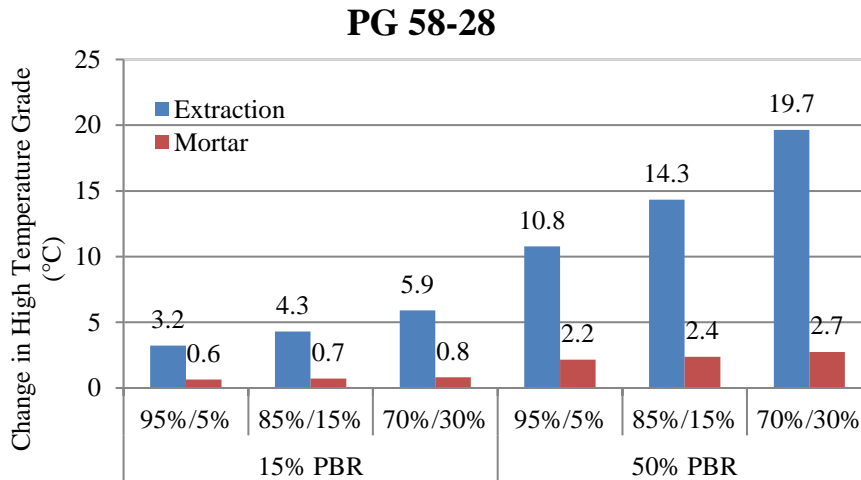


Figure 45. High Temperature Grade Change analysis for RAP/RAS Combinations (estimated from Grade Rate Changes of Figure 2).

3.3.3 Summary of Findings

Findings from the analysis of results of this experiment suggest that at low temperatures the mortar procedure for estimating blended binder properties compares closely with extraction-based linear blending charts for RAP materials. For RAS materials, the mortar procedure closely compares to non-linear (m-value) blending at low temperatures.

At intermediate temperatures the procedures can be expected to give relatively similar results, but since the grading interval at intermediate temperature is 3 °C, minor differences may result in significant difference in grade assignments.

At high temperature the procedures differ significantly, possibly due to a lack of blending in the mortar procedure and forced blending in the blending chart method. The mortar procedure offers a solvent-free alternative to extraction and recovery and may offer the advantage of directly characterizing materials based on the amount of blending that actually occurs. Since some solvents may degrade or otherwise mask

the properties of some binder modifiers, the mortar procedure may be a viable alternative over extraction and use of blending charts.

3.4 Experiment 4: In-Service Field Validation

3.4.1 Background

In 2014 WisDOT initiated a pilot program to investigate the use of higher recycled asphalt contents in mixes, as part of the program a specifications were revised to adjust volumetric mix design targets, RAP/RAS stockpiles, and new specifications were developed to include mixture performance testing as part of the mix design and production monitoring process. The new specification also required performance grading of binder recovered from the mix. Performance tests selected included the Hamburg Wheel Tracking Test, the LSU Semi-Circular Bend Test (SCB), and the Disc Shaped Compact Tension Test (DCT). The specification also includes effects of aging using the AASHTO R30 procedures, the Hamburg is tested on short term conditioned specimens and the cracking tests are conditioned on long term aging. AASHTO/ASTM test procedures were used for the HWT and DCT tests, the SCB test and limits for all three tests were selected based on other states' practices and recent research results. Four projects throughout the state were selected and constructed over the 2014 and 2015 construction seasons. The geographic location of the projects is shown in Figure 46 and a brief description is provided in Table 40. An overview of the pilot program and more detailed information on the STH 77 project have been presented at other meetings including the WAPA conference (2014 and 2015) and AAPT (2016) (Paye, 2015), (Hanz, et al., 2016).

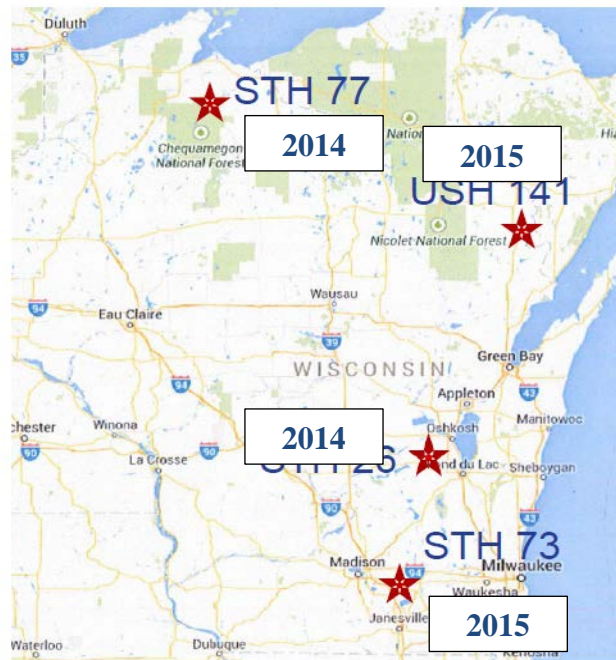


Figure 46. Location of WisDOT High RAM Pilot Projects

Table 40. Overview of High RAM Projects for WisDOT Pilot Program

Project	Project Type	Length (miles)	Description	Const. Date	Coring Date
STH 77 – Clam Lake	Mill and Overlay	4.1 (High RAM) 9.6 (Control)	E3 RAP Only (HR) 12.5 mm and 19.0mm (Control) 12.5 mm	Aug. 2014	Nov. 2015 Apr. 2016
STH 73 – USH 12/14 to I90	Reconstruction	9.6 miles	RAP & RAS in various combinations/PBR levels. Both 12.5 mm and 19.0 mm mixes.	Fall 2014	N/A
USH 141 Marinette County		5.3 miles Lower Layer: 5.3 (High RAM) Upper Layer: 2.0 (High RAM)	E3 RAP Only (HR) 12.5 mm and 19.0mm (Control) 12.5 mm	Spring 2015	Mar. 2016
STH 26 Fondu Lac County		??? Lower Layer only	E10 RAP& RAS (HR) 19.0 mm	2015	Apr. 2016

This study includes data from three of the four projects constructed as part of the High RAM Pilot Program. A total of six test sections were tested including both control and experimental mixes. All three projects were cored in spring of 2016, which corresponds to approximately 1.5 years in-service for STH 77 and six months in-service for USH 141 and STH 26. MTE cored STH 77 in November 2015 for internal research, recovered binder grading and mix performance data from both sampling times will be included in the report.

3.4.2 Analysis Methods

Forensic analysis of the cores included application of new concepts aimed at relating asphalt binder properties to performance and further evaluating mixture compaction. The asphalt binder parameter introduced is ΔT_c , is defined in Equation 4.

$$\Delta T_c = S_{crit}(60) - m_{crit}(60)$$

Where: ΔT_c = Difference in critical failure temperatures (°C).

$S_{crit}(60)$ = Low temperature stiffness continuous grade temperature (°C)

$m_{crit}(60)$ = Low temperature m-value critical continuous grade temperature (°C)

Equation 4

As shown, ΔT_c is available from low temperature grading information if AASHTO T313 is conducted at a minimum of two test temperatures that span the stiffness and m-value failure criteria. Anderson (2011) had identified ΔT_c as an indicator of pavement durability, however in their study ΔT_c was calculated and reported as a positive value. Recent consensus has adopted Equation 1 as the method of calculation resulting in negative values for ΔT_c when the binder becomes m-controlled. The ΔT_c parameter quantifies the relaxation properties of the asphalt binder; As ΔT_c becomes more negative the risk

for cracking increases (Anderson, et al., 2011). The research proposed ΔT_c values of -2.5°C and -5.0°C as cracking warning and failure limits respectively.

Recently the ΔT_c value was correlated to extent of cracking on two test sections in Minnesota, CTH 112 in Olmstead County and on MnRoad. The MnRoad test sections were constructed in 1999 with the objective of investigating use of different binder grades to reduce low temperature cracking. Three binder grades were evaluated, PG 58-28, PG 58-34, and PG 58-40. After 4 years in-service all mixes had similar cracking performance with levels of non-centerline cracking ranging from 0-90 ft, after 5.5 years the cracking in the PG 58-40 section grew exponentially to over 1000 ft. The ΔT_c parameter was determined on loose mix aged in the compacted condition for 10 days at 85°C (doubling of the AASHTO R30 protocol). The PG 58-28 and PG 58-34 were S-controlled or slightly m-controlled with the ΔT_c values ranging from 0.5 to -1.8°C , the PG 58-40 had a ΔT_c value of -4.7°C , demonstrating the ability to discriminate between materials (Reinke, et al., 2015).

The Olmstead County test section was constructed in 2006 as part of a study organized by Western Research Institute (WRI) to investigate the effect of asphalt binder crude source. The test sections included a polymer modified PG 58-34, that used a Canadian crude (MN 1-2), and PG 58-28 grades from Canadian (MN 1-3), Middle Eastern (MN 1-4), and Venezuelan (MN 1-5) crude sources. All of the mixes were virgin design placed over newly constructed base, for more information regarding the project refer to reports prepared by WRI (Pauli, et al., 2012), (Planche, et al., 2014). In 2014 a distress survey was conducted and field cores were taken from each test section. The ΔT_c parameter was measured on asphalt recovered from the top $\frac{1}{2}$ " of the cores and compared to total distress. Total distress is the sum of transverse, longitudinal, and fatigue cracking, results are presented in Figure 47.

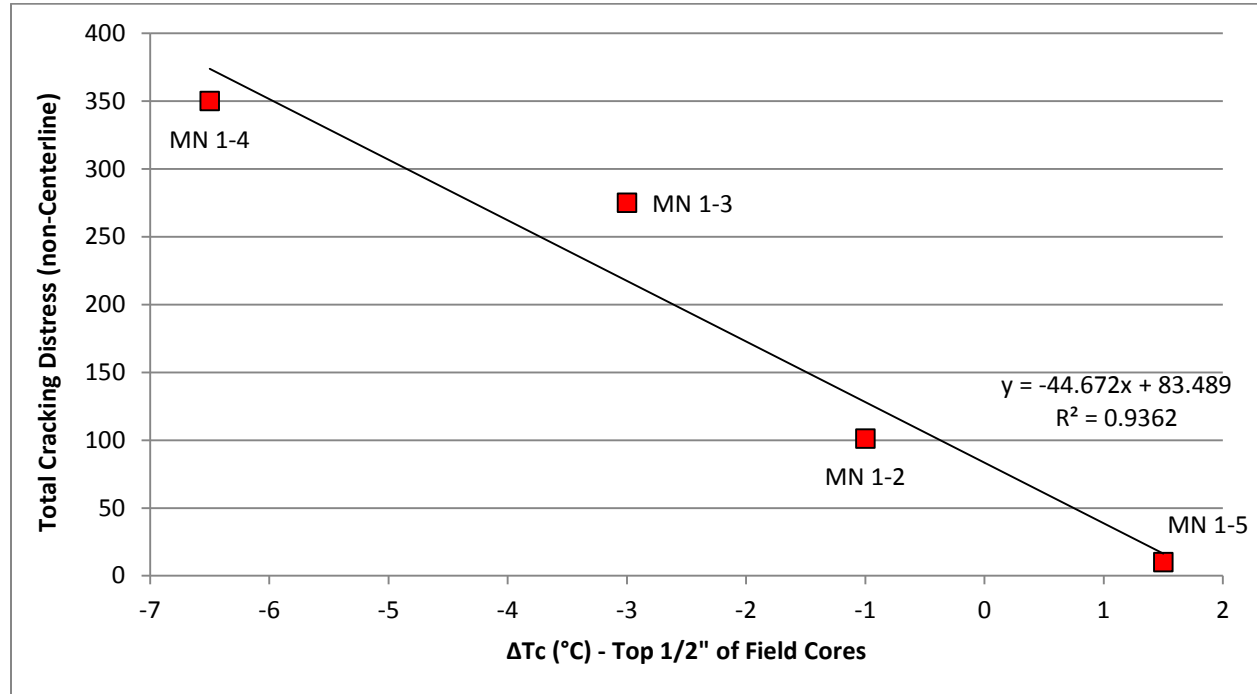


Figure 47. Total Distress vs. ΔT_c – Olmstead County Test Section, WRI Source Study (Reinke, et al., 2015)

All of the materials used in this study met the same PG grade under the current grading systems. The ΔT_c parameter introduces an additional measure of performance by quantifying changes in relaxation properties. In Figure 47 ΔT_c demonstrates a strong relationship with total cracking distress and the ability to discriminate between materials. For this test section total cracking distress ranged from 10 to 350 and the ΔT_c for the different crude sources ranges from $+1.5^\circ\text{C}$ to -6.5°C . Although the sample set is small, research completed to date and the relationship with field distress identify ΔT_c as a promising parameter to better understand asphalt binder durability and field performance.

Image processing has been widely used recently in order to evaluate the relationship between aggregate structure and mechanical properties of asphalt mixtures. In this study it was applied as a forensic tool to measure the aggregate structure of the in-service control and high RAM test sections. Recent studies have shown that the resistance to permanent deformation of asphalt mixtures can be related to the internal aggregate structure parameters such as number of proximity zones and total proximity length (Coenen, 2011), (Roohi, 2012). These parameters are focused on identifying aggregate contacts and defining the stress path traveled during loading. For proper statistical representation of the microstructure of each mixture, six sections obtained as indicated in Figure 48 were scanned using a flatbed scanner and aggregate structure was characterized using the Image Processing and Analysis Software (iPas) developed by UWMARC in cooperation with Michigan State University. For the field cores, the analysis was focused on only the layer of interest (upper or lower).

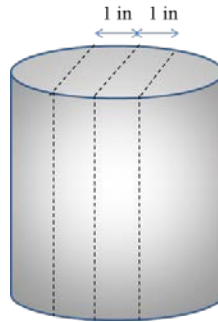


Figure 48. Schematic of Sample Cutting for Image Analysis (Roohi, 2012)

The output of the aggregate structure analysis is an estimate of the proximity or contact length between aggregates, which is used to estimate the internal aggregate structure and connectivity of asphalt mixtures. Using this parameter, a sound aggregate structure with proper aggregate connectivity is expected to adequately distribute stresses and perform better when subjected to traffic or environmental loading. The software uses common digital imaging processing (DIP) methods to convert colored images of asphalt mixtures into a binary image (i.e., black and white). The matrix representation of this binary image is then used in MATLAB for calculation of internal structure parameters. A schematic of the analysis conducted by the software is provided in Figure 49.

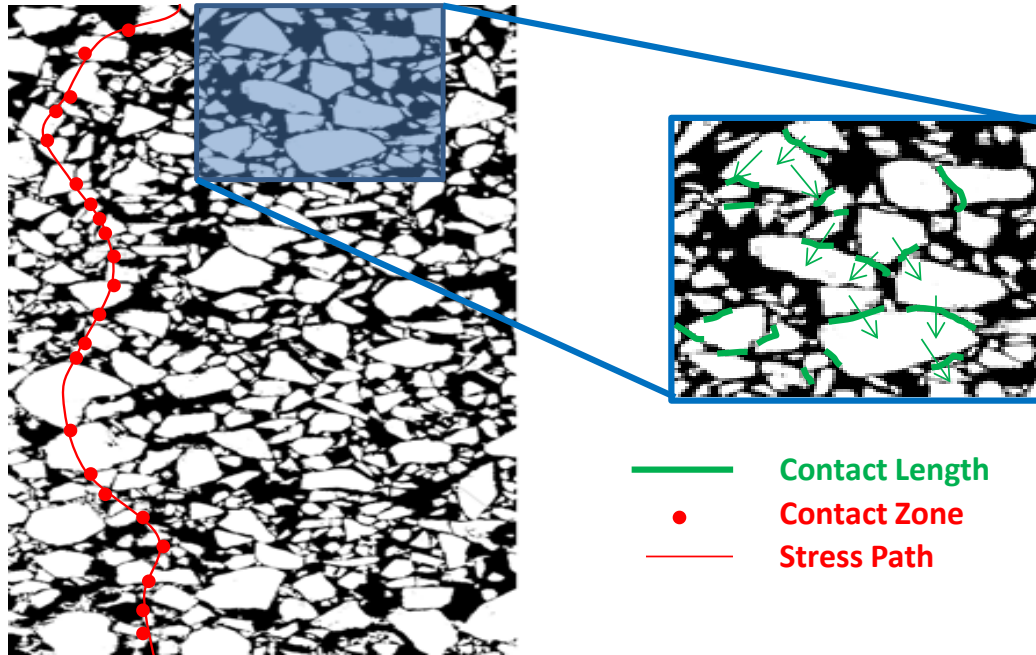


Figure 49. Microstructural parameters from imaging analysis in iPas (Roohi, 2012)

The aggregate internal structure in the mixes is characterized by means of the number of proximity zones and total proximity length. Proximity zones are defined based on a predetermined distance identified by the user. If the pixels representing two aggregates are closer than the threshold distance, the two aggregates are said to be in proximity. The proximity length between two aggregates corresponds to the summation of the pixels in the proximity zone. An example of defining the proximity zone and the length of contact is provided in Figure 50.

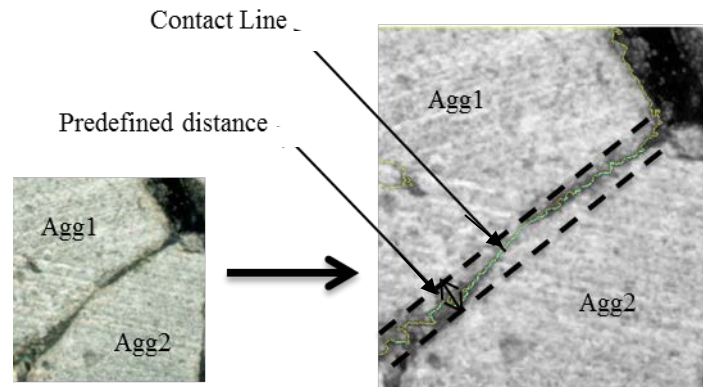


Figure 50. Schematic of Definition of Aggregate Proximity and Length of Proximity (Roohi, 2012)

3.4.3 Experimental Plan

The objective of this experiment is to establish the baseline performance characteristics of the control and high RAM mixes using recovered binder grading and selected mixture performance tests. In addition to the recovered binder grading and image analysis, performance testing was incorporated into the High RAM pilot project with the goal of producing mixtures with high recycle contents that meet or exceed the performance of control mixes. Mix performance tests to evaluate fatigue and thermal cracking were selected to address the main distresses of concern associated with increased binder replacement. Based on

results of Experiment 1b the DCT and SCB-IFIT test methods were selected to leverage existing data sets presented in other research (Al-Qadi, et al., 2015), (Braham, et al., 2009). Unfortunately mix performance testing is limited to the STH 77 project because it is the only project for which 6 inch cores were available, while 4 inch cores were taken on the USH 141 and STH 26 projects. Given the influence of ligament length, defined as the distance between the crack tip and top of the specimen, and other factors, modification of existing test methods to accommodate 4 inch cores was deemed outside the scope of this research. Cores from all projects were available for use in recovered binder grading and IPas analysis.

Previous research has shown that increased levels of binder replacement, particularly when RAS is used, have potential to accelerate the rate of aging in the pavement (Reinke, et al., 2014). In-place pavements do not age uniformly, an aging gradient with depth exists with most aging occurring at the surface due to increased exposure to air and ultra-violet radiation at the surface of the pavement (Petersen, 2009). To measure the change in properties with depth recovered binder grading was conducted on two lifts of the surface mixes sampled (STH 77 and USH 141), the top ½” and the remainder of the lift. One recovery was conducted on the STH 26 cores because a high RAM mix design was only used in the lower layer.

Recovered asphalts were evaluated using the PG grade as specified in AASHTO M320 and ΔT_c parameter. High temperature grade was determined using the AASHTO T315 test procedure and the low temperature grade was estimated using the 4mm parallel plate geometry as a surrogate for the bending beam rheometer. This change was made due to the small quantity of recovered asphalt available from the sliced sections of the core. Previous research has established a testing and analysis method for use of the 4-mm parallel plate to estimate low temperature grade (Sui, et al., 2011), (Sui, et al., 2010).

3.4.4 Results and Analysis

3.4.4.1 Recovered Binder Grading

Recovered binder results were analyzed separately for STH 77 because it was the only project with ~18 months service life and data points from two coring times were available for analysis. The first set of cores was taken in November 2015 by MTE approximately 15 months after construction; the second set was taken in by WisDOT in April 2016, approximately 20 months after construction. For the cores taken by MTE, representative sections of the control and high RAM sections were selected and six cores were taken from the EB and WB lanes for analysis. The WisDOT cores were taken at various points of the two test sections, alternating between WB and EB lanes of traffic. The High RAM mix had 36.7% binder replacement (from RAP) and was made with a PG 58-40 asphalt grade; the control mix had 24.5% binder replacement and was made with a PG 58-34 asphalt grade. In the presentation of results cores are grouped by mix type, then by location in the pavement structure to provide direct comparison of the high RAM and control mixes for each layer of the core analyzed. Results for high temperature grading are presented in Figure 51.

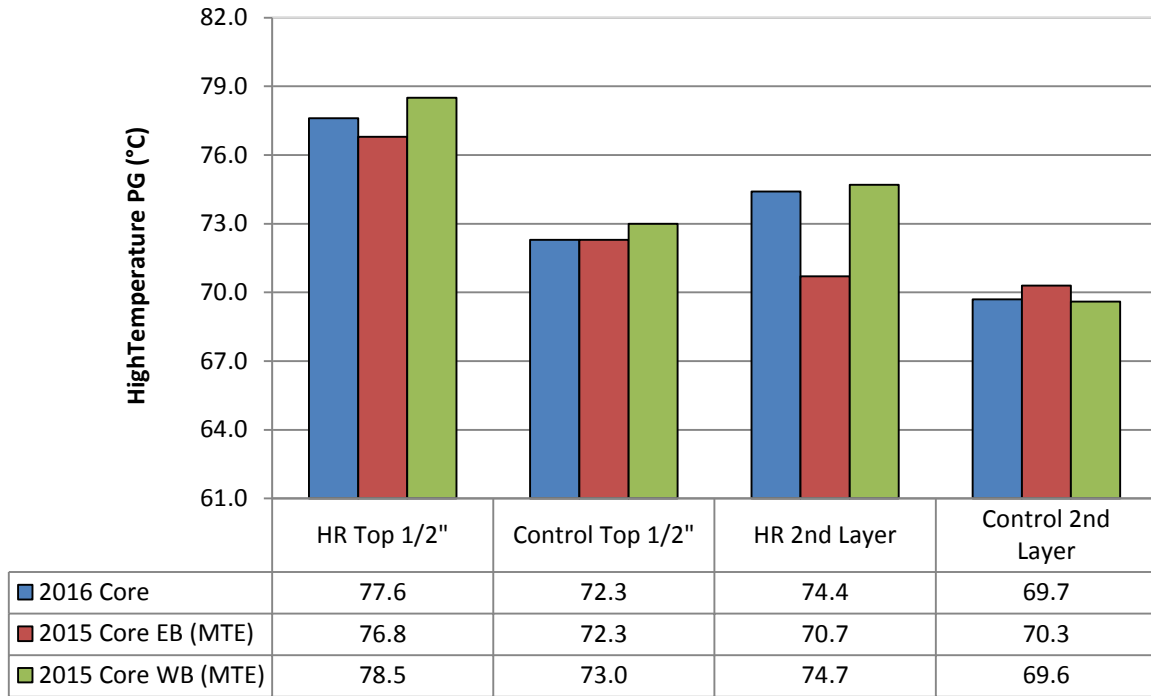


Figure 51. High Temperature PG of Recovered AC from STH 77 High RAM and Control Mixes

As shown in Figure 51 the high temperature grade of the high RAM mix is approximately 3°C higher than that of the control for both the material extracted from the top 1/2" and the remainder of the layer in the core. Furthermore, the decrease in high temperature grade with pavement depth is approximately 4°C for the high RAM mix and 2°C for the control. In most cases there is little variation between traffic lanes or time of coring, the exception being the high RAM 2nd Layer. As a frame of reference, the high temperature PG of the asphalt recovered from production sampled mix and reported during the pilot project was 80.9°C. Results of low temperature PG grading are presented in Figure 52.

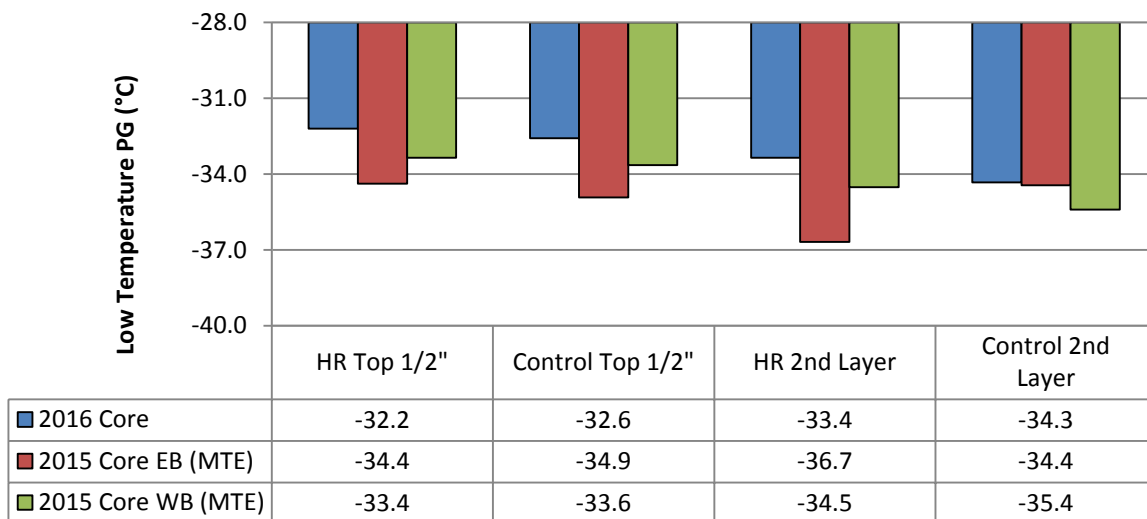


Figure 52. Low Temperature PG of Recovered AC from STH 77 High RAM and Control Mixes

The low temperature grade of the recovered asphalt from the high RAM mix sampled during production was -35.3°C. Comparison of grading results from 2015 and 2016 indicates a decrease in low temperature performance grade of approximately 2°C in the top ½” of both the high RAM and control mixes. The target low temperature grade for the project was -34, as a result of this decrease both mixes fall slightly below this requirements, but have similar performance grades. A decrease in grade was also observed for the 2nd layer of the high RAM mix, while the control remained unchanged. The low temperature grade is defined by the limiting factor of two criteria, $S(60) < 300$ MPa and $m(60) > 0.300$, the ΔT_c parameter provides insight as to which property is controlling low temperature performance. Results for ΔT_c are presented in Figure 53.

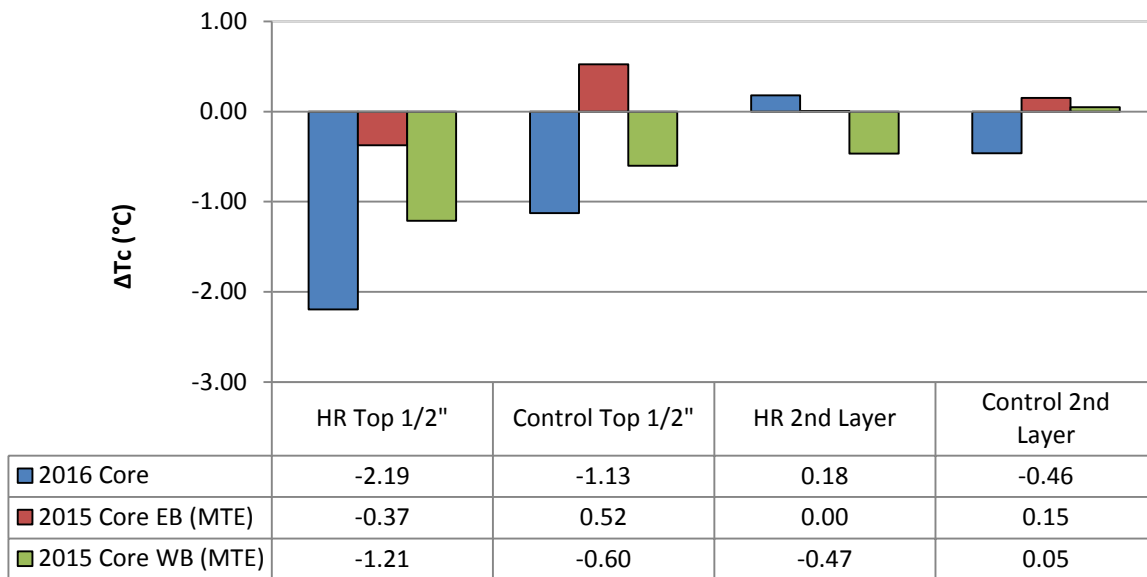


Figure 53. Low Temperature PG of Recovered AC from STH 77 High RAM and Control Mixes

In relation to performance, a positive value of ΔT_c is preferred, as it indicates that the low temperature performance grade is S-controlled. Negative values indicate m-controlled failure, as ΔT_c become more negative it is indicative of the binder losing its ability to relax, thus becoming more prone to non-load associated cracking. The results presented in Figure 53 clearly demonstrate the aging gradient that exists in in-service asphalt pavements as there are significant differences between the results for top ½” and the underlying material. The ΔT_c value of the high RAM mix sampled during production was 0.5°C, this value is within 1°C of the results for the 2nd layer indicating that the mix at that location did not substantially age over the 20 months in-service. Conversely, negative values of ΔT_c were observed in the top ½” of both cores, with significant changes occurring between 2015 and 2016 coring times. In regards to this parameter the control mix is performing better whereas the high RAM mix ΔT_c value of -2.2°C is approaching the proposed warning limit proposed by Anderson (Anderson, et al., 2011).

Data from the USH 141 and STH 26 projects is presented separately because these pavements were both constructed in 2015. The USH 141 design had a target climate of PG 58-34, the E3 12.5 mm high RAM mix design was prepared with 32% binder replacement from FRAP (AC content = 5.6%), the virgin binder grade used was not listed on the mix design. The STH 26 project had a target climate of PG 58-28, the E10 19.0 mm mix design included 44% binder replacement, 26% from FRAP (AC content = 4.9%) and

18% from RAS (AC content = 21.0%). For each mix type and location in the pavement structure results are presented comparing the high RAM to the control mixtures. The STH 26 mix was in the lower layer, so only one recovery was completed because the surface of the mix was not exposed. Results presented in Figure 54 for high temperature PG show similar trends to those presented for the STH 77 project. The PG grade of the high RAM mixes is significantly higher than that of the control for the USH 141 top 1/2" and the STH 26 binder layer. Similar values of PG were observed for the USH 141 2nd layer.

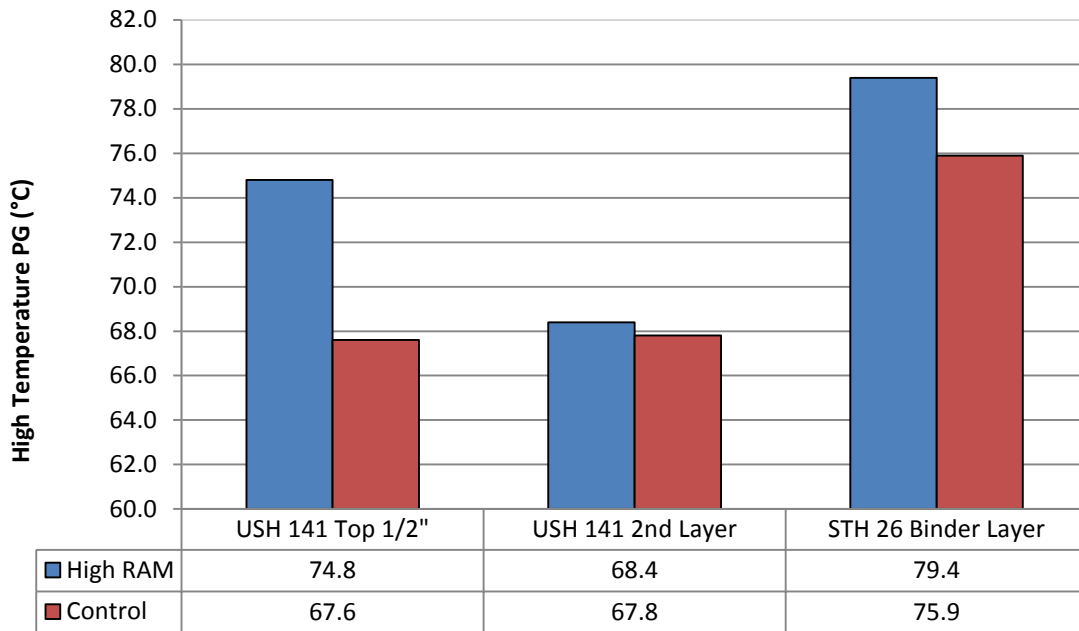


Figure 54. High Temperature PG of Recovered AC from USH 141 and STH 26 High RAM and Control Mixes

Low temperature grading results for the mixes studied are presented in Figure 55, the target low temperature PG grades for the USH 141 and STH 26 mixes are -34°C and -28°C respectively. For the USH 141 mixes the results for the top 1/2" recovery perform similarly but have low temperature grades slightly warmer than the target grade. This is again attributed to the differential aging that occurs near the pavement surface, as the material below the 1/2" layer meets performance grading requirements for both mixes with the grade of the high RAM mix 1.2°C warmer than that of the control. There was not a significant difference between the STH 26 mixes and both meet the target -28°C low temperature grade.

For USH 141 results presented in Figure 56 indicate although a change in PG grade relative to the -34°C target climate was observed with pavement depth the cracking not a risk as ΔT_c values remain near zero or slightly S-controlled. Given the age of the pavement, this result is not uncommon as the ΔT_c parameter becomes more negative as the pavement ages. Significant differences were observed between the High RAM and control mixes for the STH 26 project, with the ΔT_c values approaching -2.0°C for the high RAM mix. This result is attributed to the relatively high level of binder replacement from RAS (18%). Due to the manner in which the asphalt is processed and additional weathering shingle asphalt has very poor relaxation properties, as an example the tear-off RAS source used in this study had a ΔT_c of -28.9°C on the as-recovered material.

In summary, the data presented does not indicate substantial differences in binder grading or relaxation properties between the high RAM and control mixes. This result is promising, but not unexpected given the relatively young age of the pavements evaluated. A recognized risk of increasing binder replacement, particularly with RAS is premature cracking due to the accelerated aging caused by recycled binders (Reinke, et al., 2014). Data presented in this study serve as a baseline for continued monitoring of these projects, to allow for future work to correlate changes in pavement distress with material properties.

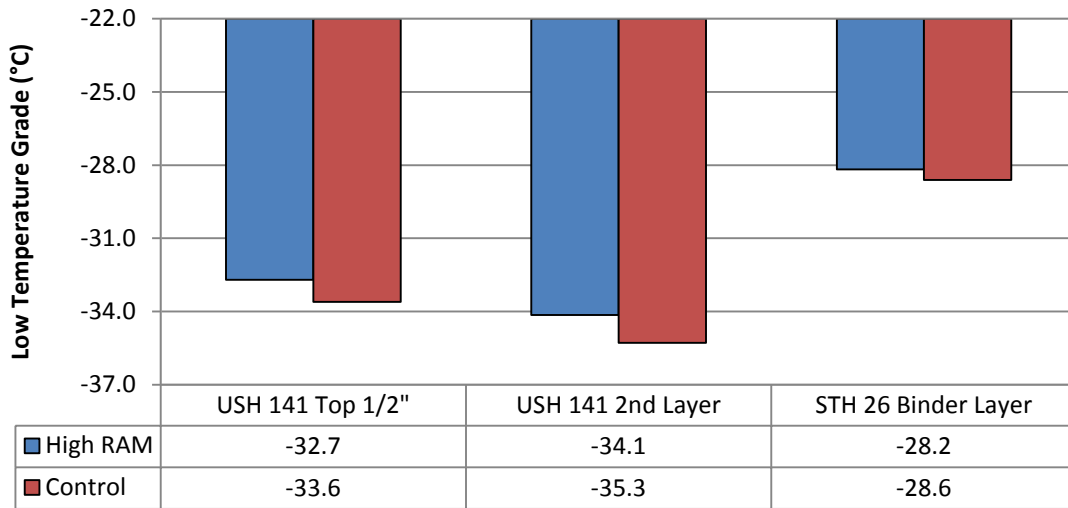


Figure 55. Low Temperature PG of Recovered AC from USH 141 and STH 26 High RAM and Control Mixes

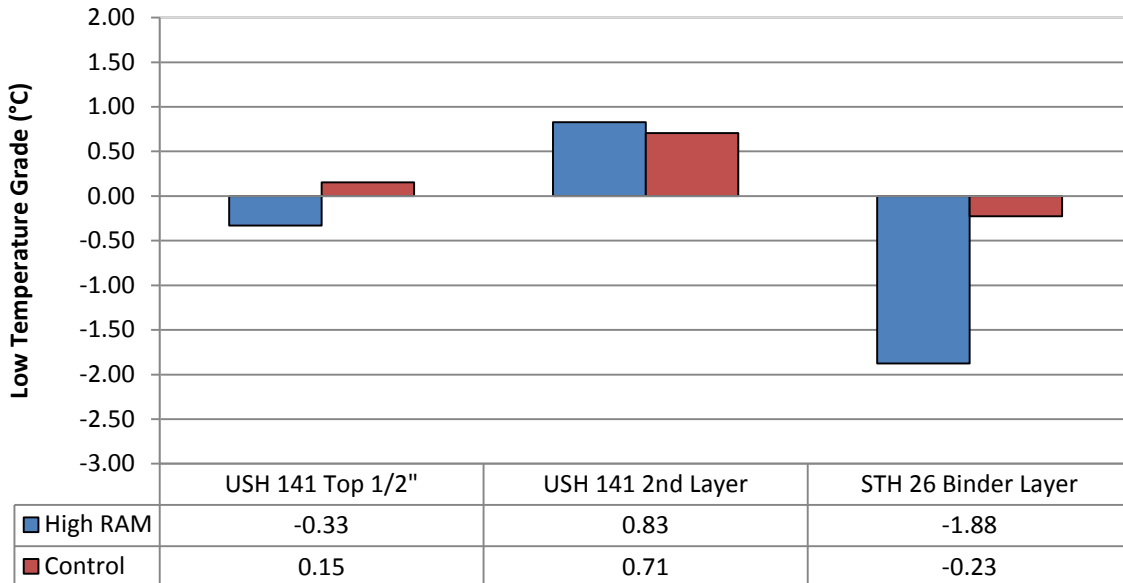


Figure 56. ΔTc of Recovered AC from USH 141 and STH 26 High RAM and Control Mixes

3.4.4.2 STH 77 Mixture Performance Results

The DCT and SCB-IFIT test methods were selected to compare the low and intermediate temperature cracking resistance of the STH 77 mixes. Data collected by MTE on the 2015 cores is also included to evaluate the effect of time in the field. Comparison of the DCT fracture energy for the mixes is provided in Figure 57, the error bars represent that standard deviation of the test for this data set (56 J/m²).

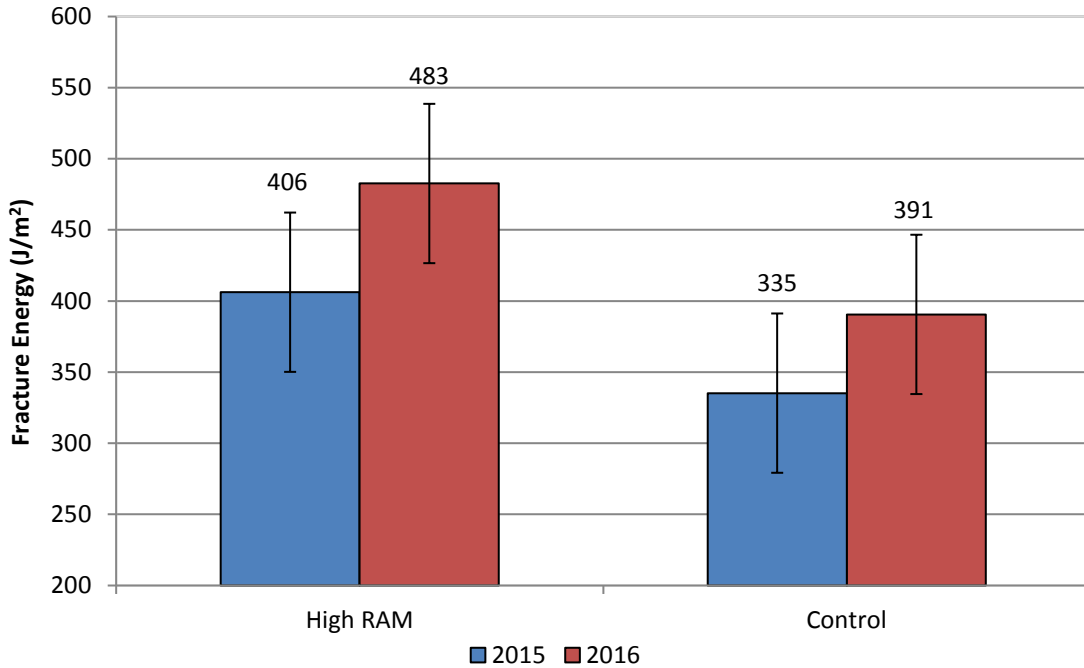


Figure 57: DCT Fracture Energy at -24°C – Comparison of STH 77 High RAM and Control Mixes

The high recycle mixture had fracture energy values after both sampling times that were 60 – 90 J/m² higher than that of the control. Effects of time were consistent with MnRoad data presented by Braham on loose mix aged samples in which he demonstrated that fracture energy increased up to 8 hours of aging then decreased (Braham, et al., 2009). The mechanism for why this behavior was observed was explained previously in discussion of the laboratory DCT results. Given the effect of aging, the relatively young age of the pavement, and the consolidation that occurs during initial traffic loading the increase in fracture energy with coring time is not unexpected. While directional trends are observed in the data, when the experimental error is considered the differences are not statistically significant.

The three reporting parameters specified by ASTM D7313 are summarized in Table 41. As a point of reference, DCT results for plant produced mix loose mix aged for 12 and 24 hours are also included (Hanz, et al., 2016). The higher fracture energy observed in the high RAM mix relative to the control for the field cores is caused by higher values of both peak load and time to peak load. Given that the aggregate structure of the mixes is similar, differences between the mix designs including effective binder content and the use of modifiers were identified as potential reasons for the difference in performance.

Table 41: Summary of DCT Parameters for Field Cores and Laboratory Aged Mixtures

Mix	Year	Peak Load (kN)		Time at Peak Load (s)		Fracture Energy (J/m ²)	
		Avg.	COV	Avg.	COV	Avg.	COV
STH 77 High RAM	12 hr @135C	4.5	1%	8.1	32%	634	11%
	24 hr @135C	3.9	1%	6.2	17%	588	22%
	2015	2.67	6%	6.70	4%	406	14%
	2016	2.29	6%	7.89	6%	482	12%
STH 77 Control	12 hr @135C	3.1	10%	6.25	1%	296	7%
	24 hr @135C	3.0	1%	6.6	5%	360	1%
	2015	1.55	0%	6.42	12%	335	0%
	2016	2.41	16%	6.64	4%	391	15%

Values of fracture energy for the long term aged laboratory produced specimens were significantly higher than the field cores for the high RAM mixes and similar to the results for the control mix. As a result the differences observed between the laboratory aged high RAM and control mixes is statistically significant. Relative to other mixes/cores the laboratory aged high RAM mixes had a much higher peak load, which contributes to higher fracture energy. Further monitoring with time of the field cores is needed to see if further differentiation between mixes and an increase in peak load is observed.

The SCB test procedure recently developed by University of Illinois (SCB-IFIT) was selected to compare intermediate temperature performance of the control and high RAM test sections. Similar to the DCT data, SCB-IFIT data is available on both 2015 and 2016 field cores. The test was selected because of existing application of the test on field cores for projects in Illinois. For these projects, the range in Flexibility Index of the cores was from ~0.5 to 12.0, performance was classified into three categories: Type I (Acceptable), Type II (Inferior), and Type III (Unacceptable). Preliminary Flexibility Index minimums for these levels on field cores are 4, 2, and 1 (Al-Qadi & Ozer, 2015). Results for the 2015 and 2016 field cores are presented in Figure 58.

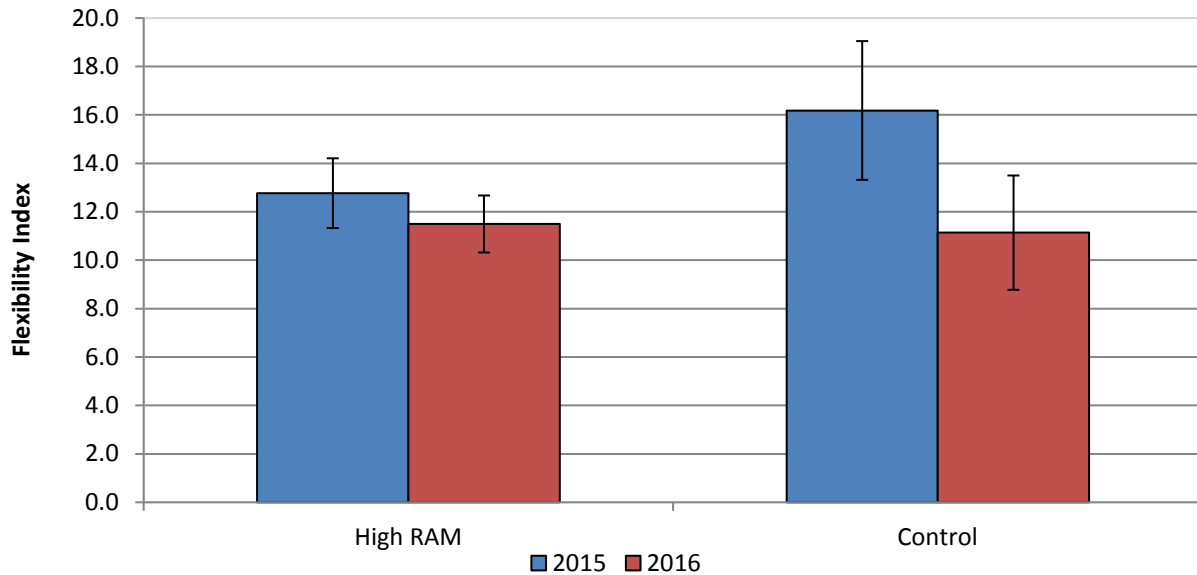


Figure 58: SCB-IFIT Flexibility Index at 25°C – Comparison of STH 77 High RAM and Control Mixes

Flexibility Index (FI) values for both sampling times are well above the 4.0 minimum value proposed as an acceptable limit in the UIUC research (Al-Qadi & Ozer, 2015). For the 2015 cores, the FI of the control mix was 3.4 points higher than that of the control, this difference was not observed in the 2016 data and FI values between mix types were equal. Additional parameters measured during the SCB-IFIT test are summarized in Table 42.

Table 42: Summary of SCB-IFIT Parameters for Field Cores

Mix	Year	Fracture Energy (J/m ²)		Post Peak Slope (kN/mm)		Stiffness Index (N/mm)		Flexibility Index	
		Avg.	COV	Avg.	COV	Avg.	COV	Avg.	COV
STH 77 High RAM	2015	1552	8%	-1.22	9%	2361	1%	12.8	11%
	2016	1411	6%	-1.23	4%	2425	9%	11.5	10%
STH 77 Control	2015	1760	7%	-1.11	13%	1793	34%	16.2	18%
	2016	1482	12%	-1.34	9%	2731	11%	11.1	21%

Trends in the data are consistent with changes that occur over time for in-service pavements. With aging mix stiffness index increased, most likely as a function of both mix consolidation under traffic loading and aging. It is interesting to note the change in stiffness that occurred between 2015 and 2016 cores for the control mix, relative to a minor change in the high RAM mix. For the 2016 core data the mixes had very similar values of fracture energy and post-peak slope. As the mix becomes more brittle the post peak slope will become more negative.

3.4.4.3 Aggregate Structure Analysis Using IPas

The IPas software was used as a measure of in-place aggregate structure in terms of the Total Proximity Length (TPL) per unit area of 100 cm². Packing of aggregates results in higher TPL values and better

resistance to rutting due to more aggregate contacts (proximity). The TPL has been related to laboratory rutting resistance via the Flow Number test in previous research (Roohi, 2012). Results for the images taken from the field sections are presented in Figure 59.

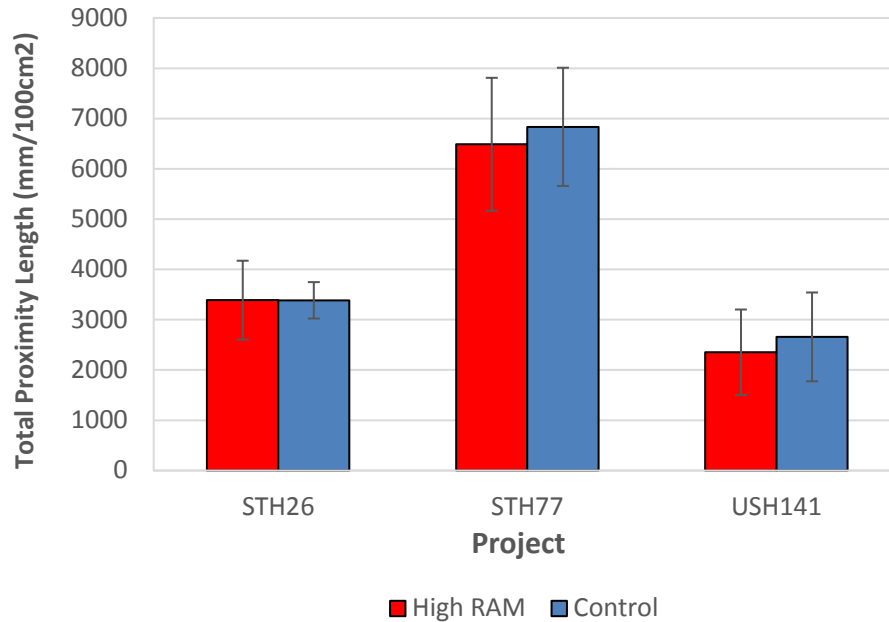


Figure 59: IPas Results for High RAM and Control Mixes – Comparison of Total Proximity Length (mm/100cm²)

Interpretation of the results is limited to a comparison between the high RAM and control mixes for a given project. Using this metric the use of high RAM mixes has no significant impact on aggregate structure as values of TPL between control and high RAM mixes are virtually identical for all through projects. Project to project comparison is not possible because both the age of the pavements and location in the pavement structure are confounding factors. For example, the STH 77 project has been in-service one year longer, allowing for more densification with traffic. Additional monitoring of the change in TPL and rutting performance with time is needed to assess the usefulness of the IPas approach as a forensic tool.

3.4.5 Summary and Conclusions

Preliminary results did not identify any significant performance concerns with the high RAM mix designs relative to the control as for most performance tests the high RAM designs performed as well or better than the control designs when tested for the Fracture Energy. The exceptions are the ΔT_c values of the top 1/2" of the STH 77 mix and the ST 26 mix were slightly more negative than the control, but did not exceed the warning limit established by previous research. Given the relatively young age of the pavements it is promising that no differences were observed, however monitoring of both materials properties and pavement performance over time is required to verify the initial laboratory work conducted as part of the High RAM Pilot Project and the initial forensic research presented in this study. This data set introduced new evaluation parameters and set baseline values for future comparisons of how these change with time. It is recommended that the most promising tests be selected and applied on an annual or bi-annual basis to continue to track material properties and to begin to develop relationships with pavement performance.

4. Conclusions and Recommendations

This study is by far one of the largest that WisDOT has undertaken to evaluate the feasibility of using performance-related properties of mixtures to supplement the SuperPave mixture volumetric specifications. The study included four experiments in which a large number of mixtures, mainly produced in the lab, were evaluated for rutting resistance, moisture damage effects, fatigue cracking resistance, and thermal cracking. The study also included short term and long term aging of loose mixtures. The results are used to propose specification framework for each of the main distresses (Rutting and Moisture Damage, Fatigue Resistance, and Thermal Cracking Resistance). The framework includes specific testing procedures and specification parameters. It also provides very preliminary limits derived based on the averages and distribution of the values measured for the mixtures tested. The following points provide a summary of the findings.

1. **Dynamic Modulus E***: The values of E* measured at 4 temperatures (4.2 C, 21.1, 37.2, and 54.4 °C) vary based on the aggregates used, the mixture design (NT or HT) and the binder grade. The E* values, at a given temperature and frequency of loading, can vary by as much as 165%, or as small as 65% of the minimum value measured due to the mixture composition variation. This range is important and could have significant impact on stresses and strains in a typical pavement section.
2. **Rutting and Moisture Damage Resistance**: The Flow Number test in the confined and unconfined condition was used, as well as the Hamburg Wheel Tracking Test (HWTT) to measure effect of repeated loading and moisture at high temperatures. It is found that the HWTT results in a very similar mechanism of rutting to the Flow Number. However there is not a one-to-one match of the rutting rate due to the fact that HWTT provides partial confinement that is lower than the confinement in the FN test. The HWTT mechanism of rutting changes significantly after the Stripping Inflection Point (SIP), which appears to be due to moisture effects. It is recommended that the HWTT is used for measuring both rutting resistance as well as moisture damage potential. The parameters selected include the creep rate, the SIP, the strip rate, and the passes to 12.5 mm rut depth. Also it is recommended to conduct the test at 45 °C. The following table represents the specification framework recommended.

Table 43. Rutting Resistance Framework: All tests done at 45 °C

Climatic Region/ Traffic		LT	MT	HT
North	Minimum Creep Rate (mm/1000 passes)	-1.50	-0.75	-0.375
	Minimum Passes to 12.5 mm	6,000	9,000	12,000
South	Minimum Creep Rate (mm/1000 passes)	-1.25	-0.625	-0.312
	Minimum Passes to 12.5 mm	7,500	11,250	15,000

Moisture Damage Potential Framework

- If Ratio of Stripping slope to Creep slope: ≥ 2.75 , passes to SIP should be checked
- Passes to the Stripping Inflection Point (SIP): Same as Passes to 12.5 mm
- Stripping Slope: $\geq - 2.25$ for all mixtures

3. **Fatigue Cracking Resistance:** Based on the literature review and a recent WHRP study the Semi-Circular Bend (SCB) test was selected as the potential test for this distress type. Two procedures (SCB-LSU and SCB-IFIT) were included in this study. Both procedures are found to have deficiencies in terms of producing logical trends in measuring effect of mixture and aging variables included in the experiments. Therefore a modified SCB-LSU procedure recommended in a recent WHRP study is recommended for the specification framework. The main reason for this recommendation is the use of the Post-Peak Slope in the analysis, which appears to be a useful parameter to measure effects of oxidative aging and use of RAP. The following table presents the framework proposed. The mixture property used is the Flexibility Index (FI).

Table 44. Intermediate SCB Test Framework

Traffic	LT			MT			HT		
Construction	Overlay	Other Construction		Overlay	Other Construction		Overlay	Other Construction	
PG-LT	-28	-28	-34	-28	-28	-34	-28	-28	-34
Test Temp.	19	19	16	19	19	16	19	19	16
Minimum FI (Short-Term Aged 4hrs)	*	6.0		*	12.0		*	18.0	
Minimum FI (Long-Term Aged 12hrs)	*	2.5		*	5.0		*	7.5	

* The limits for Overlay should be increased by 50% to account for the excessive movements at the pavement joints or cracks. This increase should be left to the discretion of the material engineer of the project.

4. **Thermal Cracking Resistance:** For thermal cracking the Disc-Compact- Tension (DCT) and the SCB test developed by the University of Minnesota (SCB-UMN) were included in the study. Due to the challenges faced in interpretation of the statistical analysis results and the lack of good fit of the regression models, it was difficult to decide if the DCT or the SCB-UMN should be used. Also there were mixed trends for the effect of long term aging on the values of the fracture energy, which is the parameter recommended for this distress. Therefore both tests and both aging conditions are included in the recommended framework until further studies allow expanding the database and validating which test and aging condition is preferred.

Table 45. Low Temperature Cracking Tests Framework

Traffic	LT			MT			HT		
Construction	Overlay	Other Construction		Overlay	Other Construction		Overlay	Other Construction	
PG-LT	-28	-28	-34	-28	-28	-34	-28	-28	-34
Test Temp	-18	-18	-24	-18	-18	-24	-18	-18	-24
DCT Minimum Fracture Energy (Short-Term Aged 4hrs) J/m ²		300			400			500	
DCT Minimum Fracture Energy		250			300			350	

(Long-Term Aged 12hrs) J/m ²						
SCB-UMN Minimum Fracture Energy (Short-Term Aged 4hrs) J/m ²		200		350		500
SCB-UMN Minimum Fracture Energy (Long-Term Aged 12hrs) J/m ²		TBD		TBD		TBD

5. **Experiment 2:** The sensitivity of fatigue cracking parameters to variability of asphalt binder content and filler content within allowable construction tolerance were studied in Experiment 2. Based on results of this experiment it is concluded that minor changes to P200 during production would not be expected to significantly affect the FI and Post-Peak Slope measured by the SCB-IFIT procedure; however, changes in asphalt within the tolerance limits could significantly affect FI, and changing aggregate sources could change all responses. This confirms the concern expressed in earlier works that the results of this procedure could be over-sensitive to the asphalt content.

Therefore, if the FI is used in the specifications, the limits should be set low enough to allow for the inherent variability in asphalt content. Also, aggregate source changes should be restricted to avoid failing of the specifications.

6. **Experiment 3:** To provide supplemental guidelines to control the properties of mixture with high RAM content, the results from binder extraction and blending charts procedure were compared with the mortar testing procedure for a limited number of combinations. The results indicate that the mortar procedure offers a solvent-free alternative to extraction and recovery and may offer the advantage of directly characterizing materials based on the amount of blending that actually occurs in high RAM mixtures. Since some solvents may degrade or otherwise mask the properties of some binder modifiers, the mortar procedure may be a viable alternative over extraction and use of blending charts.

7. **Experiment 4:** An attempt was made to validate the limits proposed in the specifications frameworks proposed from the data collected in experiment 1 of the study. However only one project could be sampled due to various challenges. However, imaging analysis of cored samples taken from 3 projects, as well as testing of recovered asphalt binders was completed. The data was also complemented by results from another recent study in WI. The limited results analyzed did not identify any significant performance concerns with the high RAM mix designs relative to the control as for most performance tests the high RAM designs performed as well or better than the control designs when tested for the Fracture Energy. The exceptions are the ΔT_c values of the top 1/2" of the STH 77 mix and the ST 26 mix were slightly more negative than the control, but did not exceed the warning limit established by previous research. Given the relatively young age of the pavements it is promising that no differences were observed, however monitoring of both materials properties and pavement performance over time is required to verify the initial laboratory work conducted as part of the High RAM Pilot Project and the initial forensic research presented in this study. It is recommended that the most promising tests be selected and applied on an annual or bi-annual basis to continue to track material properties and to begin to develop relationships with pavement performance.

5. References

- Al-Qadi, I. L. et al., 2015. *Testing Protocols to Ensure Performance of High Asphalt Binder Replacement Mixes Using RAP and RAS*, Champaign, IL: Illinois Department of Transportation.
- Al-Qadi, I. & Ozer, H., 2015. *Impact of RAS and RAP on Asphalt Mixtures' Fracture: The Need for a Cracking Potential Test*. Fall River, MA.
- Anderson, M., King, G., Hanson, D. & Blankenship, P., 2011. *Evaluation of the Relationship between Asphalt Binder Properties and Non-Load Related Cracking*. Journal of the Association of Asphalt Paving Technologists, pp. 615-663.
- Aschenbrenner, T., 1995. *Evaluation of Hamburg Wheel-Tracking Device to Predict Moisture Damage in Hot Mix Asphalt*. Transportation Research Board. Transportation Research Record 1492.
- Bonaquist, R., 2011. *Effect of Recovered Binders from Recycled Asphalt Shingles and Increased RAP Percentages on Resultant Binder PG*. Madison: Wisconsin Highway Research Program.
- Bonaquist, R., 2011. *Precision of the Dynamic Modulus and Flow Number Tests Conducted with the Asphalt Mixture Performance Tester*. Washington D.C. NCHRP Report 702, National Cooperative Highway Research Program.
- Bonaquist, R., 2011. *Characterization of Wisconsin Mixture Low Temperature Properties for the AASHTO Mechanistic-Empirical Pavement Design Guide*, Madison, WI: Wisconsin Department of Transportation.
- Braham, A., Buttlar, W. & Clyne, T., 2009. *The Effect of Long Term Laboratory Aging on Hot Mix Asphalt Fracture Energy*. Journal of the Association of Asphalt Paving Technologists, pp. 417-454.
- Braham, A., Buttlar, W. G. & Marasteanu, M., 2007. *Effect of Binder Type, Aggregate, and Mixture Composition on Fracture Energy of Hot-Mix Asphalt in Cold Climates*. Transportation Research Record, Journal of the Transportation Research Board, Volume 2001, pp. 102-109.
- Buttlar, W. G., Hill, B. C., Wang, H. & Mogawer, W., 2016. *Performance-Space Diagram for the Evaluation of High and Low Temperature Mixture Performance*. Asphalt Technology Journal of the Association of Asphalt Paving Technologists, Volume 85.
- Coenen, A. M. K. H. B., 2011. *Aggregate Structure Characterization of Asphalt Mixtures Using 2-Dimensional Image Analysis*. International Journal of Road Materials and Pavement Design.
- Dave, E. et al., 2011. *Low Temperature Fracture Evaluation of Asphalt Mixtures Using Mechanical Testing and Acoustic Emissions Techniques*. Journal of the Association of Asphalt Paving Technologists, pp. 193-225.
- Haji, E., Salazar, L., & Sebaaly, P., 2012. *Methodologies for Estimating Effective Performance Grade of Asphalt Binders in Mixtures with High Recycled Asphalt Pavement Content*. Transportation Research Record, 53-63.
- Hanz, A., Dukatz, E. & Reinke, G., 2016. *Use of Performance Based Testing for High RAP Mix Design and Production Monitoring*. Asphalt Paving Technology, Journal of the Association of Asphalt Paving Technologists, Volume 85, p. TBD.
- Johanneck, L. et al., 2015. *DCT Low Temperature Fracture Testing Pilot Project*, St. Paul Minnesota: Minnesota Department of Transportation.

McDaniel, R., & Anderson, R. M., 2001. *NCHRP Report 452: Recommended use of Reclaimed Asphalt Pavement in the Superpave Mix Design Method*. Washington D.C.: Transportation Research Board National Research Council.

Mohammad, L.N., Wu, Z., and Aglan, M.A., 2004. *Characterization of Fracture and Fatigue Resistance of Recycled Polymer-Modified Asphalt Pavements*, 4th RILEM International Conference on Cracking in Pavements, pp. 375-382.

Mull, M.A., Stuart, K., Yehia, A., 2002. *Fracture resistance characterization of chemically modified crumb rubber asphalt pavement*, Journal of Materials Science, Vol.37, pp. 557-566.

Pauli, A. T., Farrar, M. J. & Harnsberger, P. M., 2012. *Material Property Testing of Asphalt Binders Related to Thermal Cracking in a Comparative Site Pavement Performance Study*. Delft, Netherlands, Springer Netherlands, pp. 233-242.

Paye, B., 2015. *WisDOT Pilot: High Recycle Mixes*. Madison, WI, s.n.

Petersen, J., 2009. *A Review of the Fundamentals of Asphalt Oxidation: Chemical, Physiochemical, Physical Property, and Durability Relationships*, Washington D.C. Transportation Research Board of the National Academies.

Planche, J., Turner, F., Farrar, M. & Glaser, R., 2014. *Lab and Field Performance of Mixtures Containing REOB Modified Asphalt*. Washington D.C., Transportation Research Board of the National Academies.

Quintus, H.L.V., Jagannath Mallela, Ramon Bonaquist, C.W. Schwartz, and R.L. Carvalho., 2012. *Calibration of Rutting Model for Structural and Mix Design*. Washington D.C.: National Cooperative Highway Research Program.

Reinke, G. et al., 2014. *Impact of the use of Reclaimed Asphalt Shingles on Mixture and Recovered Binder Properties*. Raleigh, NC, Taylor and Francis, pp. 1088-1098.

Reinke, G. et al., 2015. *Further Investigations into the Impact of REOB & Paraffinic Oils on the Performance of Bituminous Mixtures*. Fall River, MA, s.n.

Roohi, N. L. T. H. B., 2012. *Characterization of Mixture Rutting Performance Using 2-D Imaging Techniques and Internal Structure Parameters*. Asphalt Paving Technology, Journal of the Association of Asphalt Paving Technologists, Volume 80, pp. 109-138.

Sui, C. et al., 2011. *New Low Temperature Performance Grading Method Using 4mm Parallel Plates on a Dynamic Shear Rheometer*. Transportation Research Record, Journal of the Transportation Research Board, Volume 2207, pp. 43-48.

Sui, C., Farrar, M., Tuminello, W. & Turner, T. F., 2010. *New Technique for Measuring Low-Temperature Properties of Asphalt Binders with Small Amounts of Material*. Transportation Research Record, Journal of the Transportation Research Board, Volume 2179, pp. 23-28.

Swiertz, D., & Bahia, H., 2011. *Test Method to Quantify the Effect of RAP and RAS on Blended Binder Properties without Binder Extraction*. Canadian Technical Asphalt Association, 43-60.

Swiertz, D., Mahmoud, E., & Bahia, H., 2011. *Estimating the Effect of Recycled Asphalt Pavements and Asphalt Shingles on Fresh Binder, Low-Temperature Properties Without Extraction and Recovery*. Transportation Research Record, 48-55.

Appendix A

Summary of Mixture Design Results

A database for all details of Mixture design and all E* testing results has been developed and is available to WisDOT in electronic format as part of this final report.

Material Detail		%Binder Replacement	Total AC	Added AC	RAP AC	Gmb		Gmm		Va		VMA		VBE		Pbc	AFT	P8	P200	D/B Ratio
			Rep	Rep	Rep	Rep	Ave	Rep	Ave	Rep	Ave	Rep	Ave	Rep	Ave	Rep	Rep	Rep	Rep	Rep
Cisler-15% PBR	MT-S-28	20	5.64	4.5	1.14	2.365	2.4	2.453	2.5	3.76	3.6	15.97	15.9	12.21	12.2	5.3	10.6	50.9	3.8	0.72
						2.371		2.462		3.52		15.76		12.24						
	MT-S-34		5.64	4.5	1.14	2.399	2.4	2.475	2.5	3.85	3.7	15.48	15.4	11.63	11.6	5.1	10.2	50.9	3.8	0.75
						2.408		2.473		3.57		15.23		11.66						
	MT-V-28		5.64	4.5	1.14	2.399	2.4	2.467	2.5	3.38	3.4	15.48	15.5	12.1	12.1	5.3	10.6	50.9	3.8	0.72
						2.399		2.457		3.38		15.48		12.1						
	MT-V-34		5.54	4.4	1.14	2.393	2.4	2.468	2.5	3.78	3.8	15.6	15.6	11.82	11.8	5.1	10.2	50.9	3.8	0.75
						2.393		2.464		3.78		15.6		11.82						
	HT-S-28	8	5.656	5.2	0.456	2.365	2.4	2.45	2.5	4.84	4.8	17.51	17.5	12.67	12.7	5.6	11.7	46.3	4	0.71
						2.365		2.459		4.84		17.51		12.67						
	HT-S-34		5.656	5.2	0.456	2.381	2.4	2.454	2.5	4.21	4.2	16.89	16.9	12.68	12.7	5.5	11.5	46.3	4	0.73
						2.381		2.459		4.21		16.89		12.68						
	HT-V-28		5.656	5.2	0.456	2.396	2.4	2.468	2.5	3.99	4.2	16.3	16.5	12.31	12.3	5.3	11.1	46.3	4	0.75
						2.386		2.469		4.47		16.71		12.24						
HT-V-34	5.656		5.2	0.456	2.382	2.4	2.454	2.5	4.16	4.2	16.85	16.9	12.69	12.7	5.5	11.5	46.3	4	0.73	
					2.382		2.459		4.16		16.85		12.69							
Waukesha-15% PBR	MT-S-28	18	5.726	4.7	1.026	2.419	2.4	2.502	2.5	4.19	4.1	16.04	15.9	11.85	11.9	5.1	8.5	58.3	5	0.98
						2.426		2.505		3.92		15.8		11.88						
	MT-S-34		5.726	4.7	1.026	2.417	2.4	2.496	2.5	4.04	4.1	16.11	16.1	12.07	12.1	5.2	8.6	58.3	5	0.96
						2.416		2.499		4.08		16.15		12.07						
	MT-V-28		5.726	4.7	1.026	2.416	2.4	2.501	2.5	4.1	4.2	16.08	16.2	11.98	12.0	5.2	8.6	58.3	5	0.96
						2.409		2.499		4.39		16.33		11.94						
	MT-V-34		5.726	4.7	1.026	2.404	2.4	2.503	2.5	4.55	4.7	16.49	16.6	11.94	11.9	5.2	8.6	58.3	5	0.96
						2.399		2.496		4.82		16.73		11.91						
	HT-S-28	11	5.17	4.6	0.57	2.463	2.5	2.542	2.5	4.02	4.1	14.83	14.9	10.81	10.8	4.6	9.8	47.9	3.6	0.78
						2.461		2.533		4.1		14.9		10.8						
	HT-S-34		5.17	4.6	0.57	2.454	2.5	2.523	2.5	3.77	3.6	15.22	15.0	11.45	11.5	4.9	10.5	47.9	5.1	1.04
						2.464		2.516		3.38		14.87		11.49						
	HT-V-28		5.17	4.6	0.57	2.452	2.5	2.544	2.5	4.6	4.5	15.21	15.2	10.61	10.6	4.5	9.6	47.9	5.1	1.13
						2.455		2.539		4.48		15.11		10.63						
HT-V-34	5.17		4.6	0.57	2.455	2.5	2.502	2.5	3.06	3.2	15.03	15.2	11.97	12.0	5.1	10.9	47.9	5.1	1.00	
					2.448		2.511		3.34		15.27		11.93							

Material Detail		%Binder Replacement	Total AC	Added AC	RAP AC	Gmb		Gmm		Va		VMA		VBE		Pbc	AFT	P8	P200	D/B Ratio	
			Rep	Rep	Rep	Rep	Ave	Rep	Ave	Rep	Ave	Rep	Ave	Rep	Ave	Rep	Rep	Rep	Rep	Rep	
Wimme-15% PBR	MT-S-28	15	5.555	4.7	0.855	2.402	2.4	2.493	2.5	4.57	4.6	16.08	16.1	11.51	11.5	5	8.4	58.2	3.4	0.68	
						2.402	2.491	2.5	4.57	4.6	16.08	16.1	11.51								
	MT-S-34		5.555	4.7	0.855	2.418	2.4	2.491	2.5	3.57	4.6	15.4	16.1	11.83	11.8	5.1	8.5	58.2	3.4	0.67	
						2.418	2.482	2.5	3.61	4.6	15.43	16.1	11.82								
	MT-V-28		5.555	4.7	0.855	2.425	2.4	2.495	2.5	3.36	3.4	14.93	14.9	11.57	11.6	5	8.4	58.2	3.4	0.68	
						2.425	2.494	2.5	3.36	3.4	14.93	14.9	11.57								
	MT-V-34		5.555	4.7	0.855	2.42	2.4	2.493	2.5	3.48	3.5	15.11	15.1	11.63	11.6	5	8.4	58.2	3.4	0.68	
						2.42	2.492	2.5	3.48	3.5	15.11	15.1	11.63								
	HT-S-28		5.6	15	4.7	0.9	2.389	2.4	2.498	2.5	5.31	5.0	17.18	16.9	11.87	11.9	5.2	8.1	60.3	4.5	0.87
							2.407	2.493	2.5	4.59	5.0	16.56	16.9	11.97							
	HT-S-34		5.6		4.7	0.9	2.418	2.4	2.49	2.5	3.71	4.0	15.97	16.3	12.26	12.2	5.3	8.3	60.3	4.5	0.85
							2.404	2.49	2.5	4.35	4.0	16.53	16.3	12.18							
HT-V-28	5.6	4.7	0.9		2.429	2.4	2.507	2.5	3.81	3.8	15.58	15.6	11.77	11.8	5.1	8	60.3	4.5	0.88		
					2.429	2.501	2.5	3.81	3.8	15.58	15.6	11.77									
HT-V-34	5.6	4.7	0.9		2.439	2.4	2.493	2.5	3.18	3.2	15.31	15.3	12.13	12.1	5.2	8.1	60.3	4.5	0.87		
					2.439	2.499	2.5	3.18	3.2	15.31	15.3	12.13									
Cisler-30% PBR	MT-S-28	35	5.745		3.75	1.995	2.406	2.4	2.481	2.5	4.2	4.3	15.74	15.8	11.54	11.5	5	9.4	49.1	4.8	0.96
							2.401	2.479	2.5	4.32	4.3	15.85	15.8	11.53							
	MT-S-34		5.745		3.75	1.995	2.414	2.4	2.479	2.5	3.73	3.8	15.4	15.4	11.67	11.7	5.1	9.6	49.1	4.8	0.94
							2.413	2.477	2.5	3.78	3.8	15.44	15.4	11.66							
	MT-V-28		5.745	3.75	1.995	2.421	2.4	2.469	2.5	3.18	3.4	15.09	15.3	11.91	11.9	5.1	9.6	49.1	4.8	0.94	
						2.411	2.477	2.5	3.66	3.4	15.5	15.3	11.84								
	MT-V-34		5.745	3.75	1.995	2.42	2.4	2.461	2.5	2.66	2.6	15.11	15.0	12.45	12.5	5.4	10.1	49.1	4.8	0.89	
						2.422	2.457	2.5	2.5	2.6	15.11	15.0	12.48								
	HT-S-28		5.324	34	3.5	1.824	2.423	2.4	2.49	2.5	3.82	3.8	14.63	14.6	10.81	10.8	4.7	8.8	49.1	4.7	1.00
							2.423	2.494	2.5	3.82	3.8	14.63	14.6	10.81							
	HT-S-34		5.324		3.5	1.824	2.402	2.4	2.482	2.5	4	4	15.26	15.3	11.26	11.2	4.9	9.2	49.1	4.7	0.96
							2.402	2.475	2.5	4	4	15.26	15.3	11.26							
HT-V-28	5.324	3.5	1.824		2.416	2.4	2.499	2.5	4.22	4.1	14.87	14.8	10.65	10.7	4.6	8.6	49.1	4.7	1.02		
					2.42	2.492	2.5	4.06	4.1	14.73	14.8	10.67									
HT-V-34	5.324	3.5	1.824		2.424	2.4	2.491	2.5	3.5	3.6	14.52	14.6	11.02	11.0	4.7	8.8	49.1	4.7	1.00		
					2.421	2.483	2.5	3.62	3.6	14.63	14.6	11.01									
Cisler-50% PBR	MT-S-28	50	5.75		2.9	2.85	2.435	2.4	2.495	2.5	3.55	3.9	14.72	15.0	11.17	11.1	4.8	10.9	36.5	3.8	0.79
							2.423	2.49	2.5	4.17	3.9	15.28	15.0	11.11							
	MT-S-34		5.75		2.9	2.85	2.425	2.4	2.495	2.5	3.98	4.0	15.14	15.1	11.16	11.2	4.8	10.9	36.5	3.8	0.79
							2.425	2.488	2.5	3.98	4.0	15.14	15.1	11.16							
	MT-V-28		5.75	2.9	2.85	2.427	2.4	2.493	2.5	3.81	3.8	14.93	14.9	11.12	11.1	4.8	10.9	36.5	3.8	0.79	
						2.427	2.494	2.5	3.81	3.8	14.93	14.9	11.12								
	MT-V-34		5.75	2.9	2.85	2.402	2.4	2.487	2.5	4.7	4.7	15.93	15.9	11.23	11.2	4.9	11.1	36.5	3.8	0.78	
						2.402	2.487	2.5	4.7	4.7	15.93	15.9	11.23								
	HT-S-28		5.25	60	2.1	3.15	2.437	2.4	2.519	2.5	4.57	4.4	14.21	14.1	9.64	9.7	4.1	9.2	36.5	3.8	0.93
							2.444	2.523	2.5	4.22	4.4	13.9	14.1	9.68							
	HT-S-34		5.25		2.1	3.15	2.434	2.4	2.52	2.5	4.73	4.7	14.39	14.4	9.66	9.7	4.1	9.2	36.5	3.8	0.93
							2.434	2.52	2.5	4.73	4.7	14.39	14.4	9.66							
HT-V-28	5.25	2.1	3.15		2.442	2.4	2.512	2.5	3.98	4.0	13.97	14.0	9.99	10.0	4.3	9.6	36.5	3.8	0.88		
					2.442	2.513	2.5	3.98	4.0	13.97	14.0	9.99									
HT-V-34	5.25	2.1	3.15		2.428	2.4	2.502	2.5	4.28	4.3	14.53	14.5	10.25	10.3	4.4	9.9	36.5	3.8	0.86		
					2.428	2.506	2.5	4.28	4.3	14.53	14.5	10.25									

Appendix B

Summary of “Fitted” E* Values for all Mixtures

Aggregate	Cisler								Waukesha								Wimme											
Traffic Level	MT				HT				MT				HT				MT				HT							
Binder	S-28	S-34	V-28	V-34	S-28	S-34	V-28	V-34	S-28	S-34	V-28	V-34	S-28	S-34	V-28	V-34	S-28	S-34	V-28	V-34	S-28	S-34	V-28	V-34	S-28	S-34	V-28	V-34
0.000001	18.4	17.9	23.3	20.4	18.7	21.8	20.1	29.2	21.7	20.6	38.7	33.8	20.1	22.6	17.4	28.9	24.0	27.0	26.1	27.0	28.2	28.5	23.4	26.9				
0.00001	21.0	21.4	27.6	23.2	22.6	25.3	24.8	31.0	26.9	25.5	42.2	36.5	24.9	28.3	20.9	33.3	27.7	29.3	29.5	29.1	31.0	32.1	27.1	29.3				
0.0001	26.2	27.9	35.7	28.5	29.5	31.3	33.5	34.4	36.4	33.9	49.1	41.7	33.6	38.3	28.0	41.0	34.8	33.7	35.8	33.1	36.4	38.4	33.8	33.9				
0.001	37.3	40.5	51.4	38.8	42.0	41.9	50.0	41.2	54.7	49.0	63.4	52.2	50.3	56.3	43.2	54.9	48.8	42.6	48.4	41.0	47.5	50.2	47.1	42.9				
0.01	62.5	65.8	83.5	60.5	65.8	61.5	82.8	55.6	91.3	76.7	94.3	74.3	83.5	89.4	78.4	80.8	78.2	61.6	74.6	57.4	71.7	73.0	74.6	61.9				
0.1	123.0	118.4	150.5	107.7	111.6	98.5	148.4	87.8	164.5	128.0	164.5	123.7	150.0	150.5	161.5	130.6	142.1	104.5	131.8	93.4	127.2	118.6	133.4	103.7				
1	264.9	225.3	285.4	210.6	198.5	168.7	273.9	163.1	303.7	220.8	321.2	235.5	277.7	259.6	345.0	225.3	276.8	203.7	254.7	174.7	254.6	209.9	256.6	198.1				
10	553.4	423.5	528.4	416.8	352.6	296.2	491.0	333.8	540.8	377.6	630.0	469.1	498.9	439.5	684.6	394.8	530.6	417.7	494.8	350.9	517.8	382.6	489.6	398.1				
100	1012.6	738.8	896.0	764.9	595.9	506.9	813.4	666.0	885.3	615.7	1110.1	871.5	828.4	704.5	1174.0	665.2	924.7	801.4	884.2	679.3	955.4	670.3	858.7	755.6				
1000	1563.6	1154.5	1349.4	1234.1	927.9	810.9	1215.9	1165.0	1304.0	932.7	1670.5	1401.3	1240.6	1045.9	1717.5	1034.5	1411.2	1328.9	1383.4	1161.8	1506.2	1071.1	1328.7	1255.1				
10000	2076.5	1608.5	1810.0	1737.7	1315.5	1186.4	1640.6	1723.9	1734.1	1300.5	2173.7	1933.3	1676.1	1429.6	2201.0	1460.3	1894.3	1880.0	1892.1	1705.9	2037.7	1530.1	1812.5	1792.8				
100000	2470.7	2029.8	2208.2	2183.4	1707.3	1584.8	2028.7	2208.4	2117.4	1675.7	2544.6	2361.7	2074.6	1810.2	2566.4	1879.8	2296.8	2338.7	2321.1	2192.2	2453.9	1969.8	2229.8	2256.6				

Appendix C

Draft AASHTO Standard for the RAP/RAS Mortar Testing

Standard Method of Test for

Estimating Effect of RAP and RAS on Blended Binder Performance Grade without Binder Extraction

AASHTO Designation: T XXX-12

1. SCOPE

- 1.1 This test method presents the procedure to estimate the effect of recycled asphalt pavement (RAP) or recycled asphalt shingles (RAS) on binder performance grade. The procedure measures the Superpave PG properties of asphalt binders and mortars in order to estimate the performance properties of the blended binder. Due to the use of mortars, extraction of binders from recycled materials is not required. In addition, the procedure provides blended binder performance properties at two levels of binder replacement and therefore can be used to construct a blending chart to estimate the change in performance grade as a function of percent binder replacement.
- 1.2 The values stated in SI units are to be regarded as the standard.
- 1.3 *This standard does not purport to address all of the safety problems, if any, associated with its use. It is the responsibility of the user of this standard to establish appropriate safety and health practices and determine the applicability of regulatory limitations prior to use.*
-

2. REFERENCED DOCUMENTS

- 2.1 *AASHTO Standards:*
- AASHTO M320 – Standard Specification for Performance Graded Asphalt Binder
 - AASHTO T240 – Effect of Heat and Air on a Moving Film of Asphalt Binder (Rolling Thin Film Oven Test)
 - AASHTO R28 – Accelerated Aging of Asphalt Binder Using a Pressure Aging Vessel
 - AASHTO R29 – Practice for Grading or Verifying the Performance Grade of an Asphalt Binder
- 2.2 *ASTM Standards:*
- ASTM D 7175-08 – Standard Test Method for Determine the Rheological Properties of Asphalt Binder Using the Dynamic Shear Rheometer.
 - ASTM D7643-10 – Determining the Continuous Grading Temperatures and Continuous Grades for PG Graded Asphalt Binders

ASTM D 6648-08 – Standard Test Method for Determining the Flexural Creep Stiffness of Asphalt Binder Using the Bending Beam Rheometer.

ASTM D6307 – Standard Test Method for Asphalt Content of Hot Mix Asphalt by Ignition Method.

ASTM D8 – Standard Terminology Relating to Materials for Roads and Pavements

3. TERMINOLOGY

3.1 *General Definitions:*

3.1.1 General definitions of terms used in this practice are found in Terminology ASTM D 8 determined from common English usage, or combinations of both.

3.2 Procedural Definitions

3.2.1 *Binder Performance Grade Change Rate:* Change in blended binder continuous grade due to increasing binder replacement [$^{\circ}\text{C}/\%$ RAP(S) binder replacement].

3.2.2 *Binder Replacement:* The percentage by weight of recycled binder present to the total weight of binder used to prepare the mortar.

3.2.3 *Blended Binder:* The effective asphalt binder (virgin binder blended with RAP(S) binder) in the mortar material. Blending does not need to be present to test the mortar materials in the proposed procedure. Complete blending may not occur if the mortar is prepared at low mixing temperatures, or the RAP(S) material is heavily oxidized.

3.2.4 *Burned Aggregates:* Remaining aggregates from RAP or RAS material after burning in the ignition oven according to ASTM D6307-05. This material is free from binder and consists only of the non-bituminous components of RAP or RAS.

3.2.5 *Asphalt Binder Continuous Grade:* The temperature at which an asphalt binder fails a given Superpave performance grading limit. To determine the continuous grade it is required to test at temperatures that correspond to the material passing and failing the specification limit. The performance vs. temperature relationship is used to determine the exact temperature at which the material fails by use of interpolation. Continuous grading is applicable to high, intermediate, and low grading temperatures.

3.2.6 *Virgin Asphalt Binder:* Conventional asphalt binder material used in construction of asphalt pavements. In application to this procedure virgin binder is subjected to standard SuperPave grading specified in AASHTO M320 and used for preparation and evaluation of mortar properties. Virgin binder can be modified or unmodified and used at various levels of artificial aging, as required by the test procedure.

3.2.7 *Mortar:* Laboratory produced mixture of virgin asphalt binder and R_{100} aggregates.

3.2.8 *R100 Aggregates:* Aggregates and other non-bituminous components from either RAP or RAS material that are passing sieve #50 (300 μm) and retained on #100 (150 μm).

Aggregates that do not meet this size requirement are discarded. Both aggregates sampled directly from RAP/RAS source and sampled after burning in ignition oven are used in this test procedure.

- 3.2.9 *RAP*: Recycled (Reclaimed) Asphalt Pavement.
 - 3.2.10 *RAS*: Recycled (Reclaimed) Asphalt Shingles.
 - 3.2.11 *Total Binder Content*: Weight percentage of binder (virgin binder + RAP/RAS binder) in mortar material.
-

4. SUMMARY OF METHOD

- 4.1 Evaluation of the impacts of RAP/RAS on performance requires testing of three different materials using SuperPave methods. The materials required include the virgin binder and two void-less mortar samples prepared with the virgin binder and a single sized aggregate gradation. The two mortar samples are prepared with identical gradation and total asphalt content using aggregates from recycled materials both before and after burning in the ignition oven. As a result, any difference in performance properties between the two mortars is attributed to the presence of recycled binder. The effect of the recycled binder on mortar performance is applied to estimate the performance of the blended binder.
-

5. SIGNIFICANCE AND USE

- 5.1 This test method provides an estimate of the impacts of binder replacement by recycled asphalt materials (RAP and/or RAS) on blended binder performance grade. The method is also used to define the change in binder continuous grade as a function of percent binder replacement. This relationship can be used to define the maximum allowable binder replacement before a change in virgin asphalt grade is necessary. The procedure uses mortars and thus eliminates the need, and variability associated with, chemical extraction and recovery. This test procedure is performance based and therefore the analysis is blind to RAP/RAS source, virgin binder source, and the use of binder modification.
-

6. SAMPLE PREPARATION

- 6.1 Select virgin binder, RAP, and RAS sources representative of materials used in the field for a user defined climate and geographical area.
- 6.2 Dry and sieve all RAP and/or RAS material. Arrange sieves to collect R₁₀₀ material, defined as materials passing sieve #50 (300 μm) and retained on sieve #100 (150 μm). Discard all material passing the #100 sieve (P₁₀₀). The test procedure requires at least 500 g of R₁₀₀ material. After sufficient material is collected split the R₁₀₀ material.
- 6.3 Place at least 250 g of RAP or RAS material in the ignition oven and follow ASTM D6307-05 to determine the binder content of the R₁₀₀ material. Save the aggregates that remain after burning for use in preparation of mortar samples.

- 6.4 The procedure requires preparation of two mortar types, these mortars are defined below. The quantity of mortar required and aging condition of the asphalt binder used in preparation of the mortar is user defined and depends on the performance property of interest. Guidelines are provided in Table 1.
- 6.4.1 *RAP/RAS Mortar:* Consists of R₁₀₀ RAP or RAS material from (6.2) combined with virgin binder at a user-selected level of aging. Adjust binder content to ensure that a level of workability is achieved such that DSR samples and BBR beams can be cast free of voids. A minimum total binder content of 30% by weight is recommended as a guideline.
- 6.4.2 *Aggregate Mortar:* Consists of R₁₀₀ burned aggregates from (6.3) mixed with virgin asphalt binder at a user defined aging condition and at the same total binder content as the RAP/RAS mortar prepared in (6.4. 1).
- 6.5 Select the aging condition of the virgin asphalt and quantity of the mortar based on the aging condition at and type of test required for performance evaluation.
- Note 1** – Research has indicated the blending of virgin and RAP aged binder is a diffusion process in which time and conditioning temperature can greatly affect the amount (degree) of binder blending. To ensure sufficient blending, mortar samples should be conditioned at 135 °C for two hours. It is best to determine the field production temperature and conditioning time conditions in order to simulate the actual blending in the laboratory. If possible, use these conditions in the laboratory.
- 6.5.1 *Un-aged mortar performance:* Prepare the mortar with un-aged virgin asphalt binder.
- 6.5.2 *Short and Long Term aged mortar performance:* Short-term age virgin asphalt binder in the RTFO according to AASHTO T240 and use the aged binder to prepare the mortar.
- 6.5.3 *Recommended mortar quantities:* Un-aged and short-term aged properties require at least 60 grams of mortar for DSR testing. Evaluation of long term-aged properties requires at least 200 g of mortar to allow for both the DSR and BBR testing. Example calculations for preparation of the mortar are provided in Appendix X1.
- 6.6 Long term aging requires aging of mortars in the pressure aging vessel for 24 hours under the conditions specified in AASHTO R-28 prior to testing. Place sufficient mortar in each PAV pan to ensure 50 grams total of binder is present in the pan. For example, if the total binder content of the mortar is 40 percent, the required amount of mortar in each PAV pan will be $50\text{ g} / (0.40\text{ binder content}) = 125\text{ g mortar}$.
- 6.7 Short and long term age virgin binders as required to measure SuperPave PG properties. Conduct each specification test at a minimum of two temperatures.
- The test samples required for a complete analysis procedure are summarized in Table 1.

Table 1 – Required Test Specimens for Complete Performance Grade Analysis

Performance	Low Temperature: BBR	Intermediate Temperature: DSR	High Temperature: DSR	
Asphalt Binder	Same as PG Grading			
RAP/RAS Mortar	PAV Aged: RTFO Binder + RAP/RAS	PAV Aged: RTFO Binder + RAP/RAS	RTFO Binder + RAP/RAS	Original Binder +RAP/RAS
Aggregate Mortar	PAV Aged: RTFO Binder + RAP/RAS Aggregate	PAV Aged: RTFO Binder + RAP/RAS Aggregate	RTFO Binder + RAP/RAS Aggregate	Original Binder + RAP/RAS Aggregate

7. TESTING PROCEDURE

- 7.1 *Virgin Asphalt Binder:* Conduct tests specified in AASHTO M320 to determine the SuperPave performance properties of the asphalt binder. Take measurements at two test temperatures. Select testing temperatures for a given performance property based recommendations provided in Table 3.
- 7.2 *RAP/RAS and Aggregate Mortars:* Measurement of the performance properties of mortars requires revisions to the AASHTO M320 procedure as detailed below. Evaluate each performance property at the same test temperatures as used for the virgin binder in Step 7.1.
- 7.2.1 *High Temperature Performance:* Prepare separate aggregate and RAP/RAS mortars with un-aged and RTFO aged virgin binders as detailed in Table 1. Test in the Dynamic Shear Rheometer (DSR) at a gap of 2mm at the prescribed test temperatures. All other testing conditions specified in AASHTO M320 remain unchanged.
- 7.2.2 *Intermediate Temperature Performance:* Prepare separate and Aggregate and RAP/RAS mortars with RTFO aged virgin binder. Long term age the mortars in the PAV according to (6.6). Evaluate the performance properties using the procedure in AASHTO M320 at the same test temperatures as the virgin binder tested in (7.1).
- 7.2.3 *Low Temperature Performance:* Prepare separate aggregate and RAP/RAS mortars with RTFO aged virgin binder. Long term age the mortars in the PAV according to (6.6). Prepare beams for testing in the bending beam rheometer (BBR) and test at the temperatures used for the virgin binder. Adjust test load in BBR based on test temperature selected as shown in Table 2. All other testing conditions as specified in AASHTO M320 remain unchanged.

Table 2 – Bending Beam Rheometer Test Loads in mN.

Test Temperature (°C)	PAV Binder	PAV Mortar
0	980	980
-6	980	1980
-12	980	2980
-18	980	3980
-24	980	4980

7.3 The testing procedures, evaluation parameters, recommended temperatures and deviations from AASHTO M320 are summarized in Table 3.

Table 3 – Summary of Test Procedure and Deviations from AASHTO M320 for Mortar Grading

Recommended Test Temperatures	Device and Test Parameters	Deviations from AASHTO M320		
		Virgin Asphalt	Aggregate Mortar	RAP/RAS Mortar
Low Temperature PG LT+10°C, PG LT+10°C	Bending Beam Rheometer (BBR), S(60), m(60)	None	Adjust test load for different test temperatures.	
Intermediate Temperature PG IT, PG IT+3°C	Dynamic Shear Rheometer (DSR), $G^* \sin \delta$		None	
High Temperature – Short Term Aged PG HT, PG HT+6°C	Dynamic Shear Rheometer (DSR), $G^* / \sin \delta$		Increase DSR testing gap from 1mm to 2mm	
High Temperature – Un-aged PG HT, PG HT+6°C	Dynamic Shear Rheometer (DSR), $G^* / \sin \delta$			

8. CALCULATION AND INTERPRETATION OF RESULTS

- 8.1 *Data Analysis.* The test data available after completion of Section 7 provides sufficient information to estimate the effect of recycled binders on virgin binder performance properties and to create a blending chart that establishes the relationship between %Recycled Binder replacement vs. change in binder continuous grade.
- 8.2 *Estimating the Impact of RAS/RAP on Virgin Binder Continuous Grade*
- 8.2.1 Determine the continuous grade of the virgin asphalt binder using the analysis procedure specified in ASTM D7643.

- 8.2.2 Compare the performance of the RAP/RAS and aggregate mortars at each testing temperature to estimate the performance properties of the recycled asphalt binder. The only difference between RAP/RAS aggregate mortars is the presence of the recycled binder, therefore any differences in performance are assumed to be due to the recycled binder. The difference in performance between the RAP/RAS and aggregate mortars for a given performance property at a given test temperature is defined as (δ_{Tx}). It is necessary to measure δ_{Tx} at both test temperatures.

$$\text{Eq (1)} \quad \delta_{Tx} = \frac{\text{Property RAP/RAS Mortar}}{\text{Property Aggregate Mortar}}$$

Note: To maintain agreement with ASTM D7346 δ_{Tx} values must be calculated using a logarithmic scale for all properties except the BBR m-value. Use an arithmetic scale to calculate δ_{Tx} for the m-value.

- 8.2.3 Calculate the average change in performance across both testing temperatures (δ_{RAP}) using Equation 2.

$$\text{Eq (2)} \quad \delta_{RAP} = \frac{(\delta_{T1})+(\delta_{T2})}{2}$$

Where,

δ_{RAP} = Average change in performance property due to the presence of recycled binder in the RAP/RAS mortar.

δ_{T1} = Change in performance property due to the presence recycled binder in the RAS/RAP mortar at PG testing temperature 1.

δ_{T2} = Change in performance property due to the presence of recycled binder in the RAS/RAP mortar at PG testing temperature 2.

- 8.2.4 Multiply the RAP shift factor (δ_{RAP}) by the virgin binder performance property of interest at each test temperature to determine the effect of blending of the reclaimed RAP or RAS binder with virgin binder. Calculate the blended binder continuous grade using the procedure detailed in ASTM D7643.

8.3 *Estimating the relationship between %Recycled Binder Replacement and Change in Blended Binder Continuous Grade*

- 8.3.1 The analysis method provides two points of reference for estimating the rate of change in continuous grade due to replacement of virgin binder with recycled binder, the continuous grade of the virgin binder (0% binder replacement) and the estimated continuous grade of the recycled binder blended with the virgin binder (x% binder replacement). The %binder replacement in the blended binder depends on the asphalt content of the recycled material used and the total binder content of the RAP/RAS mortar. Based on these points of reference the rate of change in continuous grade is represented by the slope of the line, provided in Equation 3.

$$\text{Eq (3)} \quad \text{Rate of Change in C. G.} = \frac{(\text{Est.Blended Binder C.G.} - \text{Virgin Binder C.G.})}{\text{Recycled PBR}}$$

Where,

Rate of Change in C.G. = Rate of virgin binder grade change per percent binder replaced. [°C/% replacement]

Estimated Blended Binder C.G. = Estimated blended binder continuous grade [°C]

Virgin Binder C.G. = Virgin binder continuous grade [°C]

Recycled PBR: Percent binder replacement [%]

8.3.2 Equation 3 is applicable to any performance property in the high, intermediate, and low SuperPave grading temperature regimes. In addition the linear relationship is applicable to any quantity of recycled binder replacement through use of interpolation or extrapolation.

8.4 An example of this calculation is provided in Appendix X2.

9. REPORT

9.1 *Virgin Binder Properties*

9.1.1 SuperPave performance properties as measured according to AASHTO M320 at high, intermediate and low test temperatures.

9.1.2 Continuous grade of virgin binder as determined by ASTM D7643.

9.2 *Mortar Properties*

9.2.1 Reclaimed Binder Replacement (See Appendix X1.1) in mortar.

9.2.2 Blended binder continuous grade as determined by ASTM D7643.

9.2.3 Rate of change in continuous grade due to the presence of recycled binders (°C/%Binder Replacement).

10. PRECISION AND BIAS

10.1 Adherence to precision and bias statements of ASTM D 6648-08 – Standard Test Method for Determining the Flexural Creep Stiffness of Asphalt Binder Using the Bending Beam Rheometer and ASTM D 7175-08 – Standard Test Method for Determine the Rheological Properties of Asphalt Binder Using the Dynamic Shear Rheometer has been found to be acceptable. Ongoing testing is being completed to further characterize precision and bias of the proposed procedure.

APPENDIX

X1. EXAMPLE MORTAR MIXTURE DESIGN CALCULATIONS

X1.1 *Mortar Mix Design.* The following calculations are an example of mortar mixture design calculations performed to determine the appropriate material proportions for the mortar samples. However, other methods of design are possible.

RAP/RAS mortar samples are prepared according to (6.4.1). The following equations are valid for RAS materials and RAP/RAS material blends, with the only adjustment being the R₁₀₀ asphalt content. The mortar total asphalt content AC_{total} and percent binder replacement AC_{RAP} are calculated from the following two equations:

$$\text{Mortar Total Asphalt Content: } AC_{totalRAP/RAS} = \left[\frac{(RAP_S * R100_{AC}) + VB}{RAP_S + VB} \right] * 100$$

$$\text{Reclaimed Binder Replacement: } AC_{RAP} = \left[\frac{RAP_S * R100_{AC}}{(RAP_S * R100_{AC}) + VB} \right] * 100$$

Where,

$AC_{total-RAP/RAS}$: RAP/RAS Mortar total asphalt content [%]

AC_{RAP} : Percent RAP/RAS binder replacement [%]

RAP_S : Sieved R₁₀₀ RAP/RAS material quantity [g]

$R100_{AC}$: R100 RAP/RAS asphalt content [%]

VB : Virgin binder quantity at prescribed level of aging [g]

Aggregate mortar samples are prepared according to (6.4.2). Here, the user will only control the quantity of burned R₁₀₀ aggregates, as the procedure requires that the total binder content matches that of the RAP/RAS mortar. To meet this requirement the following equation must hold:

$$VB = \frac{AC_{total-RAP/RAS} * RAP_{AM}}{1 - AC_{total-RAP/RAS}}$$

Where,

RAP_{AM} : Quantity of burned R₁₀₀ RAP aggregates required for aggregate mortar [g]

The Aggregate Mortar total binder content $AC_{total-AM}$ is then be expressed as

$$AC_{total-AM} = \left(\frac{VB}{RAP_{AM} + VB} \right) * 100$$

And

$$AC_{total-AM} = AC_{total-RAP/RAS}$$

Note that for the previous equation to be true, the quantity of virgin binder required for the Aggregate Mortar will be greater than the quantity used in the RAP/RAS mortar as in this mortar a portion of the virgin binder (at the prescribed aging condition) is replaced with recycled binder.

X2. EXAMPLE BLENDED BINDER CONTINUOUS GRADE CALCULATIONS

X2.1 *Estimation of Blended Binder Continuous Grade.* The following calculations are an example of calculations used to estimate the blended binder continuous grade and the rate of change in continuous grade (rate of improvement) of the virgin binder. The calculations are shown for low temperature grading but the methodology remains unchanged for performance at other grading temperatures.

An example set of low temperature test results is given in Table X2.1.

Table X2.1 – Example Low Temperature Testing Results

Binder Replacement in RAP/RAS Mortar	25%			
Test Temperature, °C	-12		-18	
Test Specimen	Average BBR Parameter		Average BBR Parameter	
	Stiffness S(60) MPa	m-value	Stiffness S(60) MPa	m-value
PAV Aged Virgin Binder	160	0.343	283	0.316
RAP/RAS Mortar	1075	0.263	1790	0.233
Aggregate Mortar	675	0.324	1180	0.278

The low temperature stiffness continuous grade of the PAV aged virgin binder is first calculated following ASTM D 7643 as:

$$T_c = T_1 + \left(\frac{\log_{10}(S_s) - \log_{10}(S_1)}{\log_{10}(S_2) - \log_{10}(S_1)} \right) (T_2 - T_1) - 10$$

Where,

T_c : Continuous grading temperature, [°C]

T_1 : Lower of the two test temperatures, [°C]

S_s : Specification requirement for stiffness; determined at the respective PG grading temperature [log MPa]

S_1 : Test result for the stiffness at T_1 [log MPa]

S_2 : Test result for the stiffness at T_2 [log MPa]

T_2 : Higher of the two test temperatures, [°C]

The low temperature m-value continuous grade of the PAV aged virgin binder is then calculated following ASTM D 7643 as:

$$T_c = T_1 + \left(\frac{m_s - m_1}{m_2 - m_1} \right) (T_2 - T_1) - 10$$

Where,

m_s : Specification requirement for m-value; determined at the respective PG grading temperature

m_1 : Test result for the m-value at T_1

m_2 : Test result for the m-value at T_2

For the test results presented in Table X2.1, the virgin binder continuous grade is calculated to be:

Stiffness Continuous Grading Temperature -29 °C
 m-value Continuous Grading Temperature -32 °C

Calculate δ_{RAP} according to 8.2.3. The calculation is shown in Table X.2.2 for the data set given above.

Table X2.2 – Calculation of δ_{RAP}

Test Temperature, °C	-12		-18	
Test Specimen	Average BBR Parameter		Average BBR Parameter	
	Stiffness S(60) MPa	m-value	Stiffness S(60) MPa	m-value
RAP/RAS Mortar	1075	0.263	1790	0.233
Aggregate Mortar	675	0.324	1180	0.278
δ_{Tx}	$\frac{\log(1075)}{\log(675)} = 1.07$	$\frac{0.263}{0.324} = 0.812$	$\frac{\log(1790)}{\log(1180)} = 1.06$	$\frac{0.233}{0.278} = 0.834$
δ_{RAP}	$\frac{1.07 + 1.06}{2} = 1.07$	$\frac{0.812 + 0.834}{2} = 0.823$		

The blended binder properties are then estimated by multiplying δ_{RAP} and the PAV aged virgin binder properties. Note that δ_{RAP} is multiplied by the logarithm of the stiffness but the arithmetic m-value. The results for the data set are shown below.

Table X2.3 – Calculation of Estimated Blended Binder Properties

Test Temperature, °C	-12		-18	
Test Specimen	Average BBR Parameter		Average BBR Parameter	
	Log Stiffness S(60) MPa	m-value	Stiffness S(60) MPa	m-value
PAV Aged Virgin Binder	2.20	0.343	2.45	0.316
Estimated Blended Binder Properties	2.35	0.282	2.62	0.260

The blended binder continuous grade is estimated using the formulas given in ASTM D 7643 and shown above using the estimated blended binder properties. For the test results presented above, the blended binder continuous grade is calculated to be:

Stiffness Continuous Grading Temperature -25 °C
 m-value Continuous Grading Temperature -17.6 °C

The rate of change in continuous grade due to replacement of virgin binder with recycled binder. Is calculated according to 8.3.1 as:

$$0.16 \frac{^{\circ}\text{C}}{\text{PBR}} = \frac{(-25) - (-29)}{25\%}$$

And

$$0.58 \frac{^{\circ}\text{C}}{\text{PBR}} = \frac{(-17.6) - (-32)}{25\%}$$

The more conservative of the two rate of change numbers for design, in this case example, the 0.58°C/PBR for the m-value represents the most extreme change in properties, and thus controls binder replacement levels. An example of the blending chart that is generated from this analysis and the sensitivity of S(60) and m(60) to binder replacement is provided in Figure 1. In the figure, dashed lines represent portions of the chart that were extrapolated.

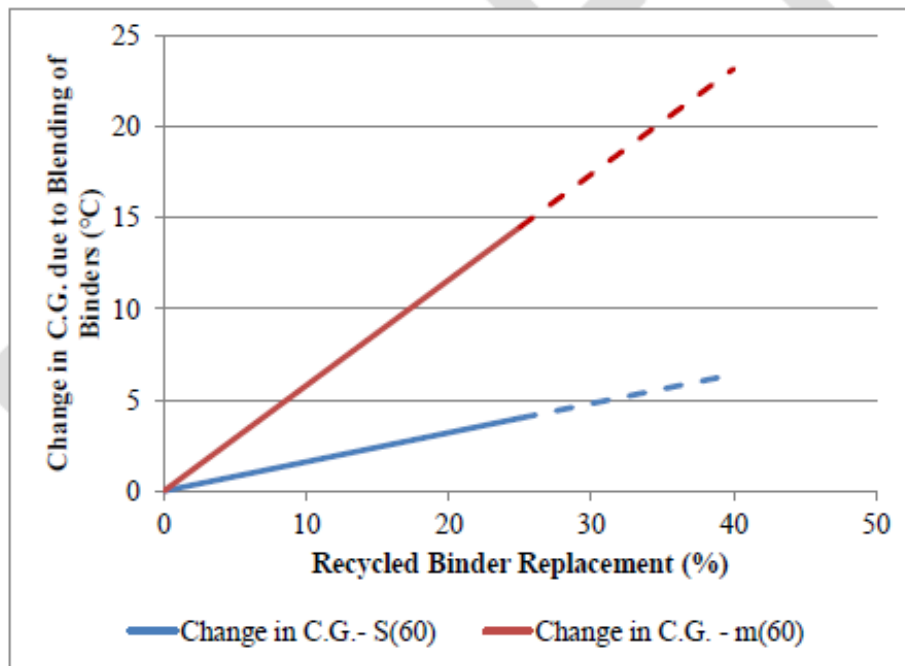


Figure X2.1 – Change in Continuous Grade based on S(60) and m(60) with Increasing Recycled Binder Replacement.